Materiomics: Dealing with Complexity in Tissue Engineering

C.A. van Blitterswijk, D. Stamatialis, H. Unadkat, B. Papenburg, J. Rouwkema, R. Truckenmuller, A. van Apeldoorn, M. Wessling, J. de Boer

Departments of Tissue Regeneration and Membrane Technology, University of Twente, The Netherlands.

INTRODUCTION: As the human body holds some 200 cell types that synthesize a multitude of both soluble and solid actives in addition to a variety of components that provide various means of mechanical support it will be clear that extremely complex interactions stand at the basis of the proper functioning of all tissues.

With the increase of complexity, certainly when this is associated with a, at best, only partial understanding of the underlying mechanisms, special strategies need to be applied to unravel or direct processes that result from such complex interactions. Rather than striving for a full understanding of the underlying mechanisms upon which to base ones actions, it might be more productive to rapidly screen a multitude of approaches and select the one with the most optimal result. Surprisingly, in tissue engineering this approach is still largely unexplored.

RESULTS: In this presentation, apart from a selective overview of the current state of high throughput in tissue engineering, we will discuss the production of large libraries of material geometries that will allow us to screen thousands to millions of substrates. We propose the name *MATERIOMICS* for the discipline of high throughput methods in biomaterials and tissue engineering science.

ADVANCED 3D-FIBRIN MATRICES FOR MOLECULAR MEDICINE

H. Hall

Cells and BioMaterials, D-MATL, ETH Zurich, Switzerland.

INTRODUCTION: Cell guidance and drug delivery is crucial when tissue engineering-based approached are followed in regenerative medicine. Here we introduce two possibilities that might be useful in stimulating tissue regeneration: a) 3D-fibrin hydrogel matrices contain covalent gradients of a cell guidance cue; namely L1Ig6 to direct cell growth; b) 3D-fibrin matrices are covalently modified with nano-condensates between (therapeutic) plasmid DNA and peptide-modified PLL-g-PEG-polymers such that the nano-condensates are released only when cells actively degrade the 3D-fibrin matrix. Both approaches will enable us to combine structural support, directed cell growth and drug delivery to improve e.g. wound healing.

METHODS: 3D-Fibrin hydrogels were produced and gradients of guidance cue L1Ig6 were formed according to [1]. Human foreskin fibroblasts (hFFs) were cultivated on top or within such fibrin gradient matrices and cell alignment with the direction of the gradient was determined at different positions after staining the cell body with DAPI and the actin cytoskeleton with phalloidin-rhodamin [1]. Homogeneous 3D-fibrin matrices were filled with different DNA-polymer nanoparticles and the release kinetics was followed over 7 days. The transfection efficiency was determined by transfection of COS-7 cells using a plasmid harbouring the sequence for enhanced green fluorescent protein (eGFP) [2-3].

RESULTS: 3D-fibrin matrices can be used as both: scaffold and release system. Here gradients of covalently attached guidance cue L1Ig6; being a ligand for integrins $\alpha v\beta 3$ and $\alpha 5\beta 1$ were assessed for their ability to direct cell alignment with the direction of increasing concentrations of the guidance cue (Fig. 1). HFFs cultivated on top and within such gradient matrices show alignment with the gradient direction at high concentrations of L1Ig6, whereas no alignment was observed at low concentrations of L1Ig6.

When peptide-modified or native PLL-g-PEG was used to complex plasmid DNA and included into 3D-fibrin matrices, it can be observed that naked DNA and native PLL-g-PEG-DNA condensates efficiently diffuse out of the matrix in 7 days (Fig. 2A). These condensates show high transfection efficiency of COS-7 cells (Fig. 2B). When PLL-g-PEG was modified with a polyArginin sequence or with a TG-peptide that allows covalent incorporation of the nano-condensates into the 3D-fibrin matrix, no release was observed. Consequently COS-7 cells were not transfected (Fig. 2 A and B).

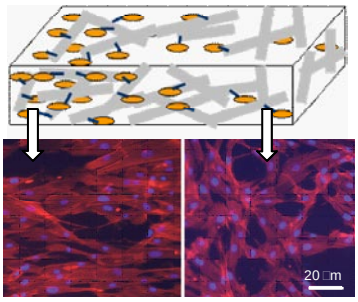

Fig. 1: Schematic of a gradient of L1Ig6 (orange ovals) covalently attached to 3D-fibrin matrices. Below: left: hFFs align; right: hFFs do not align.

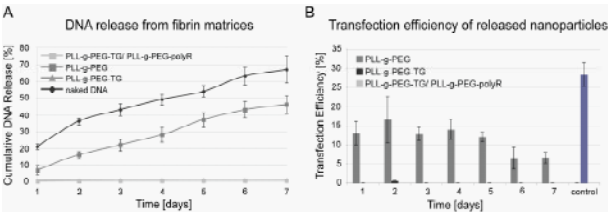

Fig. 2: Cumulative release of 4 different types of polymer-DNA-nanocondensates over 7 days (left). Transfection efficiency in COS-7 cells after release from 3D-fibrin matrices (right).

DISCUSSION & CONCLUSIONS: The experiments indicate that 3D-fibrrin matrices can be efficiently used for directed cell growth when guidance cues are covalently fixed within the matrices. Moreover, differential release of polymer-DNA-nano-condensates reveals that 3D-fibrin matrices can be used as tuneable delivery system. Both features will be explored to improve wound healing in healing deficient animal models.

REFERENCES: [1]Lühmann, T. et al. (2009) Biomaterials; 30: 4503–4512. [2]Rimann M. et al. (2008) Bioconjug Chem. 19(2):548-57. [3]Lühmann T. et al. (2008) Bioconjug Chem. **19**(9):1907-16.

ACKNOWLEDGEMENTS: The authors like to thank: Gebert Rüf Stiftung GRS/2005 and CCMX Competence Center for Materials Science and Technology.

Conductive Substrates for Stem Cell Sheet Engineering

OV. Semenov[1,2], O. Guillaume-Gentil[2], A. Malek[1], K. Maniura[3], M. Ehrbar[1], J. Voros[2], AH. Zisch[1]

[1] *University Hospital Zurich, Zurich, Switzerland.* [2] *ETH Zurich, Zurich, Switzerland.*
[3] *EMPA, St. Gallen, Switzerland.*

INTRODUCTION: Cell sheet engineering has emerged as, versatile method for direct cell transplantation or creation of three-dimensional multilayered thick tissue structures without the need of biodegradable scaffolds. Viable cell sheets from different cell types were successfully harvested from temperature-responsive polymer surfaces and already used for clinical applications [1]. We demonstrate an alternative methodology for assembling and harvesting of stem cell sheets based on applying of electrical potential to conductive indium tin oxide substrates (ITO) functionalized with polyelectrolyte multilayer (PEM) coatings [2].

METHODS: We established critical parameters for isolation of placental derived mesenchymal stem cells (PD-MSCs) [3]. Following this we created PD-MSC sheets on ITO substrates functionalized with PEM coatings assembled from 9 alternating layer pairs of cationic poly (allylamine hydrochloride) (PAH) and anionic poly (sodium-4-styrenesulfonate) (PSS). Resulting cell sheets were analyzed for morphology (light and confocal microscopy), viability (life/death stain), vitality (WST-1 assay), phenotypic profile (FACS), and plasticity (mesodermal differentiation). Live, undifferentiated PD-MSC sheets were then harvested from the conductive surface by applying of electrical potential.

RESULTS: We showed that conductive ITO substrates functionalized with [PAH-PSS] support adhesion and outgrowth of human mesenchymal stem cells and allow formation of live, dense stem cell sheets. The resulting cell sheets retained their phenotypical profile and could be differentiated towards mesodermal lineage *in vitro* (Figure 1). Moreover, we were able to recover undifferentiated PD-MSC sheets from these functionalized conductive surfaces (Figure 2).

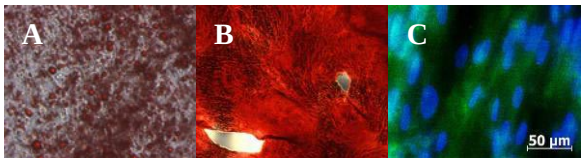

Fig. 1: Mesodermal differentiation of PD-MSC sheets in vitro on [PAH-PSS]$_9$ functionalized ITO surfaces: Adipogenic (A), osteogenic (B), and chondrogenic (C).

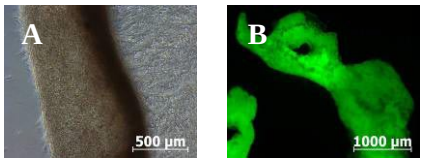

Fig. 2: Recovering of PD-MSC sheets from [PAH-PSS]$_9$ functionalized ITO surfaces: PD-MSC sheet recovering after applying of potential (A), live-dead staining of recovered PD-MSC sheet (B).

DISCUSSION & CONCLUSIONS: Conductive ITO substrates functionalized with PEM support formation differentiation and controlled recovering of intact stem cell sheets. Ongoing research is directed towards mesodermal differentiation of harvested stem cell sheets *in vitro* and their differentiation on ITO substrates by co-culture with human adult cell types.

REFERENCES: [1] J. Yang, M. Yamato, T. Shimizu, et al (2007) *Biomaterials* **28**:5033-43. [2] O.V. Semenov, A. Malek, AG. Bittermann, et al (2009) *Tissue Engineering Part A* **15(10)**:2977-90. [3] O.V. Semenov, S. Koestenbauer, M. Riegel, et al (2010) *AJOG* **202**:1-13.

ACKNOWLEDGEMENTS: This work was funded by a grant of the Competence Center for Materials Science and Technology (CCMX), Switzerland and FP6 grant “Crystal”, European Union.

Influence of scaffold pore size on extracellular matrix production by human mesenchymal stem cells cultured on silk fibroin scaffolds

S.Wüst[1], B.W.Thimm[1], S.Hofmann[1], R.Müller[1]

[1]*ETH Zurich, Zurich, Switzerland.*

INTRODUCTION: Bone tissue engineering becomes more and more important, to overcome the limited supply of grafts in orthopaedic science [1]. The main goal of the study was to obtain homogenous and fast mineralized matrix production, which is important for the applicability of tissue engineered constructs. Human bone marrow derived mesenchymal stem cells (hMSCs) were cultured on silk fibroin (SF) scaffolds with different pore sizes *in vitro* and different proliferation intervals of hMSCs prior to cell differentiation were applied. The hypothesis was that initial proliferation instead of direct differentiation along osteogenic lineage will enhance extracellular matrix (ECM) production within the scaffold by providing a higher cell number and better cell distribution through the volume of the scaffold.

METHODS: SF scaffolds (5mm diameter, 2mm height) were prepared from the silkworm *Bombyx Mori* with pore sizes of 112-224µm (small), 315-400µm (medium) and 500-600µm (large). hMSCs were seeded on SF scaffolds and cultured in control medium (DMEM, fetal bovine serum, pen/strep/fungizone), proliferation medium (control medium + non-essential amino acids, bFGF) and osteogenic medium (control medium + ascorbic acid-2-phosphate, dexamethasone, β-glycerophosphate) in static bioreactors. Proliferation intervals of 0, 3, 6 and 9 days with subsequent differentiation along the osteogenic lineage for 9 weeks were performed for scaffolds with three different pore sizes. The bioreactors were designed in-house to perform non-invasive on-line micro-computed tomography (µCT) of mineralized structures over time [2]. Cell metabolic activity, DNA, calcium deposition and alkaline phosphatase (ALP) activity were performed to complete the study.

RESULTS: Visible mineralization was achieved with hMSCs cultured on SF scaffolds in osteogenic medium only. The influence of scaffold pore sizes on ECM mineralization revealed significant differences, with the most mineralization volume achieved on scaffolds with small pores (Fig 1). This result was corroborated by the calcium assay. The proliferation phases prior to cell differentiation lead to highly significant effects on ECM mineralization on scaffolds with the small pores only; the longer the proliferation phase, the higher was the detected bone volume density (BV/TV). No difference was seen on scaffolds with medium pores and on scaffolds with large pores a longer proliferation time lead to even less ECM.

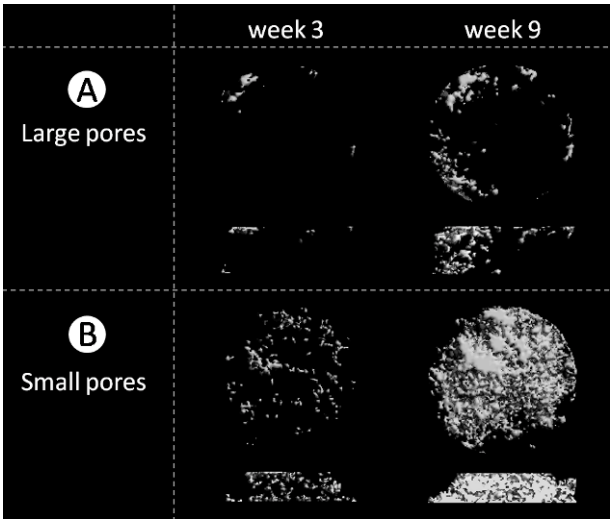

Fig. 1: µCT images of mineralization at week 3 and 9 (9 day proliferation period). (A) Scaffolds with large pores and (B) scaffolds with small pores; upper row showing top views and lower row the corresponding cross-sectional views.

DISCUSSION & CONCLUSIONS: The general hypothesis that more homogenous distribution would result from longer proliferation time prior to cell differentiation was only achieved in scaffolds with small pores. ECM distribution was still far away from the required homogeneity for implantation and has to be further improved, for example with perfused bioreactors. To analyze the influence of pore size and geometry in more detail, new scaffold production techniques must be considered. 3D printing might be the method of choice as it will allow precise control of scaffold porosity, architecture and mechanical properties in a more homogenous fashion using classical CAD.

REFERENCES: [1] L. Meinel, V. Karageorgiou, R. Fajardo, et al (2004) *Ann Biomed Eng*, **32**:112-22. [2] H. Hagenmüller, S. Hofmann, T. Kohler, et al (2007) *Ann Biomed Eng*, **35**:1657-67.

ACKNOWLEDGEMENTS: The authors would like to acknowledge funding from Robert Mathys Foundation, Bettlach. Silk was kindly provided by Trudel Silk Inc., Zürich, Switzerland.

Orientation of myoblasts in response to scaffold architecture

G. Guex[1,2], G. Fortunato[2], E. Körner[2], J. Yin[2], X. Liu[2], H. Tevaearai[1], M.-N. Giraud[1]

[1] Clinic for Cardiovascular Research, University Hospital Bern, Switzerland. [2] EMPA, Swiss Federal Laboratories for Materials testing and Research, St. Gallen, Switzerland.

INTRODUCTION: Myocardial tissue engineering aims for the repair and revascularisation of ischemic heart tissue. A crucial prerequisite is the development of a contractile muscle biograft. In the present study, we evaluate the response of muscle cell seeding efficiency and orientation to substrate architecture (microfibrous or nanofibrous constructs) and composition (incorporation of nitrogen and oxygen groups).

METHODS: By electrospinning**,** solutions of 15% w/v polycaprolactone (PCL) in chloroform/methanol or acetic acid/pyridine were processed into fibrous nonwovens. A RF plasma coating process was utilised to introduce oxygen or nitrogen groups onto the scaffold surface (using CO_2/C_2H_2 or NH_3/C_2H_2 gas, respectively). Contact angle (CA), XPS measurements and SEM allowed a first characterisation of the constructs.

Mouse myoblasts (cell line C2C12) were seeded on the scaffolds at a density of $9*10^3/cm^2$ and cultured under static conditions up to 7 days. Myoblasts were assayed for seeding efficiency and viability (MTT staining after 48 hours), morphology and alignment (SEM, Hematoxylin-Eosin staining and angle measurement). All assays were accomplished in N=3 and compared to cells cultured on TCPS. Values are given in percentage relative to TCPS as mean ± SD.

RESULTS: *Scaffold Characterisation* PCL microfibrous (3.2 ± 0.8 µm, fig. 2A) and nanofibrous (308 ± 178nm, fig. 2B) patches were obtained using, respectively, chloroform/methanol and acid/pyridine as solvents. XPS confirmed the incorporation of oxygen (increase of 14% compared to pure PCL) or nitrogen (18%), respectively. Pure PCL patches revealed highly hydrophobic properties (CA=123°), whereas the use of plasma coatings turned the patches into highly hydrophilic ones.

Cell Culture Cell seeding was optimised in order to attain a homogenous cell distribution. Pure PCL patchs, displaying fibres in the micrometre range resulted in higher seeding efficiency compared to fibres in the nanometre range. Similar seeding efficiencies were obtained for CO_2/C_2H_2 plasma coated patches. In contrast, nitrogen groups induced lower seeding efficiency for both architectures, compared to pure PCL patches (table 1). Orientation on pure PCL substrates was fibre size dependent. Cell angle measurements revealed a higher degree of orientation for C2C12 cultured on nanofibrous compared to microfibrous scaffolds (fig. 2A and 2B).

Table. 1:Seeding efficiency on scaffolds with distinct coatings and different fibre sizes.

	Seeding efficiency (%)	
functional group	microfibrous	nanofibrous
none	76 ± 10	49 ± 5
oxygen	72 ± 8	46 ± 14
nitrogen	47 ± 8	22 ± 12

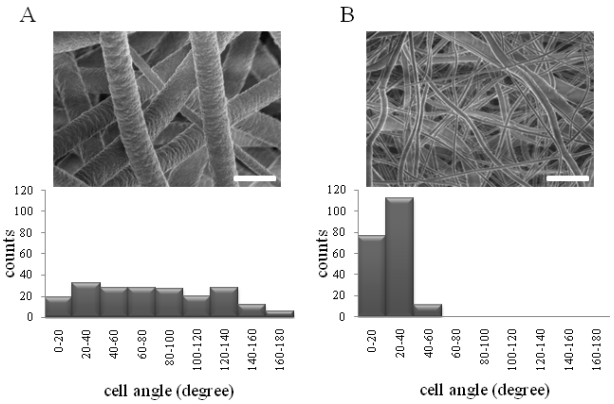

Fig. 2: SEM images of the pure PCL scaffold (scale bar 5µm) and corresponding cell angle distribution on A) microfibrous and B) nanofibrous scaffold. N=200 cells

DISCUSSION & CONCLUSIONS: By electrospinning, we produced randomly oriented fibres, displaying distinct diameters. We provide evidence, that microfibrous, pure PCL scaffolds allow highest seeding efficiency of muscle cells. Whereas nanofibrous scaffolds of the same composition induced cell alignment. Further investigations will determine if initial cell alignment favours cell differentiation into parallel and contractile myotubes.

ACKNOWLEDGEMENTS: Project was funded by SNF grant 122334

Injectable Hyaluronan Hydrogels for Cell and Drug Delivery.

M. Peroglio, D. Mortisen, M. Alini, D. Eglin
AO Research Institute, Davos, Switzerland.

INTRODUCTION: Thermo-reversible hydrogels are promising cell carriers for cartilage and nucleus pulposus (NP) repair. In this study poly(N-isopropylacrylamide) grafted hyaluronan (HA-PNP) hydrogels with well-defined molecular architecture and properties were synthesized through RAFT polymerization and "click" chemistry. Effect of PNP grafting length and density on HA-PNP properties were evaluated by methods relevant for a cell therapy (fig.1).

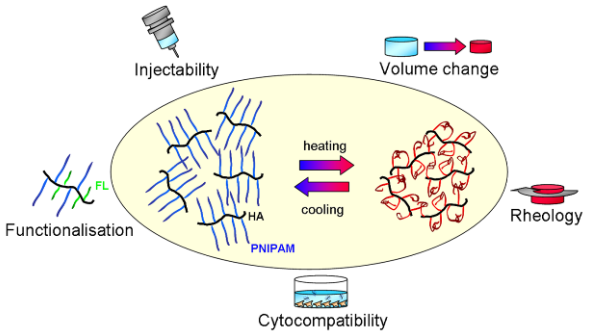

Fig. 1: Pathway to the development of HA-pNP thermo-reversible hydrogels for cell therapy.

METHODS: Synthesis of thermo-reversible HA-PNP hydrogels were synthesized by procedures reported elsewhere[1,2]. Briefly, N_3-terminated PNP of different molecular weights (Mn) were synthesized by RAFT polymerization. The PNP were grafted to propargylamide functionalized HA by copper(I) catalyzed alkyne-azide cycloaddition at different grafting density (DS) of the alkyne subunits. Gelling **reversibility** was analyzed by differential scanning calorimetry (DSC). HA-PNP rheological properties were characterized using a CVOR-Rheometer Bohlin instrument (1ºC/min, heating from 25 to 40ºC at 2 Hz). **Water retention** was calculated as the ratio of wet-dry difference of hydrogel plunged in PBS at 37°C for a time t and wet-dry difference of the blank (hydrogel at 25°C, prior to PBS plunging). **Cytocompatibility** tests were performed using a primary bovine NP cells seeded in 96 well plates (2000 cells suspended in 100 µl of DMEM-10% FCS in each well). After 14 hrs, PNP, HA-PNP and degradation products were added to achieve a final concentration from 5 to 100 µg/ml. Cell viability was measured by WST-1 assay at 24 and 48 hrs. HA-PNP simultaneously grafted with **fluorescein** bearing an azide function was performed and characterized by ^{1}H nuclear magnetic resonance and fluorescence microscopy.

RESULTS & DISCUSSION: At all stages of a cell therapy, the carrier should provide adequate properties: (1) low viscosity liquid at room temperature to facilitate cell dispersion and injection through a needle, (2) with rapid thermo-responsive gelling kinetics to ensure good space control, (3) with reversible gelling to allow retrieval of cells encapsulated and cultured *in vitro*, (4) cytocompatible, (5) with suitable mechanical properties when gelled at 37°C, and (6) readily amenable to further functionalization. Both PNP grafting length and density affects the overall properties of the hydrogels, but it was found that the grafting length had the strongest effect. In fact, increasing PNP Mn induced: (1) a decrease of HA-PNP viscosity at 25°C, (2) an increase of G' at 37°C and (3) a decrease of the water retention (table 1).

Table 1. HA-PNP compositions viscosity at 25ºC and 2 Hz, elastic moduli at 37ºC and 2 Hz and water retention after 1 hr in PBS at 37°C.

Mn (kDa)-DS (%)	η* (Pa·s)	Water retention %	G' (Pa)
10 –30	30.0	1.46 (0.3)	458.5
20 –30	13.9	1.01 (0.1)	252.8
35 –30	16.2	0.71 (0.0)	4959.7
35 – 25	10.8	0.53 (0.0)	16099.7

PNP, HA-PNP and their degradation products were cytocompatible to NP cells (cell viability > 80% at 48 hours for all compositions). Gelling reversibility was confirmed by DSC profiles for all HA-PNP compositions. Therefore, these gels can be used for cell expansion prior to delivery in the injured site. The feasibility of creating multi-functional hydrogels was assessed by PNP and fluorescein simultaneous grafting on HA backbone through "click" chemistry. Fluorescein grafting to HA-PNP was confirmed by its solubilisation and homogeneous fluorescence.

CONCLUSIONS: A composition with properties ideal for cell encapsulation was identified and characterized by a low viscosity at 20°C, rapid gelling at 37°C, absence of volume change upon gelling, and a G' of 140 Pa at 37 °C.

REFERENCES: [1] M. Li, P. De, S.R. Gondi, et al (2008) *Macromol Rapid Commun.* **29**: 1172. [2] V. Crescenzi, L. Cornelio, C. Di Meo, et al (2007) *Biomacromolecules* **8**: 1844.

Engineered RGD-Silk Scaffold for Improved Cell Adhesion

AY. Nilsson[1], AJ. Meinel[1], S. Panke[1]

[1] *ETH Zurich, Zurich, Switzerland*

INTRODUCTION: Silk is an alanine- and glycine-rich protein consisting of repeating crystalline and amorphous regions. These features give silk its outstanding mechanical properties, which are complemented with good biocompatibility and biodegradability. Together these properties make silk a suitable scaffold material for tissue engineering purposes. The objective of this work is to produce a genetically engineered spider silk-based protein with the cell signaling amino acid sequence RGD (arginine-glycine-aspartic acid) directly incorporated into the primary sequence. The hypothesis is that the engineered RGD-silk will promote receptor-mediated cell adhesion and spreading, features crucial for a functional bioactive scaffold.

METHODS:
$GRG_2LG_2QGAGA_5G_2AGQG_2YG_2LGSQG$ is the consensus sequence of the repetitive unit derived from the major ampullate spidroin 1 (MaSp1) of the spider *Nephila clavipes*. A DNA sequence coding for 15 repeats of this consensus sequence was constructed (15mer) [1] and also an analogue flanked by DNA coding for the amino acid sequence VTGRGDSPA derived from fibronectin domain III_{10} was assembled (RGD-15mer) [this work]. For affinity purification and quantification terminal His- and S-tags were attached. The two engineered silks were produced by fed-batch fermentation using a bacterial expression system, and then purified and cast into films with a surface density of 1 mg/cm^2. The films were seeded with DiI stained human mesenchymal stem cells (hMSC) at a density of 5'000 cells/cm^2, and cell adhesion was studied with time-lapse microscopy.

RESULTS: The final concentration of the engineered silks after fermentation was approximately 1'000 mg/L, and 25% of this could be recovered after purification to a purity of >95%. Films made of the engineered silks with the fibronectin derived RGD sequence (RGD-15mer) and without the RGD sequence (15mer) were cast and seeded with hMSCs. On the RGD-15mer silk the cells started to polarize and migrate, something that could not be observed on the 15mer silk over the duration of the time-lapse experiment, see Fig. 1. As a positive control fibronectin-coated 15mer silk (5 µg/cm^2) was used. All experiments were performed with serum free medium.

Analysis of the mechanical properties of the engineered silks, and long term cell culture studies to investigate proliferation and differentiation remain to be performed.

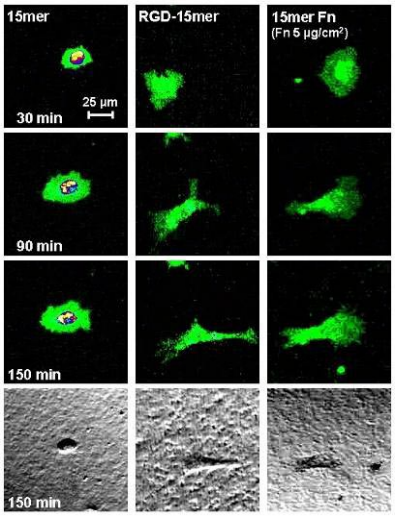

Fig. 1: Micrographs of human mesenchymal stem cells on 15mer, RGD-15mer and fibronectin-coated 15mer silks 30, 90 and 150 minutes post-seeding. Top 3 rows: fluorescence images, bottom row: differential interference contrast images.

DISCUSSION & CONCLUSIONS: We have set up a production system for tailor-made silk materials for tissue engineering applications. Furthermore we have integrated the cell signaling amino acid sequence RGD into one of the engineered silks, and we could detect an effect in adhesion of human mesenchymal stem cells on films made of this RGD-silk. These results show that this novel biomaterial has the potential to be used as a cell adhesion promoting scaffold material in the field of tissue engineering.

REFERENCES: [1] E. Bini, C.W. Foo, J. Huang, V. Karageorgiou, B. Kitchel, D.L. Kaplan (2006) *Biomacromolecules* **7**:3139-45.

ACKNOWLEDGEMENTS: We gratefully acknowledge the kind gift of the *Nephila clavipes* silk gene containing plasmid, coding for 15mer silk, from Professor David Kaplan (Tufts University, Medford, MA). Special thanks go to Dr. Kristopher Kubow (ETH Zurich) for assistance with the time-lapse studies. This work was supported by the BioEngineering Cluster (ETH Zurich).

In vivo evaluation of cotton wool-like amorphous-TCP/PLGA nanocomposites

O.D. Schneider[1], B. von Rechenberg[2], P.R. Schmidlin[3], F. Weber[4], W.J. Stark[1]

[1] *Institute for Chemical and Bio-Engineering, ETH Zurich, Switzerland.*
[2] *Musculoskeletal Research Unit, Equine Clinic, University of Zurich, Switzerland.*
[3] *Clinic for Preventive Dentistry, Periodontology and Cariology, University of Zurich, Switzerland.*
[4] *Department for Cranio-Maxillofacial Surgery, University Hospital Zurich, Switzerland.*

INTRODUCTION: In reconstructive surgery, bioresorbable implant materials are in great demand for the repair of bone defects. Many current biomaterials consist of calcium phosphates which excel in biocompatibility, bioactivity and osteoconductivity. However, many commercially available products are limited to specific clinical applications because of their brittleness, incompressibility and difficulty to shape. The present contribution shows two *in vivo* studies of entirely *in vitro* [1,2] investigated nanocomposites.

METHODS: Highly porous nanocomposites consisting of a biodegradable poly(lactide-co-glycolide) fibrous matrix and either aerosol-derived amorphous tricalcium phosphate nanoparticles (PLGA/TCP) alone or finely silver dispersed on identical TCP nanoparticles (PLGA/Ag-TCP) were prepared by electrospinning. A first *in vivo* study was performed in four circular non-critical size calvarial defects in New Zealand White rabbits, which were treated with PLGA and PLGA/TCP scaffolds (Fig. 1a). The "gold standard" in dental surgery (BioOss®) was used as a positive control and cavities left empty served as a negative control. The bone regeneration was assessed after 4 weeks implantation using histological and micro-computed tomographic analysis. The *in vivo* performance of PLGA/TCP and PLGA/Ag-TCP scaffolds was evaluated in a second study using a drill hole defect model in the metaphysis of long bone in sheep (during 8 weeks). The effect of silver on the biocompatibility and cellular reactions during bone regeneration was assessed by histological analysis applying a score system.

RESULTS: The fibrous nanocomposites showed enhanced *in vitro* mineralization in simulated body fluid (Fig. 1a), whereas silver containing fibres showed additionally strongly antimicrobial properties for 2 days against E. coli [2]. The cotton wool-like biomaterials could be applied very easy during surgical procedure. The area fraction of newly formed bone was significantly increased for TCP containing fibres compared to pure PLGA [3]. Semi-quantitative histology showed that both PLGA/TCP and PLGA/Ag-TCP scaffolds were fully biocompatible and enabled fast bone formation even to the centre of the former defect (Fig. 1c). No inflammatory reactions were observed for both biomaterials which were mostly resorbed through macrophages (Fig. 1d).

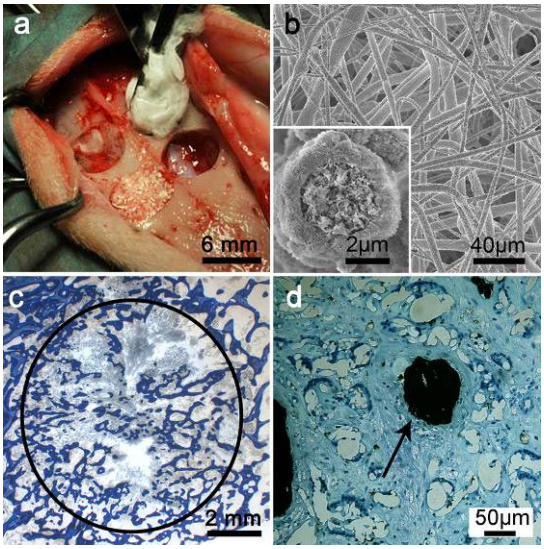

Fig. 1: (a) The Cotton wool-like biomaterial is easy-to-apply in bone defects. (b) SEM of PLGA/TCP nanocomposites after in vitro mineralization. (c, d) Histological sections showing bone formation and resorption of material in sheep.

DISCUSSION & CONCLUSIONS: The easy applicable biomaterial suggests application for non-load bearing complex shaped bone defects. The advantageous use of this compressible material could be valuable in minimally invasive surgery or for specific indications in dental surgery (i.e. sinus augmentation, augmentation procedures of the alveolar bone, socket preservation after tooth extraction) where the antimicrobial properties of PLGA/Ag-TCP could be beneficial.

REFERENCES: [1] O.D. Schneider et al (2008) *J Biomed Mater Res Part B* **84B(2)**:350-62. [2] O.D. Schneider et al (2008) *J Mater Chem* **18**: 2679-2684. [3] O.D. Schneider et al (2009) *Acta Biomater* **5(5)**: 1775-1784.

ACKNOWLEDGEMENTS: Financial support by the Swiss Commission for Technology and Innovation, CTI project 9141.1 is kindly acknowledged.

The role of mechanical load on the chondrogenesis of human bone derived mesenchymal stem cells in fibrin-polyurethane scaffolds

Stoddart MJ., Li Z., Eglin D., Alini M.

AO Research Institute, Davos, Switzerland.

INTRODUCTION: The differentiation of stem cells into chondrocytes is highly dependant on the signals the cells receive. TGFβ is used to induce chondrogenesis and yet this would not be supplemented within an articular defect. We have developed a biodegradable polyurethane-fibrin scaffold system which has been shown to be highly favorable for chondrogenesis under classical chondrogenic stimuli (TGFβ containing medium). The aim of this study was to determine the effectiveness of this scaffold composite in supporting chondrogenesis in the absence of an exogenous TGFβ signal, but under the influence of a loading regime similar to that which might be experienced during a patient rehabilitation protocol.

METHODS: The scaffolds were prepared by a salt leaching-phase inverse technique consisting of the mixing in equal weight of a porogen (sodium phosphate heptahydrate dibasic salt, particles size range from 90 to 300 μm) with a solution containing a mixture of solvents and the polyurethane synthesized from hexamethylene diisocyanate, poly(epsilon-caprolactone) diol and 1,4:3,6-dianhydro-D-sorbitol in a one step solution polycondensation reaction. P3 hMSCs were suspended in fibrin and seeded at a cell density of $5x10^6$ per polyurethane scaffold. All groups were cultured in medium consisting of DMEM, ITS, Pen/Strep, ascorbate-2-phosphate, 5 μM ε-amino-caproic acid, and 10^{-7} M dexamethasone. 0 ng/ml, 1 ng/ml, or 10 ng/ml recombinant human TGF-β1 was added into the medium of 3 groups respectively. Load was applied using our previously described bioreactor system[1] with ball oscillation of ±25° at 1 Hz and dynamic compression 1 Hz with 10% sinusoidal strain, superimposed on a 10% static offset strain. Mechanical loading was performed 1h a day over 7 consecutive days. DNA content was measured spectrofluorometrically using Hoechst 33258. The amount of GAG in the scaffolds and medium was determined by the dimethylmethylene blue dye method. mRNA expression of collagens type-I (COL1), type-II (COL2), type-X (COL10), aggrecan (AGG), proteoglycan4 (PRG4), osterix (Sp7), transforming growth factors -β1 (TGFB1), and β3 (TGFB3) were investigated and compared to 18S ribosomal RNA as the endogenous control.

RESULTS: Total GAG synthesized was normalized to DNA content. The control samples cultured in medium with 1 ng/ml ($P<0.01$) or 10 ng/ml TGF-β1 ($P<0.001$) had significantly higher GAG/DNA value compared to samples cultured in medium without TGF-β1. In all the 3 groups where samples were cultured in medium with different concentrations of TGF-β1, the total GAG/DNA value showed a trend of up-regulation by mechanical load, this difference was significant in the groups with 0 ng/ml or 10 ng/ml TGF-β1.

As expected, the addition of TGF-β1 led to an increase in chondrogenesis in a dose dependant manner. By day 14, in the absence of load, addition of 1 ng/ml TGF-β1 increased the COL2 ($P=0.004$), AGG ($P=0.002$), COL10 ($P=0.002$) and Sp7 ($P=0.004$) gene expression compared to cells cultured in the absence of TGF-β1. This increase was greater when 10 ng/ml TGF-β1 was added to the medium

When investigating the effect of load on chondrogenesis increasing concentrations of TGF-β1 lead to a diminished response. The greatest response to load was seen in the groups without TGF-β1. When hMSCs were cultured in medium without TGF-β1, mechanical load significantly stimulated gene expression of COL2 ($P=0.018$), AGG ($P=0.004$), COL10 ($P=0.004$) and Sp7 ($P=0.006$). This suggests that under natural in vivo conditions mechanical load would be required to fully realise the chondrogenic potential of stem cells within this scaffold system.

DISCUSSION & CONCLUSIONS: This study demonstrates that the scaffold composite described is able to support chondrogenesis. The requirement for TGF-β1 in the medium can be removed when sufficient mechanical stimulation is applied. This study also shows that to more accurately determine the in-vivo response of a cell-biomaterial implant all stimuli, including mechanical load, must be considered.

REFERENCES: [1]Grad *et al.* Tissue Eng **11**, 249, 2005

ACKNOWLEDGEMENTS: Supported by Swiss National Fund (SNF 320000-116846/1).

Surface modification to optimize nanogel-based antigen delivery

C. A. Schütz[1°], L. J. Harwood[2°], P. Käuper[3], K. C. McCullough[2], C. Wandrey[1]

[1]Laboratory for Regenerative Medicine and Pharmacobiology, EPFL-SV-IBI-LMRP, station 15, Lausanne, Switzerland. [2]Institut für Viruskrankheiten und Immunprophylaxe, Sensemattstrasse 293, 3147 Mittelhäusern, Switzerland. [3]Medipol SA, PSE-B, 1015 Lausanne, Switzerland. °The authors have equally contributed.

Hydrophilic nanogels (Ng) have potential as nanocarriers in the development of biomedical and pharmaceutical applications. Here, we present Ng, which were optimized for antigen delivery. The components to form the core of a vaccine carrier have to protect the antigen and assure best biocompatibility. Through careful selection and modification of the carrier surfaces the delivery processes can be optimized. The core of the Ng is based on chitosan, a naturally derived polysaccharide, cationic in acidic conditions. Formation occurs by electrostatic interaction between chitosan and small molecules and/or other anionic biopolymers[1]. After the final surface decoration with polyanions, the Ng surfaces exhibit negative charges. The surface decorating alginate (Alg) was specifically functionalized to promote the targeting potential towards dendritic cell uptake.

MATERIALS AND METHODS: Two sources of chitosan were used: crustacean chitosan (Primex, Island) and ultra-pure chitosan of fungal origin (KitoZyme, Belgium), purified and characterized. Ng were formed through a robust protocol previously described[2]. The Ng shape and size were characterized. Using carbodiimide chemistry, highly purified Alg intended for surface decoration was additionally modified with the targeting moieties Pam3cys-SKKKK (Pam3) or α-D-mannopyranosyl-phenyl isothiocyanate) (Mann). As an antigen model, recNcPDI (PDI) and ovalbumin (OVA) were incorporated in the Ng according to an existing protocol. *In vitro* interactions between Ng and porcine monocyte-derived dendritic cells (MoDCs)[3] were assessed by flow cytometry and confocal microscopy. For *in vivo* studies, Swiss white mice (n=5) were immunized and blood was collected weekly for 8 weeks. A second OVA immunization was performed at day 75 and blood was collected at subsequent days 0, 2, 4, 7, and 10. OVA antibody production was measured by ELISA.

RESULTS AND DISCUSSION: Ng, loaded with PDI or OVA, were taken up *in vitro* by MoDCs within 4h incubation in a dose dependent manner. Binding of the antigen to the MoDCs was first demonstrated by flow cytometry and then internalisation of the Ng by confocal microscopy. Activation of the MoDC in response to the Ng was shown by the translocation of NFκB from the cytosol into the nucleus.

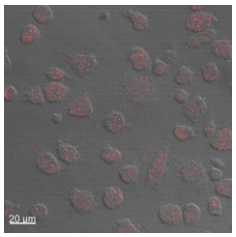

Fig. 1: MoDC uptake of PDI loaded Ng (red).

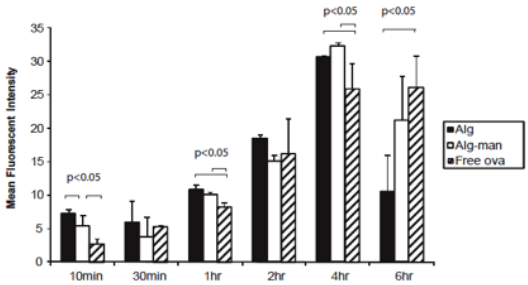

Fig. 2: Flow cytometric analysis of kinetics of uptake of free OVA and OVA loaded Ng.

Incubation of Ng with peripheral blood mononuclear cells from an OVA-immunised pig in ex vivo restimulation assays further confirmed the interaction of the particles with MoDCs and produced both T- and B- cell responses.

In vivo, the immune response to Ng treatment was dose dependent. Although primary antibody response was less than for controls, a higher memory response was observed for the groups treated with Ng with Alg-Pam3 surface, after a second antigen injection.

REFERENCES: [1]Käuper P., Laue C., 2005, WO2007031812. [2]Schütz C.A. et al., Chimia 2009, 63(4) 220-222. [3]Carrasco C. et al., Immunology 2001, 104, 175.

ACKNOWLEDGEMENTS: The research is supported by the FNS, grant 404740-117323, Medipol SA and the EU Sixth Framework Program Panfluvac (FP6-2005-SSP-5B).

Corrosion Behaviour of Metallic Implant Materials in Simulated Body Solutions

A.E.Örs, M.Diener, R. Spolenak

Laboratory for Nanometallurgy, Department of Materials, ETH Zurich, Switzerland

INTRODUCTION: Medical implants or devices have to fulfill different requirements depending on the specific biomedical demands. For instance, biodegradable implants are expected to dissolve gradually and excrete from the body after a certain time, which will enhance the patient care and avoid additional operation. Currently, the research focuses on iron, iron based alloys and tungsten as biodegradable metal implant materials [1-3]. In this work, we investigate the corrosion behaviour of metallic materials in different physiological solutions.

METHODS: Selected materials were evaluated according to immersion and electrochemical corrosion tests. In this study, five different simulated body solutions (Tab. 1) were used to simulate the human blood plasma. Although the solutions do not contain any proteins or other organic components of blood, they simulate the pH value and the inorganic components of blood. The immersion tests were performed according to ASTM standard G31. The electrochemical impedance and potentiodynamic experiments were measured with the Autolab PGSTAT12. The influence of immersion time on the corrosion behaviour was investigated by impedance measurements after 12h. Surface morphologies were examined before and after corrosion tests with a Zeiss Leo 1530 scanning electron microscope (SEM).

Table 1. Ion concentration of used solutions.

Component	0.9%NaCl (mmol/L)	Ringer's (mmol/L)	Hanks (mmol/L)	SBF (mmol/L)	PBS (mmol/L)	Human Blood Plasma (mmol/L)
Na(+)	155.20	155.20	142.77	127.76	157.17	131-155
K(+)	-	4.00	5.85	5.03	4.17	3.5-5.6
Ca(++)	-	2.70	1.27	2.52	-	1.9-3.00
Cl(-)	155.20	163.4	145.87	109.82	140.70	96-111
HCO_3(-)	-	1.20	4.17	27.01	-	16-31
HPO_4(--)	-	-	0.34	-	9.58	1-1.50
Mg (++)	-	-	0.81	1.00	-	0.70-1.90
SO_4(--)	-	-	0.81	1.00	-	0.35-1.00
H_2PO_4(-)	-	-	0.44	1.00	1.47	2.00

RESULTS: The electrochemical behaviour of iron, high carbon steel and tungsten wires depend on the used solution and the immersion time. In 0.9% NaCl and Ringer's solution, independent from the electrochemical method used, iron and high carbon steel corrode faster. On the other hand, tungsten shows slower degradation in Ringer's solution but faster in PBS. According to electrochemical impedance measurements after 12h of immersion, almost all the wires showed higher impedance values in SBF and Hanks' solution (Fig. 1). PBS was the only solution in which tungsten wire did not show higher corrosion resistance after 12h. In all solutions other than PBS, pH- measurements revealed different values after 12h of immersion.

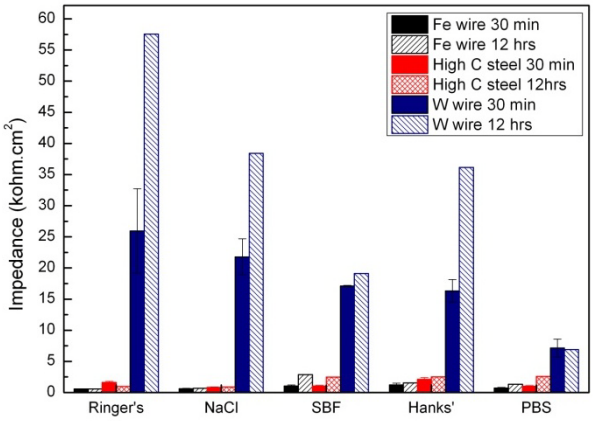

Fig. 1: Dependence of the impedance of wires on solution content and immersion time.

DISCUSSION & CONCLUSIONS: According to the results obtained from the in vitro corrosion tests corrosion mechanism, kinetics and products depend on ion concentration of the solution used. Due to the high Cl^- ion amount in 0.9% NaCl and Ringer's solutions, pitting and high corrosion rates are observed for the iron and high carbon steel wires. However, additional inorganic compounds such as bicarbonate, magnesium, phosphate and sulfate present in the solution affected the corrosion behaviour. The formation of a protective film in SBF, PBS and Hanks' solutions lowers the corrosion rate. Moreover, tungsten wires exhibit much higher corrosion resistance than iron and high carbon steel wires. The results of electrochemical impedance measurements showed time dependency of corrosion resistance.

REFERENCES: [1]M. Peuster, et. al. (2001) *A novel approach to temporary stenting*. Heart; 86:563, [2]TJ. Butler, et. al. (2000) *In vivo degradation of tungsten embolisation coils*. British Journal of Radiology; 73:601, [3] H. Hermawan, et. al. (2008) *Iron-manganese: new class of metallic degradable biomaterials prepared by powder metallurgy*. Powder Metallurgy; 51:38.

ACKNOWLEDGEMENTS: The authors would like to thank CARAG AG for providing the examined samples and Ringer's solution.

Melt-Spun Fibers From Polyhydroxyalkanoate And Polylactate For Fiber Implant Applications

M. Zinn[1], S. Dilettoso[1], S. Lischer[1], K. Maniura[1], S. Milz[2,3], B. Weisse[4], R. Hufenus[1]

[1] Empa, St. Gallen Switzerland, Switzerland. [2] Anatomische Anstalt, LMU, Munich, Munich, Germany. [3] AO Research Institute, Davos, Switzerland. [4]Empa, Dübendorf, Switzerland.

INTRODUCTION: In nature many bacteria are able to accumulate polyhydroxyalkanoates (PHAs) as a carbon storage compound. Depending on the cultivation conditions and the type of microorganism, these polyesters can be tailored and range from thermoplastic to elastomeric porperties [1]. Poly(3-hydroxybutyrate) (PHB) and the copolyester poly(3-hydroxybutyrate-*co*-3-hydroxyvalerate) (PHB/HV) exhibit the cristallization rates required for an extrusion processes. The melt-spinning of fibers from PHAs has been reported but is a tedious process that can be applied only at small scale using special equipment [2]. Poly(L-lactate) (PLLA) is a polymer that is considered to be a renewable plastic since its raw material, lactic acid, is produced by bacterial fermentation from corn starch or sugar cane. The polymer is synthesized by a ring opening polymerization in a pure chemical process using stannous octoate. PLLA is certified by FDA as an implant material, whereas for PHA so far only academic studies have been reported. The goal of this project was to develop biodegradable fibers that are suitable for tendon repair.

METHODS: PHB and PHB/HV up to a 3-hydroxyvalerate content of 80 mol% have been produced in *Cupriavidus necator* in continuous cultivation [3]. The polymers were solvent extracted [1]. For melt-spinning larger quantities of PHA were required and therefore PHB was bought from Biomer (D) or Biocycle (Br), PHB/HV with 8 mol% HV content from Tianan (Enmat Y1000, CN). PLLA was bought from Nature Works (PLA 6200D, U.S.A.). All polymers were characterized using differential scanning calorimetry (DSC), thermogravimetry (TGA), and gel permeation chromatography (GPC). The meltspinning of PHAs and PLLA was carried out on Empa's custom-made pilot melt-spinning plant that allowed production of mono- and bicomponent fibers [4]. The fibers were tested using a tensile tester Zwick (CH) equipped with a 400 N load cell. Biocompatibility was assessed using human dermal fibroblasts (HDF).

RESULTS & DISCUSSION: PHB with a molecular weight of approx. 500 kDa could not be drawn to a fiber mainly because of the low crystallization rate of PHB. As a consequence large spherulitic structures formed which caused poor mechanical properties. The content of HV could be set during biosynthesis and resulted in a decrease of the cristallinity. Optimal performance was expected for PHB/HV with a HV content of 8 mol%. PHB/HV Enmat Y1000 with a molecular weight of 490 kDa, showed better melt stability due to a lower melting temperature (Tm = 170°C). Nevertheless, a pure PHB/HV fiber could not be produced due to winding problems (stickiness of the fiber). On the other hand, PLA 6200D by NatureWorks could be spun to fibers with reasonable mechanical properties. To overcome the difficulties with spinning PHB, bicomponent fibers with a PHB/HV core and a PLA sheath were successfully spun and were strong enough for the construction of a textile fabric. *In vitro* biocompatibility studies with HDF showed no toxicity of the bicomponent fibers. Fibroblasts emerging from cell reaggregates adhered to the textiles and grew along single fibers, covering them well after a cultivation period of 1 week. *In vivo* studies in rats are currently evaluated and first results showed no inflammation in the muscle around and only localized inflammatory reaction within the meshes of the textile implant structure.

CONCLUSIONS: The processing of poly(3-hydroxyalkanoates) to fibers can be done using the bicomponent spinning method with PLLA as the sheath material. We therefore propose that the degradation rate of the fiber/textile can be controlled by the content of the PHB/HV (slowly degrading) and PLLA (quick hydrolysis). Thus, the material has properties that are in particular interesting for tendon repair applications.

REFERENCES: [1]M. Zinn, B. et al., (2001) *Adv. Drug Del. Rev.* **53**:5-21. [2]R. Vogel *et al.*, (2008) *Macromol. Biosci.***8:** 426-43. [3]M. Zinn, (2003) *Eur. Cell. Mater.* **5 Suppl. 1, 38**. [4]S. Houis, *et al.*, (2007) *Appl. Polym. Sci.* **106**, 1757-1767.

Properties of NiTi-structures fabricated by selective laser melting

T. Bormann[1,2,3], R. Schumacher[1], B. Müller[2,3], M. Mertmann[4], U. Pieles[1] and M. de Wild[1]

[1] *University of Applied Sciences Northwestern Switzerland, IMA, Muttenz, Switzerland.* [2] *School of Dental Medicine, University of Basel, Basel, Switzerland.* [3] *Biomaterials Science Center, University of Basel, Basel, Switzerland.* [4]*MEMRY GmbH, Weil am Rhein, Germany.*

INTRODUCTION: Shape memory alloys (SMA) have exceptional properties as they can change their shape as the result of thermal or mechanical stimuli. Due to their biocompatibility, NiTi-SMAs are successfully used in the field of biomedical engineering.[1] We demonstrate that selective laser melting (SLM) permits producing NiTi structures with the typical material properties of SMAs. Designing and optimizing SMA bone scaffolds, implants with advanced performance will be realized.

METHODS: For the preliminary study, pre-alloyed NiTi-powder (MEMRY GmbH) with a d50 value of 60 µm served for specimen fabrication. Differently designed test objects such as spiral springs were built by means of the SLM Realizer 100 (MTT Technologies) operated with a power of 100 W and a continuous wave Ytterbium fibre laser with a wavelength between 1068 and 1095 nm. The melting process was carried out in a highly pure argon atmosphere. Differential scanning calorimetry (DSC) and energy dispersive X-ray spectroscopy (EDX) were accomplished with both the NiTi-powder and the SLM-structures. DSC measurements were performed between -50 and +150 °C using the DSC 30 (Mettler-Toledo). The SwiftED-TM EDX spectrometer dedicated for the TM-1000 tabletop microscope (Hitachi) provided the chemical composition. The shape memory effect of the SLM structures was verified using the thermo-mechanical system TMA 40 (Mettler-Toledo) measuring the length of a deformed SLM spring as the function of temperature.

RESULTS & DISCUSSION: The NiTi-powder and the SLM-structures do show a phase transition in the related DSC measurements, see figure 1. The austenite peak temperature A_p of the powder corresponds to 19 °C, whereas the SLM-objects exhibit a value of 40 °C. The martensite peak temperature M_p lies at -4 °C for the powder and -13 °C for the SLM-structure. The EDX measurements reveal a loss of Ni up to 2%w/w in the SLM processed samples compared to the powder. As expected from the lower vapour pressure of Ti, the Ni-content of the alloy decreases during processing. The shift of the phase transition temperatures, as summarized above can be referred to this composition change, since the phase transition temperatures strongly depend on the Ni/Ti ratio.[2] TMA-measurements (data not shown) demonstrate the pseudo-plastic behaviour of the SLM materials as the one-way effect could be clearly identified.

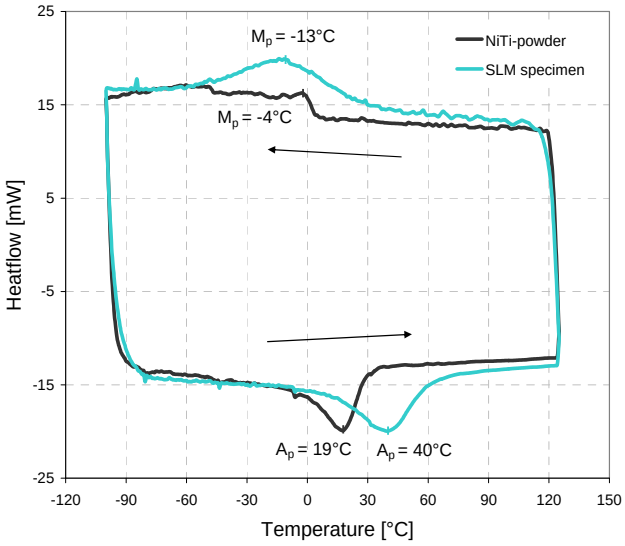

Fig. 1: DSC measurements of NiTi-powder and a selected SLM specimen.

CONCLUSIONS: The preliminary experiments reveal that SLM is an appropriate method for the fabrication of constructs with shape memory phenomena. Optimizing this process, bone scaffolds and implants of complex morphology can be realized. The final aim is the production of SMA-implants for a great variety of applications and for the benefit of patients.

REFERENCES: [1] ASTM International, F 2063 - 05. [2] W. Tang et al., (1999) *Acta Mater* **47**:3457-3468.

ACKNOWLEDGEMENT: The multi-disciplinary team gratefully acknowledges the financial support of the Swiss National Science Foundation within the program NRP 62 ‘Smart Materials‘.

In-vitro Investigation and Tailoring of Corrosion Mechanisms for Biodegradable Mg-Alloys Implants

P.Schmutz[1], M.Berg[1,2], N.Homazava[1], A.C. Hänzi[2], S. Tosatti[2,3], P.J. Uggowitzer[2]

[1] *EMPA, Dübendorf, Switzerland.* [2] *ETHZ, Zürich, Switzerland.* [3] *SuSoS, Dübendorf, Switzerland.*

INTRODUCTION: The electrochemical reactivity of Mg alloys makes them interesting as degradable implants. Mg is also essential for metabolic processes, is biocompatible and, as a metal, shows higher strength than polymers. A fundamental understanding of corrosion mechanisms is however a key prerequisite for this technology to succeed. This aspect together with a temporary corrosion protection concept obtained through surface oxidation is necessary for surface functionalization and to guarantee initial implant integrity.

METHODS: A combination of "electro"chemical techniques and surface analytical characterization of the oxide has been selected to cover a wide timescale (up to weeks) The experimental part is focused on: 1) **Inductively Coupled Plasma Optical Emission Spectroscopy** (ICP-OES) measurements that allow defining reaction mechanisms by measuring the individual dissolved ionic species amount at different immersion time. 2) Time resolved **Electrochemical Impedance Spectroscopy** (EIS) that identifies the different dissolution kinetics and surface processes based on their frequency dependence.

RESULTS: The reference solution for the in-vitro investigations was a TRIS buffered **SBF27** (pH 7.4) with concentrations (mmol): **100.0** NaCl, **4.0** KCl, **27.0** $NaHCO_3$, **1.0** $MgSO_4*7H_2O$, **2.5** $CaCl_2*2H_2O$, **1.0** KH_2PO_4. Fig.1 presents the influence of different ionic species of the SBF (solutions 1 to 5) on dissolution processes measured by ICP-OES. WE43, WZ21 and ZW12 Mg-alloys containing 4, 2 and 1% Yttrium respectively, have been compared. Yttrium dissolution shown in Fig.1b represents an excellent example of selective interaction with solution species. A small amount of phosphate hinders Y dissolution (solution 3) without major influence on Mg dissolution. Calcium which did not influence Mg dissolution alone is able to slow-down corrosion in conjunction with high Y-content and phosphates.

EIS measurements then allow the simultaneous identification of multiple reactions (three time constants visible as loops). This indicates laterally heterogeneous uniform corrosion, Fig.2. Mg is actively dissolving (first left loop representing high frequency fast processes) but formation of corrosion products on the surface depending on the ionic species of the solution induce complex degradation mechanisms. EIS measurements evidenced **diffusion limiting processes** (second loop) indicating that uniform corrosion takes place through corrosion products or **inductive components** (third loop, negative impedance) induced by re-deposition of species of the solution.

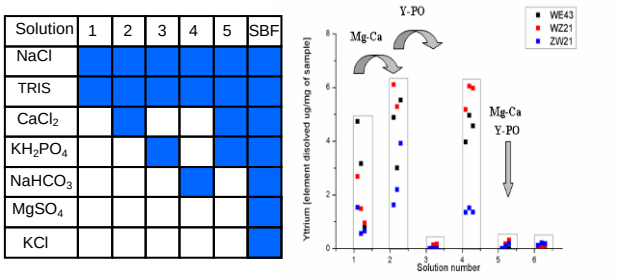

Fig. 1: ICP-OES investigation of WE43, WZ21, ZW21alloy. a) different solutions used b) dissolved yttrium concentration after 1,4 and 7 days.

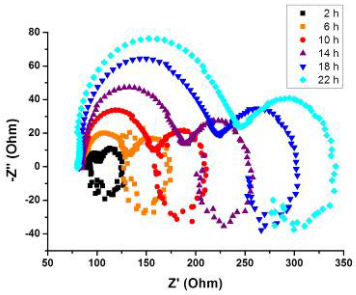

Fig. 2: Time-dependant EIS Nyquist plot for WE43 immersed in TRIS-buffered (pH 7.4) NaCl solution

DISCUSSION & CONCLUSIONS: An important conclusion is that, although fast corrosion rates are measured, the mechanism is a conversion of the metal into calcium-phosphate Y-containing oxide more than a straight dissolution. The largest corrosion rate decrease is found for the SBF and 4% Y containing alloy. A further investigation step should also include interaction with serum, proteins and cells.

REFERENCES: [1] N.C.Quach-Vu, *Comptes Rendus de Chimie*,11(9), *pp. 1043-1055 (2008).* [2] A.C. Hänzi, *Acta Biomaterialia*, 5, *pp.162-171 (2009).*

ACKNOWLEDGEMENTS: The authors thank CCMX MatLife for financial support.

BLOOD COMPATIBILITY OF DLC FILMS

Ali S. Alanazi[1] and Kenji Hirakuri[2]

[1] *King Saud University, Saudi Arabia.* [2] *Tokyo Denki University, Japan.*

INTRODUCTION

Amorphous hydrogenated carbon (a-C:H) films have been expected a surface modification coating to medical appliances [1]. In this study, we focus on the a-C:H film deposition in order to improve biocompatibility of the synthetic vascular graft. It is well known that a-C:H film has been expected to improvement of biocompatibility. However, evaluation of the biocompatibility, which is deposited a-C:H film on a synthetic vascular graft inner-wall, has not been reported enough. The biocompatibility of the a-C:H film coating on synthetic vascular graft inner-wall was investigated for biological response under cell cultures and protein adhesion for biological response.

EXPERIMENTS

i) Film deposition

a-C:H film was deposited on synthetic vascular grafts (ePTFE vascular: φ=16mm, L=60mm, polyester vascular: φ=24 mm, L=60 mm) inner-wall. In the film deposition, r.f. (13.56 MHz) plasma decomposed CH_4 gas at 10 Pa and the r.f. power was kept at 100W. The deposition time was 30 minutes. After the film deposition, structure conditions of the a-C:H films were investigated by an Ar-laser Raman spectrophotometer (Raman) and X-ray photoelectron spectrometer (XPS). The X-ray source was Mg/Kα.

ii) Plasma protein adsorbent test

Investigation of the plasma protein adsorbent was carried out using albumin from human serum, fibrinogen from human plasma, and γ-globulin from human serum. The mixture solution (1mL/1mg) of these plasma protein including 0.1 mol/L phosphate-buffered saline solution (PH=7.4, PBS(−)) were used for the estimation of the protein adsorption on the a-C:H films. The a-C:H film coated ePTFE and polyester vascular grafts (a-C:H/ePTFE and a-C:H/polyester), which were divided to 100 mm^2, was immersed in the mixture solution for 3 hours, respectively. The amount of protein absorbance was determined by using a protein adsorption measurement at a wavelength of 450 nm.

iii) Cell culture

Mouse fibroblasts (NIH 3T3) were grown as a monolayer culture in the Dulbecco's Modified Eagle Medium(D-MEM) that was supplemented with 10% bovine calf serum and antibiotics (penicillin) at 37 °C in an atmosphere of 100% humidity composed of 5% CO_2 and 95% atmosphere. After the preparation of the D-MEM solution and adjusted to a density of 2×10^4 cells/mL, the fibroblast suspensions were seeded onto the a-C:H/ePTFE and a-C:H/polyester inner-wall, which were divided into 100 mm^2, respectively. The fibroblasts were cultured on the samples in each well of a 24-multiwell insert system for 4 days.

RESULTS AND DISCUSSION

i) Film deposition

a-C:H film deposition was carried out by the cylindrical electrode with r.f. plasma CVD technique. In the Raman analysis, Raman spectra of the a-C:H/ePTFE and a-C:H/polyester films were fitted to *D*-peak and *G*-peak, respectively.. However, these peaks were shifted to downside. It is well known that such a Raman shift depends on dc self-bias voltage under film depositions [2]. From the Raman analysis, the a-C:H film was deposited successfully on the synthetic vascular grafts inner-wall.

Additionally, in XPS analysis, it was observed that each synthetic vascular surface condition was changed. The difference in the chemical structure of the surface can be understood by analyzing the carbon (C_{1s}) and fluorine (F_{1s}). The results of XPS analysis indicates that the ePTFE and polyester inner-wall surface was completely covered with the a-C:H film coating, respectively.

ii) Plasma protein adsorbent test

The synthetic vascular graft has the serious problem of the thrombosis. Formation of thrombus depends on the surface of materials conditions. Plasma protein adsorption is incipient reaction of thrombus formation. In the protein absorption, albumin of plasma protein is known to reduce thrombosis, and fibrinogen of plasma protein is an adhesive protein. The fibrinogen enhances the adhesion and activation of thrombus. It was observed that the albumin level of a-C:H film was higher than normal vascular grafts (ePTFE and polyester) or same. On the other hand, the fibrinogen and the globulin level was reduced by a-C:H films. Therefore, a-C:H film deposition is expected to improvement of biocompatibility of synthetic vascular graft such an ePTFE and polyester.

iii) Cell culture

As a result, for the cytocompatibility of the a-C:H film, which was deposited by cylindrical electrode, it was observed that there is no evidence of significant cytotoxicity. It was observed that the a-C:H film deposition onto inner-wall of synthetic vascular grafts (ePTFE and polyester) had a higher level of cell growth than the synthetic vascular grafts. Therefore, the improvement of the cytocompatibility can be expected of a-C:H film deposition onto inner-wall of synthetic vascular grafts.

CONCLUSION

In this study, a-C:H film was deposited on synthetic vascular grafts inner-wall by cylindrical electrode with r.f. plasma CVD technique. The a-C:H films was deposited successfully on inner-wall of synthetic vascular grafts. The success of uniform a-C: film deposition indicates that the a-C:H film coating is applicable to improve cell adhesion and cytocompatibility for biomaterials such as a synthetic vascular grafts.

REFERENCE

[1] WJ. Ma, AJ. Ruys, RS. Mason, PJ. Martin, A. Bendavid, Z. Liu, M. Ionescu, H. Zreiqat, Biomaterials, **28** (2007) 1620.

[2] Y. Taki, and O. Takai, Thin solid films, **316** (1998) 45.

PEEK Substrates for Measurement of Contractile Cell Forces of Primary Cells

Jasmin Althaus[1,2], Uwe Pieles[2], Kirsten Peters[3], and Bert Müller[1]

[1]*Biomaterials Science Center, University of Basel, Switzerland.* [2]*Institute for Chemistry and Bioanalytics, University of Applied Sciences, Northwestern Switzerland.* [3]*Department of Cell Biology (Junior Research Group), University of Rostock, Germany.*

INTRODUCTION: Polyetheretherketone (PEEK) gains increasing interest as biomaterial for traumatologic, orthopaedic and spinal implants.[1] The PEEK-cell interactions should be optimized tailoring chemistry, morphology and rigidity of the substrate. These parameters influence the attached cells, directly observable by their shape and gene regulation.[2] Adherent cells exert contractile forces via their actin cytoskeleton and integrin-mediated focal adhesions. To quantify these contractile cell forces as the function of substrate preparation using cantilever bending is the aim of our project. Starting from commercially available medical grade PEEK, substrate modifications by plasma treatment have been developed. To study cytocompatibility, cell lines (rat-2 and mouse 3T3 fibroblasts) and human primary cells (i.e. dermal microvascular endothelial cells/HDMEC and adipose tissue-derived stem cells/ASC) were exposed to the modified PEEK substrates.

METHODS: Hot embossing of the PEEK foils was performed at the glass transition temperature of 143°C and a pressure of 100 kN. Subsequently, the embossed foils were ammonia or oxygen/argon plasma treated (100 W, 30 sccm), before cell seeding (2 x 10^4 cells/cm^2). ASC were isolated from liposuction-derived adipose tissue, HDMEC from juvenile foreskin. Cell cultivation was under standard conditions (i.e. 37°C, 5% CO_2). Cells were cultured 48 h on the PEEK substrates and subsequently depicted by the fluorescence stainings Calcein-AM (vital stain) and Hoechst 33342 (nuclear stain).

RESULTS: As primary cells are especially relevant in biomaterials research, the effect of plasma treatment on HDMECs and ASCs besides cell lines was studied. Microscopic images of the stained cells, as represented in Fig. 1, indicated that plasma treatments positively influenced cell attachment and proliferation. Plasma treatment induced similar cellular phenotypes as on tissue culture polystyrene (TCPS). Interestingly, the cell lines did not show this effect in the same specificity.

DISCUSSION & CONCLUSIONS: Our still preliminary results demonstrated that primary cells attach and spread appropriately on plasma-treated PEEK substrates. Other substrate modifications, such as micro-grooves fabricated by hot embossing induced cell alignment. Clinically more relevant replicas from sandblasted and acid-etched Ti disks with pre-defined roughness were also produced. Using contractile cell force measurements we are going to take advantage from a physical method to optimize the cell-substrate interactions for future polymeric implants.

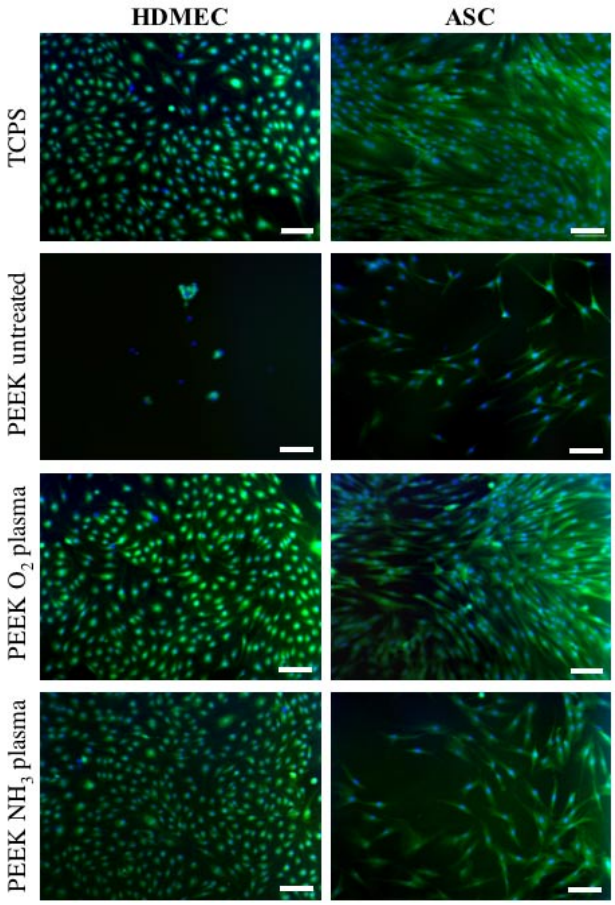

Fig. 1: Primary cells on plasma-treated PEEK and on TCPS, used as reference (green: vital staning with Calcein-AM, blue: nuclei, scale bar: 100 µm)

REFERENCES: [1] S.M. Kurtz and J.N. Devine (2007) *Biomaterials* **28**:4845-69. [2] D.E. Discher et al. (2010) *Journal of Cell Science* **123**: 297-308.

ACKNOWLEDGEMENTS: The presented research activity belongs to the project 'DICANS', a collaborative initiative between the BMC, PSI, FHNW and Concentris GmbH funded by the Swiss Nanoscience Institute at the University of Basel. Further financing was by the EU and the Federal State of Mecklenburg-Vorpommern, Germany.

Compression Tests On Heat-Curing Dental Resins

O. Bolos[1], C. Bortun[2], A. Cernescu[3], A. Bolos[4], L. Szabo[5], S. Gaman[6]

[1,2,4,5,6]*„Victor Babes" University of Medicine and Pharmacy, Timisoara, Romania University School of Dentistry,* [3]*Politehnica University Timişoara, Romania*

INTRODUCTION: Complete dentures′ repairs are frequent at elderly patients. These dentures are made from different acrylic resins, which have different mechanical properties [1,2,3,].

METHODS: 18 pairs of complete dentures were manufactured at Faculty of Dentistry Timisoara, using the classical technology. These were realized on the same model type, from different heat-curing dental resisns: Superacryl, Triplex, Vertex. A group of 6 pairs (2 from each material) were tested directly on the mechanical testing machine LBG 100T, other 6 had as support the plaster model and other 6 were adapted on models with help of silicone (Lastic Xtra, Kettenbach, Germany). The prostheses were tested at compression, until they broke, by applying forces on their occlusal surfaces.

a.

b, *c.*

Fig.1. a. Mechanical testing machine LBG 100T; b, c. Force applying detail

RESULTS: The results emphasized a rapid braking of the prostheses that didn't have any support; slower braking and multiple pieces fracture of plaster model and then that of the prostheses (Fig. 2b). The slowest fracture took place at prostheses adapted on model with help of silicone (Fig. 2a). The braking happened at 2,1 kN, as seen in the graphic below (Fig. 3b- on silicone). Figure 3a (without silicone, directly on model) shows the moment of model braking; by continuing the force application on denture′s occlusal surface, we notice a peak of its deterioration at 2,079 kN. Vertex material had the best behaviour, in all three situations.

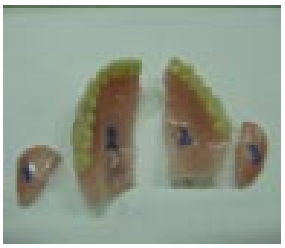

a. *b.*

Fig.2. a, b. Fractured complete denture

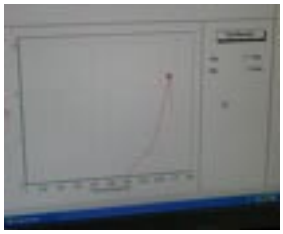

a. *b.*

Fig.3. Compression load diagrams: a. denture is situated directly on model; b. denture is adapted on model with silicone

DISCUSSION & CONCLUSIONS: We can conclude that, by imitating the soft tissue with help of silicone, we are closer to the reality from the mouth. The more intimate adaptation to prosthetic field the prostheses have, the more resistant they are (from the mechanical resistance point of view). In case of using silicone, the compression resistance force was higher and, that way, it happened a slower braking in comparison with the case of applying the denture directly on model, as shown in diagrams above. Also, we observed that, denture′s mechanical beahviour is connected to resin′s properties.

REFERENCES: [1] Diaz-Arnold AM, Vargas MA, Shaull KL, Laffoon JE, Qian F: *Flexural and fatigue strengths of denture base resin***.** J Prosthet Dent. 2008 Jul; 100(1):47-51. [2]D.L., Dixon, K.G. Ekstrand, L.C. Bredding, (1991). *The transverse strengths of three denture base resins.* J. Prosthet. Dent., 66: 510–513. [3] G. Uzun, N. Hersek. (2002 Jul): *Comparison of the fracture resistance of six denture base acrylic resins.* J Biomater. Appl.; 17(1):19-29.

ACKNOWLEDGEMENTS: This study was supported by **Ideas** grant CNCSIS type A, no. 1878/2008 from Ministry of Education and Research of Romania.

Analysis of molecular interactions between focal adhesion proteins talin and vinculin using FRET

A.-K. Born[1], V. Vogel[2], K. Maniura-Weber[1]

[1]*Empa, Material-Biology Interactions, St. Gallen, Switzerland*

[2]*ETH Zürich, Biologically Oriented Materials, Zürich, Switzerland.*

INTRODUCTION: The development of cell based sensors as well as new material concepts for medical applications will be greatly advanced by tools that allow online life monitoring of cellular processes. Cell adhesion and generation of force on the extracellular matrix (ECM) play an important role for cell viability, migration and differentiation[1].
Primary sites of adhesion are formed between integrin receptors and the underlying substratum. Within the cell, integrin receptors bind to a large number of proteins. Binding of talin head to the intracellular integrin domains cause integrin activation followed by accumulation of talin in focal contacts. Talin rod contains up to eleven vinculin binding sites that are buried in its native, un-stretched structure[2].
The recruitment of vinculin to focal adhesions sites is force dependent. Tensile forces that are applied to newly formed adhesion sites cause stretching of the talin rod thereby activating talin's vinculin binding sites. Binding to the talin rod causes vinculin activation. Vinculin containing focal adhesions are capable of exerting migration forces.

Fluorescence resonance energy transfer (FRET) microscopy offers the capability to study the fate and function of biomolecules in living cells[3]. Using CFP and YFP as the donor-acceptor pair for FRET we study the molecular interaction of talin and its binding partner vinculin in focal adhesions. Responses of talin-vinculin interaction to mechanical properties of the underlying substrate are examined by culturing cells on tissue culture plastic (TCP) or collagen-coated polydimethyl-siloxane (PDMS) substrates.

METHODS: For FRET measurements we generated several constructs in which the yellow fluorescent protein is inserted in close proximity to vinculin binding sites of talin rod. As the binding sites for talin are located in the N-terminal vinculin head domain we positioned CFP in front of vinculin. These FRET constructs were used for nucleofection of human fibroblasts.
PDMS substrates with Young's modulus between 1 MPa and 0.1 MPa were prepared by varying the cross linking reagent and coated with collagen to facilitate cell adhesion. Fluorescence localization of FRET constructs was monitored by confocal laser scanning microscopy.

RESULTS: Human fibroblasts transfected with the fluorescently-labelled vinculin or talin showed the expected accumulation of fluorescence signal at focal adhesion sites. The correct localizations of both proteins was confirmed by staining against endogenous talin or vinculin, suggesting that both tagged proteins are correctly synthesized. Cells transfected with a control vector and analysed for FRET by the acceptor depletion method showed that our setup allows FRET determination. Increased FRET signals were observed in pronounced focal adhesion sites of fibroblasts co-transfected with fluorescently tagged talin and vinculin.

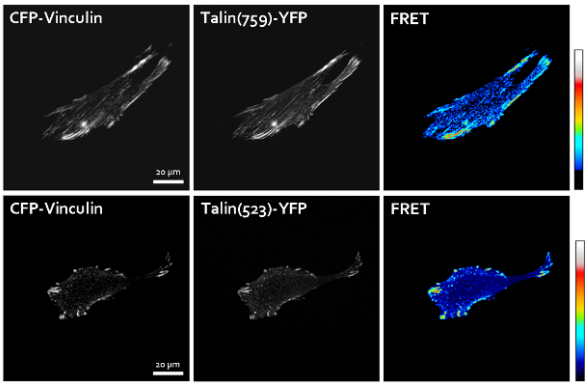

Fig. 1: Fibroblasts co- transfected with fluorescently-tagged vinculin (CFP-vinculin) and talin (Talin-(523 or 759)-YFP). Molecular interaction between vinculin and talin is displayed as intensity image (right) whereas scale ranges from blue (low interaction) to white (high interaction).

DISCUSSION & CONCLUSIONS: Our primary results suggest that transfection of human cells with our fluorescently labelled reporters is efficient and therefore qualified for FRET measurements and determination of interaction between focal adhesion proteins talin and vinculin in cells. The FRET technique allows testing the ability of cells to form adhesion complexes on a material surface and dynamics associated with this process. It has therefore been chosen as the tool of choice to evaluate cell-material interactions at the molecular level and will be of use especially to study substrates with different mechanical properties.

REFERENCES: 1. Watt, F.M., Jordan, P.W., and O'Neill, C.H. *Cell Shape Controls Terminal Differentiation of Human Epidermal Keratinocytes.* Proc Natl Acad Sci USA, 85, 5576, 1988.
2. Gingras, A.R., Ziegler, W.H., Frank, R. Barsukov, I.L., Roberts, G.C.K., Critchley, D.R. and Emsley, J. *Mapping and Consensus Sequence Identification for Multiple Vinculin Binding Sites within the Talin Rod.* JBC, 280, 37217, 2005.
3. Sekar, R.B., and Periasamy, A**.** *Fluorescence resonance energy transfer (FRET) microscopy imaging of live cell protein localizations.* JBC, 160, 629, 2003

ACKNOWLEDGEMENTS: We thank Viola Vogel for stimulating discussion about talin structure and Vesa Hytönen for sharing his ideas for development of talin FRET constructs.
The present study is supported by the European Commission through the specific targeted research project CellForce (Contract N°: NMP4-CT-2005-016626) and CCMX Matlife.

European Cells and Materials Vol. 20. Suppl. 1, 2010 (page 19) ISSN 1473-2262

THE INFLUENCE OF SURFACE TOPOGRAPHY AND CHEMISTRY ON THE BEHAVIOUR OF HUMAN BONE MARROW STROMAL CELLS

C. Brose [1], M. Bitar[1,3], V. Friederici[2], P. Imgrund[2] and A. Bruinink[1]
[1]EMPA Materials Science & Technology, Lerchenfeldstrasse 5, 9014 St. Gallen, Switzerland
[2] IFAM, Bremen, Germany; [3] Current address: Novartis, Basel, Switzerland

.

INTRODUCTION:

For the integration of implants in the human body surface topography plays an important role. Currently, medical implants are fabricated using a multistep procedure including implant manufacturing and surface treatment to obtain nano- and microstructured surfaces. Here an optimised µ-metal injection moulding (µ-MIM) process was used to produce medical grade nanostructured stainless steel. This material is characterised by excellent mechanical properties and the surfaces bear a microarray hemisphere-like protruding structures and a submicrometer surface roughness. The goal of the study was to elucidate the effect of surface roughness and surface microstructuring on human bone marrow stromal cells (HBMC) performance and in how far surface chemistry (stainless steel, titanium) is able to modify this.

METHODS:

Sample preparation: Using the optimised µ-MIM process[1] stainless steel samples bearing microarray hemisphere patterning (hemisphere diameter: 30 or 50 µm; interhemisphere distance: 20 µm; termed 30_20 and 50_20) and plane surfaces all exhibiting a defined sub-µm roughness were prepared. Two different surface roughnesses were prepared by adding different quantity of nanoparticles to the feedstock. Some samples were coated with 50 nm titanium.

Cell culture: HBMC were isolated from femur marrow tissue samples of patients undergoing total hip arthroplasty were maintained until sub-confluence in expansion medium. Cells of the first passage were seeded on the samples using osteogenic medium without dexamethasone.

Effects on cell performance: At day 7 cell cultures were fixed and stained for bone specific alkaline phosphatase, actin, and vinculin. Cell nuclei were stained using BOBO™-1 iodide. Relative mRNA quantity encoding osteocalcin, ALP and collagen-I were assessed after 7 and 14 days in culture. Calcium deposition was estimated after 21 days by Alizarin Red S staining.

RESULTS:

As preliminary data suggest the behaviour of cells was differently affected by stainless steel and titanium treated surfaces. 1) Morphology: On stainless steel cells were stretched between the hemispheres with nearly no contact to the planar area as previously described[2]. On titanium coated steel surfaces, however, cells preferred to be located between the hemispheres (Fig. 1). At high cell density a kind of mesh network of cells around the hemispheres were seen with the highest density of actin fibres centred between the hemispheres. 2) Differentiation: The osteogenic differentiation of HBMC seems to be enhanced on the 30_20 and 50_20 surfaces.

DISCUSSION & CONCLUSIONS:

Preliminary experiments suggest that cell morphology and differentiation were affected by each surface modification.

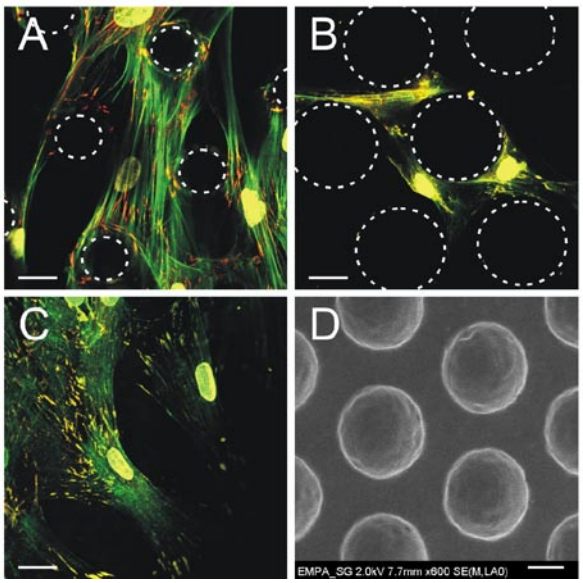

HBMCs cultured for 7 days onto 50_20 surfaces. (A) Stainless steel: Cells were attached to the hemispheres with a limited or no contact to the neighbouring planar surface between the hemispheres. (B) Titanium coated steel: Cells were observed on the plane surface between the hemispheres. (C) Planar titanium coated steel surface: Cells were well-spreaded. (D) SEM picture of the sample. Actin green; focal adhesion plaques red; nuclei yellow; scale bar 20 µm; (A-B) equal magnification, but different level.

REFERENCES:

1: V Friederici et *al.*, Mat. Sci. Eng. (submitted);
2: Bitar et *al.* Biomaterials (submitted)

ACKNOWLEDGEMENTS:

The present project is supported by the VW-Foundation (I/82 297).

Brushite Cement Samples for XRD Phase Analysis Prepared under Simulated Physiological Conditions

N. Döbelin, M. Bohner

RMS Foundation, Bischmattstr. 12, 2544 Bettlach, Switzerland.

INTRODUCTION: Since their discovery in the late 1980s, calcium phosphate-based cements setting to brushite (DCPD, $CaHPO_4 \cdot 2H_2O$) have been thoroughly investigated as an alternative to apatitic and polymeric bone cements, as well as to solid bone void fillers. However, under certain conditions the product of this cement reaction is not brushite but monetite (DCPA, $CaHPO_4$), which can exceed the maximum amount of tolerated impurities. Routine XRD analysis is usually employed to determine the phase composition of cured, dried and milled samples, but the conditions the material is exposed to during sample preparation are vastly different from in-vivo conditions. Especially drying never occurs after injection into a living organism. Drying processes may lead to phase changes never observed in-vivo, such as formation of monetite in brushite cements.

In the present study we propose a test setup allowing to measure XRD data from cement samples without the need for drying, and we compare the effect on formation of monetite with conventionally prepared, dried and milled samples.

METHODS: Brushite cements were prepared from β-TCP, MCPM, and small amounts of $Na_2H_2P_2O_7$ mixed with deionized H_2O. The paste was poured into a ring-shaped sample holder lying on a metal plate. After initial setting the ring was clamped to a plastic disc and immersed in phosphate buffer solution (PBS) at 37 °C, once for 96 hours and once for 24 hours. One surface was covered with the plastic disc, the opposite surface was in open contact with the PBS. Afterwards the ring was removed from the PBS and XRD data was collected on the covered and on the open surface. A control sample was prepared the same way, but instead of immersing in PBS it was left in air at 37 °C for 96 hours. The composition in the bulk was determined by sanding off approximately 1 mm from the covered surface of an incubated sample and measuring in wet condition. In case of the dried control sample the material was crushed and milled. The phase composition was quantified by Rietveld refinement.

RESULTS & DISCUSSION: Refined phase compositions are shown in Tables 1 and 2. β-CPP was an impurity in the β-TCP powder.

The phase compositions in Table 1 show what happened during incubation for 24 hours:

- Dissolved MCPM was washed out from the open surface of the incubated sample, leaving large amounts of unreacted β-TCP.
- The covered surface and the bulk reacted completely.
- The covered surface is an adequate approximation of the bulk composition.

Table 1: Phase compositions (rel. wt-%) 24 hours after mixing, measured at different locations of the same specimen (inc = incubated).

Sample/Surf	DCPD	DCPA	β-TCP	β-CPP
inc/open	67	2	24	7
inc/covered	90	4	< 1	6
inc/bulk	90	4	< 1	5

Table 2 shows the phase composition of the sample incubated for 96 hours on the covered surface versus the bulk composition of the sample dried for 96 hours. Drying caused a change of the phase composition from brushite (DCPD) to monetite (DCPA) far below the dehydration temperature of brushite.

Table 2: Phase compositions 96 hours after mixing, measured on an incubated and a dried specimen (inc = incubated).

Sample/Surf	DCPD	DCPA	β-TCP	β-CPP
inc/covered	90	1	< 1	8
dry/bulk	21	72	< 1	6

CONCLUSIONS: The test setup proposed here is simple and works with most self-setting cements. It can be further optimized to mimic physiological conditions by using different amounts and compositions of incubation solution. The results demonstrate that conventional sample preparation can alter the phase composition. This was effectively eliminated by using the proposed setup. The ring-shaped sample holders also allow to analyze the composition of surfaces in direct contact with surrounding liquid and in the bulk using the same specimen. Furthermore, the sample is not destroyed by sample preparation, which allows multiple data acquisitions on the same specimen.

Influence of Particle Size Distribution on Injectability of CaP-Based Pastes

L. Galea[1], M. Habib[2], G. Baroud[2], M. Bohner[1]

[1] *RMS Foundation, Bettlach, Switzerland.* [2] *Université de Sherbrooke, Sherbrooke, Canada.*

INTRODUCTION: Injectability of suspensions depends among others on particle size, particle size distribution, viscosity of liquid phase, liquid-to-powder ratio (LPR) and inter-particle interactions. The aim of this study was to assess the potential of a reduction of the mean particle size [1,2] via low sintering temperature on the injectability of a suspension. The idea was that reducing the mean particle size decreases the size of the interstices, reducing the flow of the liquid between the particles which improves injectability by reducing phase separation or filter-pressing.

MATERIALS & METHODS: Fine β-TCP powders were prepared using hydroxyapatite (HA) + dicalcium phosphate (DCP) reactive sintering. HA and DCP were mixed in appropriate amount for Ca/P ratios of 1.475 and 1.5, calcined at 850°C, and then wet milled (water) in a planetary mill (1-step sintering). Parts of the powders were further calcined at 850, 900 or 950°C (2-step sintering). A commercial β-TCP powder (Fluka) was also used as a reference powder [1,3].

Particle size and appearance of the powders were observed by SEM. Specific surface area (SSA) was measured using N_2 adsorption and applying the BET model. The crystalline composition was calculated with Rietveld refinement from XRD data sets. Particle size distribution (PSD) was measured using laser diffraction and water as a suspending medium. The plastic limit (PL) of the powders was as well assessed.

Pastes were prepared by mixing each powder with deionised water in a liquid-to-powder ratio (LPR) of 0.40ml/g. Pastes were inserted into 1-mL syringes. The injection was tested through needles with inner diameter of about 0.21mm (n=3). Compression force was applied by a compression testing machine with a displacement speed of 0.4mm/s.

RESULTS & DISCUSSION: The Rietveld refinement of XRD results revealed that all powders contained HA (2-16 wt-%), but no $Ca_2P_2O_7$. One-step sintering and Ca/P ratio of 1.5 led to higher HA content than 2-step sintering and Ca/P ratio of 1.475. SSA varied between synthesis procedures, but without correlation with sintering temperature, Ca/P ratio or sintering step. All in-house produced β-TCP powders had SSA between 5 and 8m^2/g and the commercial β-TCP from Fluka had a SSA of 0.9±0.1m^2/g. No significant difference was found between plastic limits of all powders, including Fluka powder. SEM pictures suggested that the particle size increased with the sintering temperature and decreased with the Ca/P ratio. A 2-step sintering seemed to increase the particle size. PSD measurements confirmed this evolution and revealed trimodal PSD for 1-step sintered powders. 2-step sintering and higher sintering temperature reduced the tri-modal distribution to bi-modal distribution (Figure 1).

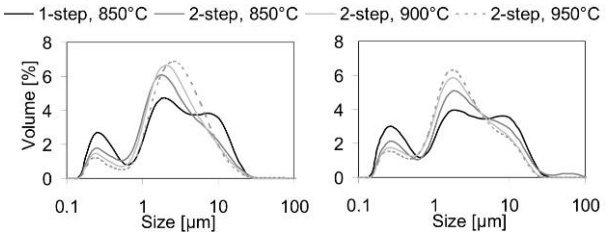

Fig. 1: PSD of the powders with Ca/P=1.475 (left) and 1.5 (right)

Increasing the Ca/P ratio significantly improved the injectability of the pastes (from 27 to 50%), but the sintering temperature did not affect significantly the paste injectability. A 2-step sintering significantly decreased the injectability compared to 1-step sintering (from 57 to 19% for Ca/P=1.475 and from 82 to 45% for Ca/P=1.5).

Fluka β-TCP powder was 31±2% injectable, which is significantly lower than powders produced with a Ca/P ratio of 1.5 or by one-step sintering.

CONCLUSIONS: As expected, decreasing the sintering temperature decreased the particles size, but surprisingly this had no influence on injectability. Increasing the Ca/P ratio reduced the particles size and significantly improved the injectability. The use of a two-step sintering seemed to slightly increase the particle size and decreased injectability. A tri-modal PSD seemed to improve injectability.

REFERENCES: [1] M Bohner, G. Baroud (2005) *Biomaterials* **26**: 1553-1563. [2] U. Gbureck, K. Spatz, R. Thull, J. E. Barralet (2005) *J Biomed Mater Res B Appl Biomater* **73**: 1-6. [3] M. Habib, G. Baroud, F. Gitzhofer, M. Bohner (2010) *Acta Biomaterialia* **6**: 250-256.

Mussel-mimetic sealant for fetal membrane repair

C.M.Haller[1],C.Brubaker[2], J.Egger[3], A.S.Mallik[1], N.Ochsenbein-Kolble[1,4], P.B.Messersmith[2], E.Mazza[3], R.Zimmermann[1,4], M.Ehrbar[1,4], A.H.Zisch[1,4].
Corresponding Author: Claudia.haller@usz.ch
[1] *Deptartment of Obstetrics, University Hospital Zurich, 8091 Zurich, Switzerland.*
[2] *Biomedical Engineering Dept., Northwestern University, Evanston, Illinois, USA.*
[3] *Mechanical Engineering Department, Swiss Federal Institute of Technology Zurich, 8092 Zurich, Switzerland.*
[4]*Task force of the European program for soft tissue engineering for children with birth defects (http://eurostec.tv.nl).*

INTRODUCTION: Premature rupture of the fetal membranes is a devastating complication of pregnancy. Medical invasions into the intrauterine cavity for diagnostic or surgical interventions carry a significant risk for persisting membrane leakage and subsequent rupture - which seriously limits the developing field of fetal surgery. The effort goes to take action *before* membrane rupture rather than react *after* obvious or symptomatic rupture.

METHODS: Our direction of research concerns preventive plugging of fetoscopic access sites in fetal membranes at the time of intervention to inhibit leakage and rupture. We introduce a novel biomechanical test device that permits to test closure of fetal membrane under close to physiological conditions. A new type of poly(ethylene glycol)-based hydrogel, mussel-mimetic tissue adhesive, showed efficient, non-disruptive, non-toxic bonding to fetal membranes in previous studies [1]. This mussel-mimetic tissue adhesive was used to seal membrane defects of up to 3.3mm. Biomechanical stretching tested the integrity of the sealant and its efficiency for possible in-vivo applications.

RESULTS: Leak-proof repair that withstood membrane stretch in an ex vivo model were successfully accomplished using the synthetic hydrogel-type mussel-mimetic tissue adhesive.

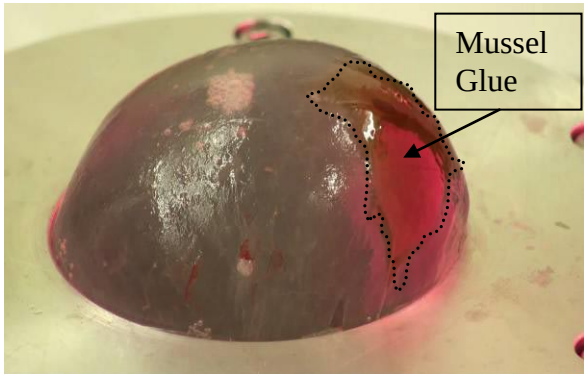

Fig. 1: Mussel-Glue-sealed fetal membranes clamped and stretched on the novel inflation device.

DISCUSSION & CONCLUSIONS: We present a new potential sealing modality for iatrogenic membrane defects that merits further evaluation in vivo.

REFERENCES: [1]Bilic G, et al (2008), Injectible candidate sealants for fetal membrane repair: Bonding and toxicity ex vivo. *American Journal of Obstetrics and Gynecology*, in press.

ACKNOWLEDGEMENTS: This work was supported by the Swiss National Science Foundation grant no. 31000-108270;
by the European Commission in its 6th Framework Programme ('EuroSTEC' (European program for soft tissue engineering for children (http://eurostec.tv.nl); LIFESCIHEALTH-2006-37409); and the Zurich Centre for Integrative Human Physiology. Portions of this work were supported by National Institues of Health (NIH, USA) grant DE014193 to P.B.M. C.B. was supported by a NIH Regenerative Medicine training grant (5 T90 DA022881).

COMPARISON OF SURFACE TOPOGRAPHY OF BONE RESORPTION PITS AND STRUCTURED TITANIUM SURFACES

T. Hefti[1,2], *M. Frischherz*[1]; *H. Hall*[1], *F. Schlottig*[2], *N. D. Spencer*[1].
[1] ETH Zürich, Zürich, Switzerland; [2] Thommen Medical AG, Waldenburg, Switzerland

INTRODUCTION: It is crucial to understand the bone remodelling process in order to potentially improve the interface between an implant and its surrounding bone tissue. In the remodelling process mineralized bone is dissolved by osteoclasts and subsequently rebuilt through the deposition of osteoblasts. The mineral phase (CaP) and the organic phase (mainly collagen type I) of bone are dissolved and digested by osteoclasts. Osteoclasts leave behind traces of resorbed bone called resorption pits or trails. For osseointegration surface topography of the implant is of critical importance for clinical success. Rough surfaces proved to achieve better mechanical anchorage in bone and higher bone to implant contact (BIC)[1].
The aim of this study is to compare the surface structures of osteoclastic resorption pits on bone with surface features of clinically tested and experimental titanium surfaces.

METHODS: A RAW 264.7 mouse macrophage cell line was seeded on bone slices, RANKL (Receptor Activator for Nuclear Factor κ B Ligand) was added (50 ng/ml) to initiate differentiation into osteoclast cells. After 14 days of cultivation cells were removed from the bone by ultrasonication in ammonia, samples were then critical point dried.
Titanium surfaces were either sandblasted and hot acid etched or only hot acid-etched.
Substrates were subsequently analyzed by SEM and stereo SEM where the region of interest was imaged from two angles differing by 10°. With the help of MeX software (Alicona) the images were converted into 3D data and the profiles of resorption pits and the topographical features of the titanium surfaces respectively were calculated.

RESULTS: After 14 days of cultivation resorption pits produced by osteoclasts were found distributed over the entire bone surface. These resorption pits could be identified as areas where the mineral phase of the bone (calcium phosphate) was locally dissolved and where partly resorbed collagen fibres were exposed (Fig. 1 top).
The sandblasted and hot acid-etched titanium surfaces showed a micro-roughness originating from sandblasting overlaid with submicron roughness originating from etching whereas the hot- etched only titanium surface showed only the submicron roughness.
The dimensions of resorption pits and surface features of the etched only titanium surface were similar with a length of 5-25 µm and a depth of 0.5-4 µm whereas the sandblasted and acid-etched surface exhibited features with a depth of 5-12 µm and a length of 10-50 µm.

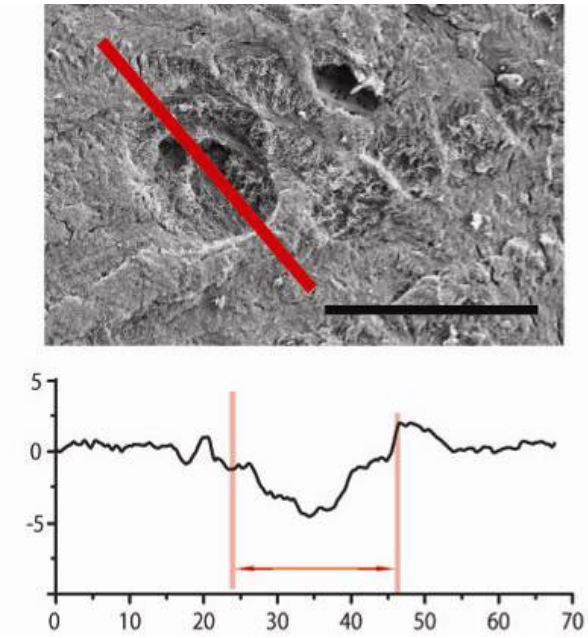

Fig. 1: Osteoclastic resorption pits (top) (scale bar 50 µm). The redline indicates the position of the corresponding height profile (bottom).

DISCUSSION & CONCLUSIONS: Both titanium surfaces and the bone surface showed similar surface features with respect to the length. The depth of natural resorption pits and clinically successful sandblasted and etched titanium surfaces was different. The titanium surfaces demonstrated significantly deeper structures. These quantifications and comparison of osteoclast resorption pits and surface features of titanium surfaces may give some hints for production of more biomimetic surfaces for optimal osteoblast attachment. This could finally lead to new insights for the improvement of currently used implant surfaces.

REFERENCES: [1] Ferguson SJ. et al. (2008), Int J Oral Maxillofac Implants, 23(6),1037-46

ACKNOWLEDGEMENTS: Thommen Medical for a scientific fellowship for TH.

SINGLE WALLED CARBON NANOTUBES AFFECT CELL PHYSIOLOGY OF EPITHELIAL CELLS

J.-P. Kaiser, X. Maeder, H.F. Krug and P. Wick

Materials-Biology Interactions Laboratory, Swiss Federal Institute for Materials Testing and Research (Empa), CH-9014 St Gallen, Switzerland

Introduction: Particle in the nanoscale range and among them the single walled carbon nanotubes (SWCNT) possess new chemical, physical and electrical properties, which differ from the properties of the bulk material. Therefore these materials were already used in various industrial applications. Despite all precautions CNT may come in contact with organisms and may be taken up by them (Helland et al., 2007, Kaiser et al., 2009). Since knowledge about impact of single walled CNT (SWCNT) on cell physiology is still rare, we investigated in this study effects of SWCNT on cell physiology of human epithelial cells (A549). For this purpose the influence of SWCNT (purified SWCNT and SWCNT raw material) on cell parameters such as cell viability, cytoskeleton organization, apoptosis, cell migration and cell adhesion had been investigated.

Materials and Methods: Cell physiology was assessed using human lung epithelial cells (A549). Cell number (cell viability) was estimated by counting the cells using a Neubaur cell chamber. Cytoskeleton organization was analyzed by staining of the cell components, such as actin, vinculin and nuclei with fluorescent dyes and thereafter microscopically analyzed. Apoptosis/necrosis was quantitatively investigated by FACS analysis. Cell migration analysis was carried out as previously described (Kaiser et al., 2006). The effect of SWCNT on cell adhesion was estimated by comparing the centrifugal force necessary to detach cells from a control culture as well as cells from cultures exposed to SWCNT.

Results and Discussion: Epithelial cell cultures grown in presence of up to 30 µg/ml purified SWCNT showed a negligible reduced cell viability compared to the untreated control culture. SWCNT raw material affected cell viability in a higher manner, than a similar concentration of purified SWCNT. Exposure of epithelial cells to purified SWCNT and SWCNT raw material (15 µg/ml and 30 µg/ml) had no notable effect on programmed cell death (apoptosis). Regarding cell migration the velocity of epithelial cells were not affected by 15 µg/ml purified SWCNT, but cell velocity was slightly decreased, when cells were incubated in presence of the same concentration of SWCNT raw material. Cell parameters such as cell viability, cell activity, cell spreading, cytoskeleton organization and cell adhesion are correlated to each other. Integrins (transmembrane proteins) mediate the binding of the actin cytoskeleton to the extra-cellular matrix via their extra-cellular domains. The adhesion strength is dependent from a variety of factors, such as the interconnections between cytoskeleton elements, the quantity, size and kind of the focal adhesions and the quantity of integrins connected to the surface and the characteristics of the substratum. Cell adhesion of epithelial cells had been estimated in this study by measuring the centrifugal force necessary to detach the cells from the surface. Cells, which were incubated in presence of SWCNT showed a weaker adherence than cells in the control cultures without treatment. A possible explanation for the observed reduction in cell adhesion is the reduction of integrins interacting with the substratum. Possible explanations are that the SWCNT were affecting area and arrangement of focal adhesion points, and in addition SWCNT might weaken the adhesion by binding to the integrins. Integrins, which bind to the SWCNT won't be able to bind in a similar way to the underlying surface.

Conclusion: The effect on cell physiology were dependent from SWCNT suspension (purified SWCNT or SWCNT raw material), SWCNT concentration and incubation time. Purified SWCNT affected only cell adhesion, whereas SWCNT raw material (30 µg/ml) affected cell adhesion, cell viability, and to a minor extend cell spreading and cytoskeleton organization. Other cell parameters such as apoptosis and cell migration were not severely affected.

References

J.-P. Kaiser, et al (2006) *Biomaterials* **27**: 5230-5241.

A. Helland, et al (2007) Environ. Health Perspect. **115**: 1125-1131.

J.-P. Kaiser, et al., (2009) Nanomedicine **4**: 57-63.

qPCR as a screening method to investigate the influence of surface features and soluble factors in matters of Osteoblast differentiation for hMSCs

P. Kleiner[1], J. Branch[2], J. Bushman[2], J. Kohn[2], R. Burgkart[1]

[1] *Klinikum rechts der Isar, TU München, München, Germany.* [2] *New Jersey Center for Biomaterials, Piscataway, NJ, USA.*

INTRODUCTION: We are interested to understand better how surface properties in combination with soluble factors influence the cell fate of human mesenchymal stem cells (hMSCs). This issue is important in materials research to improve surfaces for medical applications. Therefore we used quantitative real-time PCR (qPCR) to validate gene expression associated with differentiation. This method is a commonly used, however also an expensive screening method to investigate the differentiation process. The following genes were chosen for our experiments: GAPDH as housekeeping gene, Runx-2 and alkaline phosphatase (ALP) to check the differentiation towards osteogenic cells. Runx2 and ALP are specific markers and classified as early indicators of osteogenic differentiation.[1,2]

METHODS: The hMSCs (passage 2) were seeded at a density of 10.000 per well in a 96 well plate and incubated in basal media. We tested six different polymers that were solvent cast into wells of a 96 well plate for high through-put screenings (produced within Prof. Kohn's lab). The control surfaces were tissue culturing plastic and poly lactic acid (PLLA). 24 hours after plating, the media was changed to osteogenic media for half of the wells while the other half were left in MSC basal media. The media was replaced every two days. After seven days the RNA was purified by SV 96 Total RNA Isolation System from Promega. In the next step we generated cDNA from the RNA by using the QuantiTect Reverse Transcription Kit from Qiagen. With this cDNA real-time PCR (LightCycler 480 from Roche) was performed for GAPDH, Runx-2 and ALP. We calculated the ΔCp values by normalizing to the GAPDH reference[3] and further standardized the data to the value on PLLA.

RESULTS: In basal media a clear increase of expression can be seen on no surface for Runx-2 or ALP (data not shown). In contrast, a decrease appears on two surfaces (P1 and TC), all other values are between 90% and 105% in comparison to the PLLA surface.

Fig. 1 illustrates the expression level of the two genes in osteogenic media. On three surfaces (P1, P6 and TC) the gene Runx-2 is decreased, whereas on two surfaces (P2 and P5) the expression is raised. The gene expression on the remaining surfaces is equivalent to the PLLA control. For ALP the increase of gene expression is considerable on four surfaces (P2, P3, P4 and P5) and on the other polymers the levels are similar to the reference on PLLA.

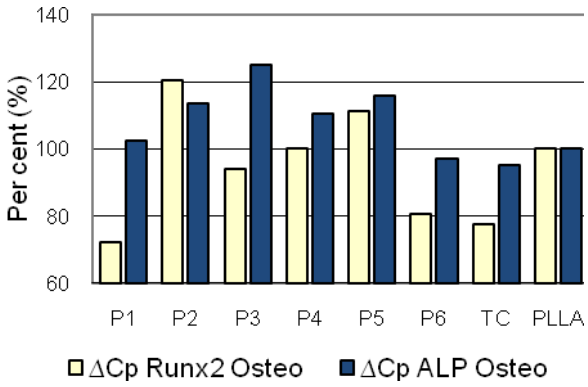

Fig. 1: ΔCp values of Runx-2 and ALP in osteogenic media normalized to PLLA

DISCUSSION & CONCLUSIONS: We can summarize that on some surfaces (P2, P3, P4 and P5) the ALP expression in osteogenic media is increased, two of these surfaces (P2 and P5) also show elevated Runx-2 expression in this media. Hence the cells produce osteoblast specific markers and start to differentiate into osteogenic cells. In basal media we cannot detect any clear raising neither for ALP nor Runx-2 expression; therefore we assume negligible osteoblast differentiation. We have shown that the media as well as the surface have a significant influence on the cell fate. In further experiments we will focus on the investigation of the surface features that cause these differences in the differentiation.

REFERENCES: [1]A. Schoolmeeters et al (2009) *PloS One* **4**, e5605. [2] G. Karsenty, (2001) *Endocrinology* **142**:2731-33. [3] M.W. Pfaffl, (2001), *Quantification strategies in real-time PCR in A-Z of Quantitative PCR* (eds. S.A. Bustin) Academic Press, pp 87-112

ACKNOWLEDGEMENTS: This work was supported by RESBIO (Integrated Technology Resource for Polymeric Biomaterials) funded by National Institutes of Health (NIBIB and NCMHD) under grant P41 EB001046 and the International Graduate School for Science and Engineering, TU München.

Contractile Cell Forces on Rigid Substrates

Jochen Köser[1], Uwe Pieles[1], and Bert Müller[2]

[1] *University of Applied Sciences Muttenz, Switzerland.* [2] *Biomaterials Science Center, University of Basel, Switzerland.*

INTRODUCTION: In recent years biomechanical parameters have been evolved as crucial factors for the determination and characterization of cell fate, e.g. for the differentiation of stem cells or the malignant transformation in cancerogenous cells.[1,2] Several methods to evaluate the contractile forces, which cells exert on the underlying substrate, have been developed since the early 1980s. These methods, however, rely on the significant deformation of the substrate and are thus suitable to mimic cell biomechanics on softer substrates. Here, we present results from an approach to determine cell forces on stiff substrates using nanomechanical cantilever sensors that is much more relevant for load bearing implants and cell culture dishes. The technique allows for the quantification of cell forces generated on different substrates and can thus be applied to characterize cell-materials interactions in many biomedical applications, aiding e.g. the development of implant surfaces and investigate fundamental cell characteristics.

METHODS: For the cell force determination cells were cultured on nanomechanical cantilever sensor arrays 500 µm long, 100 µm wide and 1 µm thick, which allow for the detection of forces as small as 10^{-5} N/m. Following adhesion and contractile force generation the cantilever sensors are transferred to the Cantisens Research system (Concentris GmbH, Switzerland) to monitor changes in cantilever bending upon trypsin-mediated release of the cells from the substrate as shown in *Fig. 1*.

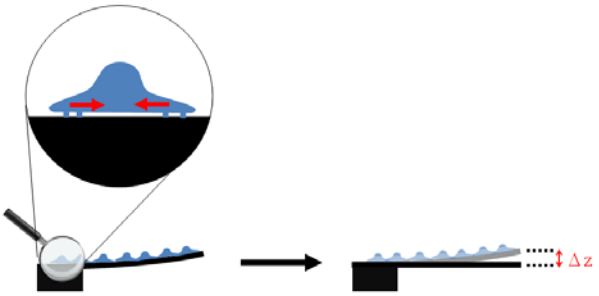

Fig. 1: Principle of the cantilever-based cell force quantification.

RESULTS: For the establishment of the cell force determination standard cultured cell lines where used. When rat2 fibroblasts are seeded on cantilevers they adhere and develop a morphology indistinguishable from that on a standard culture dish. Upon release of the cells from the sensor surface the cantilever relax with an amplitude correlating to the release of contractile cell forces (*Fig. 2*).

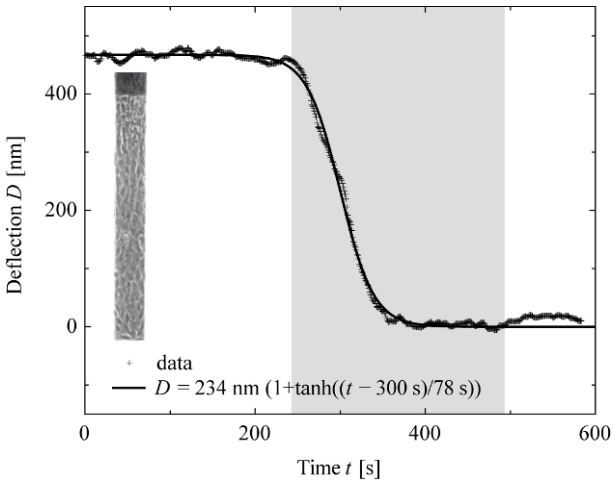

Fig. 2: Cantilever bending signal during the release (grey shaded area) of cells from the substrate.

The release kinetics can be perfectly described using the following empirically determined function:

$$\Delta z = 0.5 z_0 \, (1\text{-}\tanh((t\text{-}t_0)/\tau))$$

where z_0 corresponds to the deflection amplitude, τ denotes the time constant and t_0 relates to the start of experiment.

DISCUSSION & CONCLUSIONS: This communication deals with a method which allows the determination of contractile cell forces on different kinds of rigid substrates with materials properties similar to the ones used for implants and standard cell culture dishes. By modifying the cantilever geometry both single cell measurements and the quantification of forces in organized cell layers become feasible. We expect this method aids to the understanding of fundamental aspects of cell-materials interactions with important implications for future implant design.

REFERENCES: [1] Engler et al. (2006), *Cell* **126**, 677-689. [2] Cross et al. (2007), *Nature Nanotechnology* **2**, 780-783.

ACKNOWLEDGEMENT: These research activities belong to the project 'DICANS', a collaborative initiative between BMC, PSI, FHNW and Concentris GmbH funded by the Swiss Nanoscience Institute of the University of Basel.

Antibacterial yet still cytocompatible plasma nanocomposite coatings by controlled Ag^+ release properties

E. Körner, D. Hegemann

Empa, Swiss Federal Laboratories for Materials Testing and Research, Lerchenfeldstrasse 5, 9014 St. Gallen / Switzerland.

INTRODUCTION: Specifically in the medical sector, new materials are often investigated regarding their antibacterial or cell adhesion promoting properties. Bacterial colonization is a complex process and different strategies, e.g. biopassive, bioactive or release systems are used to prevent the colonization. Silver (Ag) is an efficacious and useful antibacterial agent. Small amounts of Ag (nano-scale) already show antibacterial properties. It is important to develop antibacterial products that contain an optimal amount of Ag for specific applications, which helps to save resources and to avoid (cytotoxic) overdoses.

METHODS: Functional hydrocarbon plasma polymer coatings with embedded Ag particles were deposited using an asymmetric RF plasma reactor at low pressure (10 Pa)[1]. The plasma polymer is produced with a reactive gas/monomer mixture of CO_2/C_2H_4. Ar was added in order to sputter Ag atoms from the Ag cathode and form nanoparticles in the growing polymer matrix. The influence of the gas ratio and different power inputs were investigated at constant pressure. The Ag content is quantified with ICP-OES and compared with the XPS surface analysis. The quantity of the Ag^+ ion release is determined for the different conditions in bi-distilled water with ICP-OES. Bacterial assays were performed with gram- and gram+ bacteria. The cytocompatibility of the coatings was tested with 3T3 mouse fibroblasts and compared to the antibacterial effectiveness.

RESULTS & DISCUSSION: The matrix functionality is an important element in the design of the coating showing a clear dependence on the CO_2 ratio in the process gas. An increase of the CO_2 ratio leads to a higher incorporation of oxygen functionalities. The Ag content of the coatings was found to be adjustable by power input and gas ratio[2]. An increasing Ag content of the coatings consequentially yields a higher Ag release over a timescale of 14 days. Differently growing sections of the particle distribution could be classified in different sections with TEM measurements. The particle size can be controlled by CO_2 addition and power input (Fig. 1).

The coatings exhibit an excellent effectiveness against the gram- bacteria. Although these coatings show the lowest Ag concentration and thus smallest Ag release within the examined range, no bacterial surface contamination could be observed. A higher amount of Ag, on the other hand, was found to be required for the gram+ bacteria. The coatings with a Ag content lower than 0.1 g/cm^3 were found to be cytocompatible.

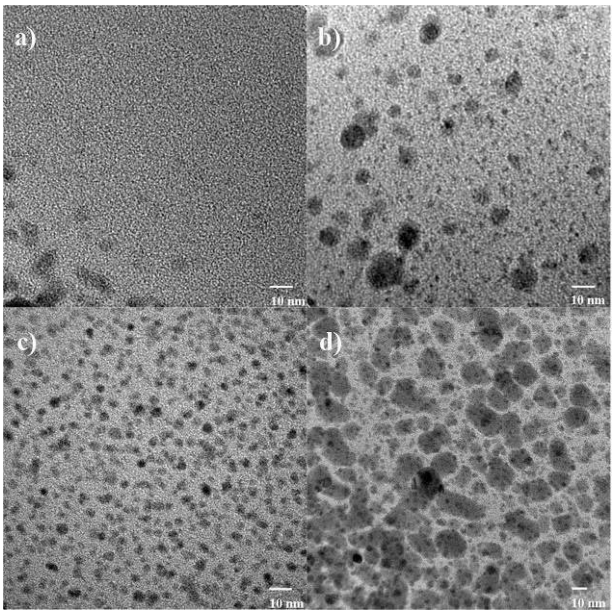

Fig. 1: Ag nanoparticle distribution for coatings prepared with various gas ratios and power inputs of a) CO_2/C_2H_4 2:1 – 50 W, b) 4:1 – 50 W, c) 6:1 – 50 W and d) 6:1 – 100 W

CONCLUSIONS: Plasma technology was found to be a versatile tool to produce and design effective antibacterial and cytocompatible coatings which can be adjusted for various applications.

REFERENCES: [1] E. Körner, G. Fortunato, D. Hegemann, *Plasma Process. Polym.* **2009**, *6*, 119-25 [2] E. Körner, M.H. Aguirre, G. Fortunato, A. Ritter, J. Rühe D. Hegemann, *Plasma Process. Polym.* **2010**, in press.

ACKNOWLEDGEMENTS: This work is part of the EU-funded project EmbekI "Development and analysis of polymer based multifunctional bactericidal materials", grant #211436 of the seventh framework program.

Microstructured Open-Porous Ceramic Scaffolds for Orthopedic Tissue Engineering

F.Krauss Juillerat[1], UT.Gonzenbach[1], C.Scaletta[2], S.Gerber-Lemaire[3], LA.Applegate[2], L.Juillerat-Jeanneret[2], LJ.Gauckler[1]

[1] ETH Zurich, Zurich, Switzerland, [2] CHUV, Lausanne, Switzerland,

[3]EPF Lausanne, Lausanne, Switzerland.

INTRODUCTION: Bone substitute materials suitable for the development of a vascular system are needed for the repair of large bone defects. In this feasibility study, the potential of permanent foam scaffolds made from an alumina-calcium aluminate composite to host cells of different types, and the influence of the material composition and microstructure on the cell behavior and biocompatibility was studied.

METHODS: Particle-stabilized ceramic foams were produced from alumina particles and calcium aluminate cement and their microstructure analyzed as described in [1-3]. Different human derived cells were tested on the scaffolds, namely a human endothelial cell line (HCEC), two commercially available human osteosarcoma cell lines (U_2Os and SaOs) and primary human fetal osteoblasts derived from the femoral bone [3]. *In scaffold* [^{3}H]-thymidine tests, MTT assays, AlamarBlue tests and SEM observations were performed to verify the biocompatibility of the foam scaffolds [3].

RESULTS: Ceramic foams were produced showing different pore sizes, porosities and permeabilities [2]. Upon setting and sintering (heat treatment) the foam scaffolds could easily be machined into the desired shapes as shown in Fig. 1. Human fetal osteoblasts, osteosarcoma cells and endothelial cells attached to the scaffolds within 24 hours of incubation and colonized the porous material for up to 6 days. *In scaffold* determination of cell attachment, cell metabolic activity and cell proliferation proved the good acceptance of the cells to the newly developed material (Fig. 2). The different microstructures of the scaffolds influenced the migratory potential of the cells, permitting either localized or widespread colonization of the scaffolds [3].

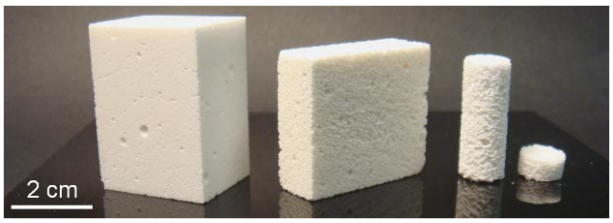

Fig. 1: Ceramic scaffolds with different microstructures machined into the desired shapes.

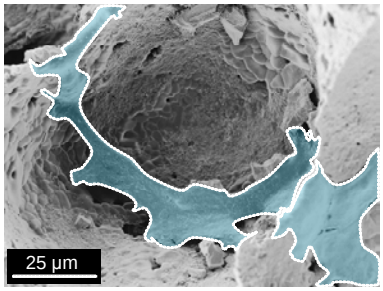

Fig. 2: SEM micrograph of an osteosarcoma cell (U2Os) cultured during 4 days inside a foam pore.

DISCUSSION & CONCLUSIONS: These results demonstrate the biocompatibility and non-toxicity of such scaffolds and provide a proof of concept for their potential as permanent implants. This information gives important indications for the development of optimized scaffold materials for large bone defect repair allowing the development of a functional vascularization and colonization with bone-derived cells, a prerequisite for the bone healing process.

REFERENCES: [1] UT. Gonzenbach et al (2006) *Angewandte Chemie-International Edition* **45** (21):3526-3530. [2] F. Krauss Juillerat et al (2010) *J Am Ceram Soc* **to be submitted**. [3] F. Krauss Juillerat et al (2010) *Mater Lett* **submitted**.

ACKNOWLEDGEMENTS: We would like to thank J. Maillardet, C. Chappuis-Bernasconi and P. Elser for the excellent technical assistance. This work is supported by the Swiss National Research Foundation (grant CR23I2-124753/1), the Sandoz Family Foundation and Foundation S.A.N.T.E.

Measuring corrosion resistance of metallic alloys in the oral cavity

Josef-Michel Kutschy[1], Fredy Schmidli[1], Markus Jungo[1], and Bert Müller[1,2]

[1]*Materials Science Institute, School of Dental Medicine, University of Basel, Switzerland.*
[2]*Biomaterials Science Center, University of Basel, Switzerland.*

INTRODUCTION: Metallic alloys are widely used materials in dentistry. Common dental metallic alloys are classified as high or reduced gold, Co-based, Ni-based, or Pd-Ag alloys, all characterized by a high degree of mechanical stability and elasticity. One of their main disadvantages, however, is the limited corrosion resistance, especially if more than one metal was incorporated in the patient's oral cavity. Therefore, many patients complain of taste irritations, metal taste, tongue burning, dry mouth, pain or irritation of the mucous membrane. These phenomena are often the result of metal ions released from the applied alloys during corrosion. Therefore, it is highly desirable to establish an objective tool for the *in vivo* measurement of corrosion resistance, as the recently introduced ec-pen.[1,2] The thin electrodes allow for electrochemical measurements directly at different locations within the oral cavity of the patient, which finally allow identifying the ion-releasing parts of the applied dental metals. The dentist together with the affected patient can search for more appropriate dental treatments that avoid the release of trouble-generating metal ions.

MATERIALS AND METHODS: The present study is based on the ec-pen that contains two electrodes as sensing heads shown in Fig. 1. Pushing the white-gray coloured tip towards the metal part of interest such as a crown (see Fig. 1), electrolyte is emitted to wet the surface and form electrical contact. This simple and fast procedure allows measuring the corrosion resistance within an area of about 2 mm^2. The present investigation comprises 26 patients, who received a crown or dentures and, subsequently, have complained of one or more of the symptoms mentioned above. The examined dental materials include alloys with high and reduced gold content as well as cobalt-based alloys exclusively from well-established suppliers as verified by means of energy-dispersive X-ray fluorescence analysis (EDX).

RESULTS: The ec-pen serves for impedance measurements to determine the corrosion potential. The visual inspection permits the discrimination between different levels of corrosion, which might be classified according to three levels: below detection limit, perceptible, and major corrosion. In more than 40% of the patients, corrosion was explicitly detected. In these cases, the measured impedance resistance was definitely well below 200 Ωcm^{-2}. Comparing the visual inspection with the ec-pen experiments, we have found a strong correlation. Impedance resistance values below 150 Ωcm^{-2} correspond to major corrosion, data between 150 Ωcm^{-2} and 250 Ωcm^{-2} can be associated with a perceptible level of corrosion, and an impedance resistance measurement with results above 250 Ωcm^{-2} does not exhibit any detectable corrosion on the metallic parts.

DISCUSSION & CONCLUSIONS: The results apply for the average values. Unfortunately, an individual experiment can lead to mis-interpretations. Therefore, several data are necessary to be acquired and faults cannot be entirely excluded. There exist numerous reasons that help to explain such problems. Firstly, the composition of saliva is patient-specific. Secondly, there is some minor variation in the chemical composition and microstructure of the dental alloys from the different suppliers. Thirdly, the handling of the ec-pen can become difficult for smaller metallic parts, which can be even covered by non-conducting ceramics or polymers. Finally, metals are frequently soldered, which can induce strong corrosion and can be identified performing EDX-measurements on fragments.

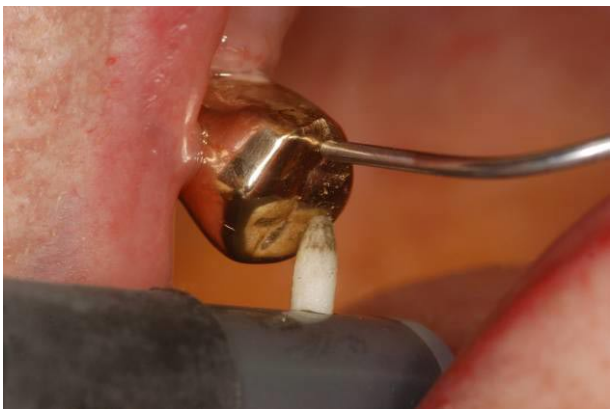

Fig. 1: Placement of the ec-pen electrodes on the crown.

REFERENCES:

[1] F. Schmidli, M. Jungo, K. Jäger, H. Lüthy and M. Büchler (2009) *Schweiz. Monatsschr. Zahnmed.* **119**:584–588.
[2] F. Schmidli, M. Büchler, M. Jungo, and B. Müller (2008) *Eur. Cells Mater.* **16**:52.
[3] M. Jungo, F. Schmidli, and B. Müller (2009) *Wissen Kompakt* **3**:3-13.

Silver Releasing Hydroxyapatite Coatings for Implant Application

S.Lischer[1], C.R. Bradbury[2], B.Wampfler[1], Q.Ren[1], Ph.Gruner[3], K.Maniura[1]

[1] Empa, Swiss Federal Laboratories for Materials Testing & Research, Lerchenfeldstr. 5, CH-9014 St. Gallen, [2] Empa, Feuerwerkerstr. 39, CH-3602 Thun, [3] Medicoat AG, Gewerbe Nord, CH-5506 Mägenwil

INTRODUCTION: Biomaterials releasing silver are of high interest as more and more bacteria develop resistance to antibiotics. After an implant surgery there is always a competition between tissue integration and bacterial colonization. Bacterial infections have dramatical consequences for the patient and cause high medical costs especially if the implant has to be removed. The incidence of infections for total hip and knee arthroplasties is around 1% to 3% [1]. Therefore, it would be highly desirable that biomaterials used for implants promote tissue integration and provide antibacterial properties in parallel. A common feature in implant technology is the surface modification, especially the application of hydroxyapaptite (HA) which is known to promote osseointegration. The additional integration of silver particles into the HA coating creates an antibacterial coating due to release of silver ions.

Fig 1: Implant coating by VPS process

METHODS: HA coatings containing silver were produced by vacuum plasma spraying (VPS) by Medicoat and Empa Thun. X-ray diffraction was used to determine the crystallinity and the composition of the coatings. The coatings were subjected to adhesion tests according to ISO 13779. Release of silver was measured by ICP-OES. The antibacterial activity of the coatings was analyzed by standard agar diffusion test as well as biofilm formation on the coating with two bacteria strains *S. aureus* (Gram-positive) and *P. aeruginosa* (Gram-negative). The cytotoxicity assay is based on the ISO-10993-5 *biological evaluation of medical devices* and quantified by MTT and DNA assay. Bone cell compatibility was determined by direct cell seeding of primary human bone cells onto the coatings. To determine cell proliferation, cells were monitored by immunohistochemical staining and SEM imaging or harvested off the sample and counted.

RESULTS: HA coatings with a range of crystallinity and different concentrations of silver could be produced by VPS technology. Material properties were shown to be in line with regulations as investigated in adhesion tests and measurements of crystallinity. XRD analysis showed that no foreign phases (TTCP, TCP or CaO) occur during the spraying process. Silver is released at a high rate in the first 24 hours of exposition and decreases continuously within 4 days to a constant value. The silver release is dependent on the coating thickness, the thicker the coating, the higher the release. Coatings with high concentrations of Ag exhibited antibacterial properties to *S. aureus* and *P. aeruginosa* whereas low concentrations of Ag showed no antibacterial effect. The results of the cytotoxicity showed that HA coatings with and without silver are biocompatible to primary human bone cells. Direct cell seeding experiments showed that there is no clear correlation between the degree of crystallinity and cell proliferation. Furthermore, it was seen that cells do not cover the coatings homogeneously. SEM analysis showed an alteration of the HA surface in the culture media over the incubation time.

DISCUSSION & CONCLUSIONS: Implants with an antibacterial HA coating might have the potential to significantly reduce the incidence of bacterial infections in orthopaedic surgery. In this project silver containing HA coatings could be produced in a reproducible way. The coatings exhibit antibacterial properties and are cytocompatible. Direct cell seeding experiments showed that the cell cultivation on HA coatings is a complex issue. The fact that the coating surface underwent alterations during the incubation time leaves many parameters open and calls for further investigations.

REFERENCES: Harris W, Sledge CB (1990) Total hip and total knee replacement *Part II. N Engl J Med*, 323:801-807

ACKNOWLEDGEMENTS: The commission for Technology “CTI Medtech” is acknowledged for financial support of the project under the contract 9071.1PFLS-LS.

3D Porous Casein – loaded Hydrogels. Calcification Induction

A.Lungu[1], D.M.Dragusin[1], I.C.Stancu[1], C.Tucureanu[2], A.Salageanu[2], D.S.Vasilescu[1], H.Iovu[1]

[1] Polytechnics University Bucharest, Romania. [2] Cantacuzino National Institute for Research and Development on Microbiology and Immunology, Bucharest, Romania.

INTRODUCTION: 3D models mimicking the trabecular bone microarchitecture and the chemical functionalities of the mineralization regulating bone proteins seem to be a successful approach towards bone regeneration. In this context, casein has been used as phosphorylated protein and its influence on the morphology of the matrix and on the induction of biomimetic mineralization has been explored when immobilized in porous poly(2-hydroxylethyl methacrylate) (PHEMA).

METHODS: Casein has been solubilised with 0.1M sodium hydroxide (to a pH of 9). Then, the so formed solution was added to the mixture of monomer containing 3% ethyleneglycol dimethacrylate (EGDMA – used as crosslinker). The ammonium persulphate, the polymerisation initiator has been added dissolved in distilled water. The mixture has been homogenized under stirring, degassed and then polymerized in polymerization tubes for 6 hours at 60^{o}C, followed by a post-polymerization treatment at 90^{o}C. Control PHEMA has been synthesized in the presence of distilled water. Sodium azide (0.1% with respect to casein) has been used to prevent bacterial growth on protein containing samples. Different loadings have been realized in hydrogels prepared with 40, 50 and 60% distilled water (v/v). All scaffolds have been purified through extraction with fresh distilled water using a Soxhlet extractor. Then the hydrogels have been freeze dried. Swelling tests in aqueous solution have been performed. The samples' morphology and porosity has been studied using scanning electron (SEM) and optical microscopy. Mineralization has been explored based on the method developed by Prof. Kokubo; briefly, the samples have been incubated for 14 days, at 37^{o}C, in an acellular solution with ionic composition nearly equal to that of human plasma; the solution has been refreshed every two days. The cytotoxicity has been evaluated through in contact test using the cellular line L929 of murine fibroblasts.

RESULTS: The presence of the protein has been confirmed through infrared spectroscopy; specific amide I and amide II absorptions have distinguished as protein diagnose peaks on the PHEMA spectrum. Casein immobilization in the hydrogel has been associated with important morphological changes when compared to control samples.

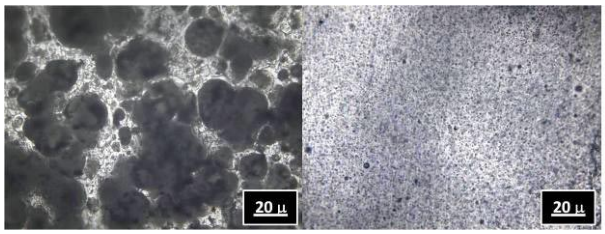

Fig. 1: Microscopic appearance of the Casein-loaded hydrogel (left) vs. non-loaded hydrogel (right).

Phase segregation has been observed and the morphological differencies between the protein-containing samples and the corresponding control are evident as displayed in Figure 1. Although the polymerization mixture containing solubilised casein was homogeneous, two phases are present in the final hybrid material; studies are on going to confirm the presumed hydrophilic PHEMA and more hydrophobic casein domains. The different water content in the polymerization mixtures has lead to different 3D organization of the hydrogels. The mineralization in synthetic human plasma seemed to be favoured both by the hydrophilic PHEMA as well as by the 3D structure and casein presence. The cytotoxicity results have indicated that the materials are suitable for implantation purposes.

DISCUSSION & CONCLUSIONS: The hybrid hydrogels seem promising scaffolds for bone sunstitution and regeneration. Further researches on the biomechanical performances and on the biomineralization potential are ongoing.

ACKNOWLEDGEMENTS: The National Authority for Scientific Research from The Ministry of Education, Research and Youth of Romania is gratefully acknowledged for the financial support through the exploratory project "Polymeric Biomaterials For Bone Repair. Biomimetism Through Nanostructured Surface", PN-II-ID-2008-2, number 729/2009.

Alginate-Poly(ethylene glycol) Hybrid Microspheres for Immobilization and Delivery: Synthesis and Physical Properties

R. Mahou, C. Wandrey

Laboratoire de Médecine Régénérative et de Pharmacobiologie (LMRP)

École Polytechnique Fédérale de Lausanne (EPFL) Station 15, 1015 Lausanne, Suisse

INTRODUCTION: Microspheres, beads and capsules, mainly composed of alginate (alg) have advantages but also drawbacks such as low mechanical stability, limited durability and insufficient adjustability of the permeability. Commonly used coating or reinforcement with polycations has a negative impact on the biocompatibility. The approach in this study is to combine ionotropic gelation of alg and covalent cross-linking of poly(ethylene glycol) (PEG) derivatives and to design a process which yields hybrid alginate-PEG microspheres (Alg-PEG-M) and after liquefaction of the calcium-alginate network (Ca-alg) spherical PEG microspheres (PEG-M).

METHODS: Alg-PEG-M and PEG-M were prepared at 37°C under physiological conditions employing a coaxial airflow droplet generator (Fig.1)

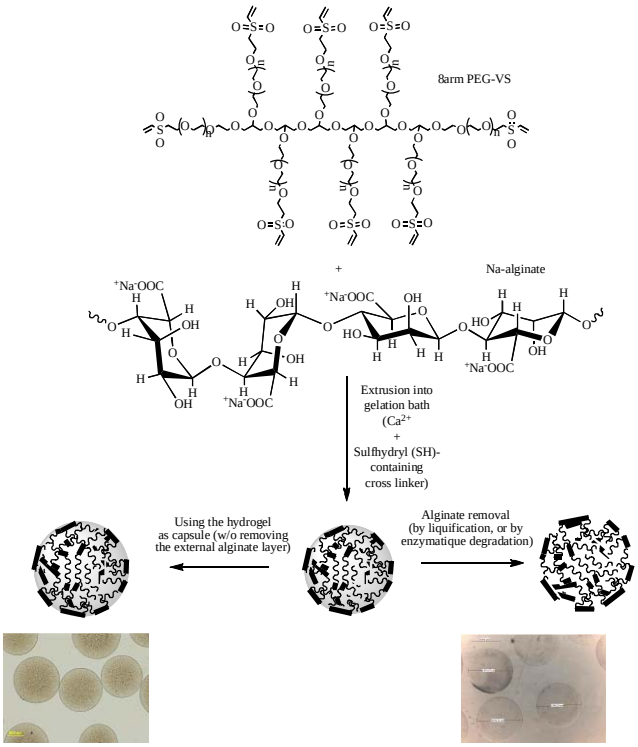

Fig. 1: Formation process. Both Alg-PEG-M (left) and PEG-M (right) were obtained spherical and uniform.

RESULTS: The diameter of the microspheres was tuneable modifying the process conditions such as airflow, syringe diameter, or the extrusion rate.

Minimal degree of swelling and maximal mechanical resistance of Alg-PEG-M were obtained for the molar ratio thiol/VS=2.75 (Fig. 2).

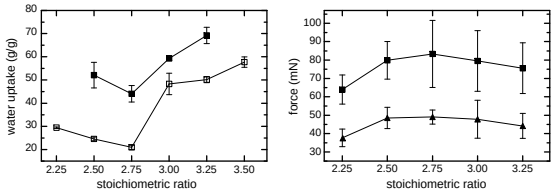

Fig. 2: Swelling (left) and mechanical resistance (right) of Alg-PEG-M as a function of the molar ratio thiol/VS.

For Alg-PEG-M prepared from the same PEG precursor, the initial precursor concentration influenced swelling and mechanical resistance (Fig.3). Increasing the concentration of PEG-VS creates a denser and more rigid network. The dissolution of Ca-alg slightly raised the resistance to compression.

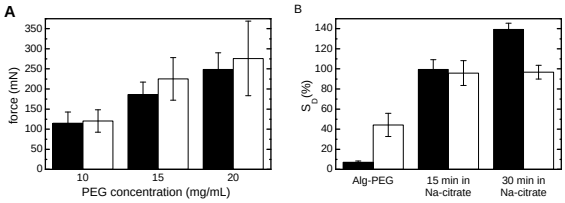

Fig. 3: (A) Mechanical resistance to 80% compression for different initial PEG-VS concentrations (■) before and (□) after Ca-alg liquefaction. (B) Swelling degree of Alg-PEG-M in water (■) and in PBS (□) after gradual dissolution of Ca-alg.

The permeability of the hydrogels could be tailored by adequate choice of the arm length of PEG-VS. The MWCO was identified in the range between 70 and 150 kg/mol.

CONCLUSIONS: A new type of hydrogel microspheres was synthesised. Important physical properties are obtainable in a range requested for biomedical and pharmaceutical applications.

REFERENCES: R. Mahou, C. Wandrey (2010). Macromolecules 43(3):1371-1378.

ACKNOWLEDGEMENT: We thank the SNF, Grant 205321-116397/1, COST 865 /STSM, and Dr. I. Lacik, Polymer Institute Bratislava.

A New Design for 3D Loading of Cells Using Controlled Alginate Gelation

Rami F. Mhanna, Philippe Schlink, Janos Vörös and Marcy Zenobi-Wong

Institute for Biomedical Engineering, Laboratory of Biosensors and Bioelectronics, ETH Zurich, Switzerland

INTRODUCTION: Chondrocytes have been shown to dedifferentiate when cultured in monolayers. Culturing chondrocytes in 3D environments help maintaining their chondrogenic phenotype [Benya, 1982]. Furthermore, the application of certain kinds of mechanical loads can increase the synthesis of extracellular matrix proteins. In this study we designed a new method to apply 3D loads to cells embedded in an alginate gel. The alginate was polymerized using an internal gelation process [Kuo, 2001] which, under load, deforms much more uniformly than conventionally polymerized alginate.

METHODS: 1% or 1.5% alginate gels were polymerized using CaCl2 gelation, or a $CaCO_3$-GDL (D-(+)-glucono-δ-lactone) system where the molar ration of CaCO3 to GDL was 0.5 to obtain a neutral pH in the alginate. The STREX device (ST-140-10, B-Bridge International) was used to apply loads to the gels. STREX PDMS chambers were modified with a series of support ridges to hold the alginate gels during load (Figure 1). The homogeneity of the applied loads was assessed by measuring the displacement of 10-30um glass beads before and after load. Bovine chondrocytes isolated from 6 month old calves were used to assess the ability of the gel to prevent dedifferentiation and enhance chondrogenic activity. Real-time quantitative PCR was used to quantify genetic expression of chondrocyte specific genes such as Sox9, aggrecan, collagen2 and others. Light microscopy was used to evaluate the viability and phenotype of embedded cells.

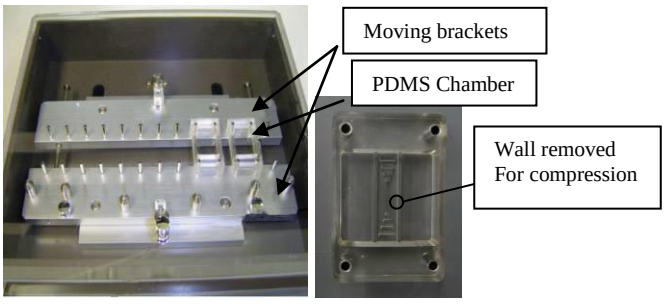

Fig. 1: STREX stretching device (left) design for 3D application of load (right).

RESULTS:

The strain distribution was found to be homogeneous throughout the gel (Figure 2).

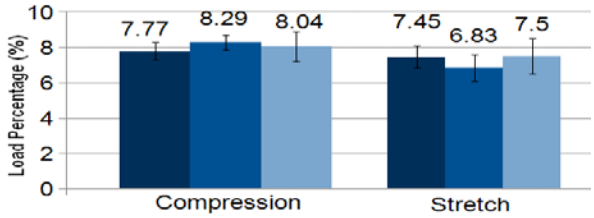

Fig. 2: Measurements of the load in different parts of 1.5% alginate gels using CaCO3-GDL gelling system for compression and tension, (n=3)

Collagen2 was upregulated 5-folds and SOX9 was upregulated 10-folds in the CaCO3-GDL system compared to the CaCl2 gelation system at 1% alginate concentration. For the 1.5% Alginate concentration, a slight upregulation of SOX9 was observed for the CaCO3-GDL system over the CaCl2 system while collagen2 gene expression was not affected.

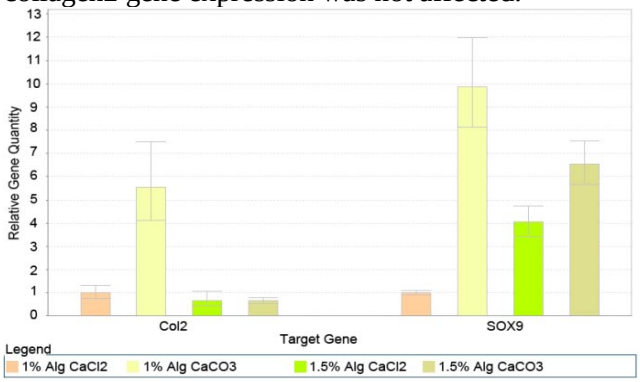

Fig. 3: Gene expression of type 2 collagen and Sox9 for the two gelation systems for 1% and 1.5% alginate concentrations.

Conclusions

The proposed system can be used for culturing and loading chondrocytes and might be superior to conventionally $CaCl_2$ gelled alginate.

Acknowledgements

The work was funded by a Marie Heim-Vögtlin grant No. PMPDP2_122997 from the Swiss National Science Foundation and the European Grant No: 229292.

References:

Benya, P.D., Shaffer, J.D; Dedifferentiated chondrocytes reexpress the differentiated collagen phenotype when cultured in agarose. Cell 30 (1982) 215–224.

K. Kuo, Peter X. Ma; Ionically crosslinked alginate hydrogels as scaffold for tissue engineering: Part 1. Structure, gelation rate and mechanical properties. Biomaterial 22 (2001) 511-521.

Comparison of two cell culture set-up for identification of optimal textile scaffold regarding cell response

M. Moczulska[1,2], M. Bitar[2], W. Święszkowski[1], A. Bruinink[2]

[1] *Faculty of Materials Science of Engineering, Warsaw University of Technology, Warsaw, Poland*
[2] *MaTisMed, Materials-Biology Interactions Lab EMPA – Swiss Laboratory of Material Testing and Research, St. Gallen, Switzerland*

INTRODUCTION: Scaffolds are designed to be temporary structure providing cells a framework and guiding structure. They are used for *in vitro* and *in vivo* tissue engineering [1]. Textile based scaffolds have the advantage of having defined porosity and structural elements (fibres). So far it is still unclear how the scaffold structure influence cell behaviour. The few existing reports mention that at least the fibre diameter is able to greatly affect cell migration and cell shape [2, 3].The aim of the present study is to identify optimal textile scaffold characteristics regarding the biological response. For this we investigated the influence *in vitro* of surface chemistry, fibre diameter and interfibre mesh spaces of woven textile scaffolds on the behaviour of primary adult human osteoblasts and dermal fibroblasts. The biological effects were characterised using a common test-set-up measuring total number and percentage of proliferating cells seeded as single cells on the scaffold. Furthermore, a new test set-up was developed mimicking the *in vivo* situation more appropriate, i.e. by placing cell reaggregates onto the scaffolds and assessing the areacell outgrowth.

METHODS: *Samples:* Five types of plasma cleaned woven fabrics were used for this study. Two fabrics were made of polyethylene terephthalat (PET) and three of polyamide 6.6 PA (Sefar, CH). The fabrics varied regarding fibres diameters (42-45 versed 77-86μm) and distance between fibres (100-105 versed 200μm). *Cell culture:* Primary normal human dermal fibroblasts (NHDF) were purchased from Cambrex and primary adult human bone cells (HBC) were obtained by cultivating trabecular bone pieces from patients receiving hip prosthesis. *Cell proliferation:* Single cells were seeded onto the nets. The culture flasks were kept for 24 hours on the gyratory shaker to obtain a homogeneous cell distribution. In the following 7 days cells were cultured under static conditions. The proliferating cells were labelled by adding BrdU 24 hours before immunostaining on day 1, 4 and 7. The cells were additionally stained with DAPI to visualize the nuclei of all cells. The BrdU positive and negative cells were counted using a fluorescent microscope. *Cell spreading:* Cell reaggregates were prepared by gyratory shaking of cell suspensions for three days under cell culture conditions. Single reaggregates were seeded onto the scaffolds and kept under cell culture conditions for 10 days. Cell outgrowth was examined every day. The area was measured using Motic Images Plus 2.0 software. The cell outgrowth was expressed as a percentage of the projected area of the reaggregate on the first day of culture.

RESULTS & DISCUSSION: We could show that HBC and NHDF could attach, proliferate on the PET and PA fabrics with various diameters and distance between fibres. In comparison to the common test set-up, the new test set-up (measuring the cell outgrowth area starting from a cell reaggregate seeded on the scaffold) was detecting differences in scaffold characteristics with greater sensitivity. Only with this new set-up we were able to distinguish between the biological effects of two different fibre diameters (42-45 with 77μm) and surface chemistries (PET and PA), with the PET fabric with 42 fibre diameter being of the evaluated materials significantly the best scaffold in promoting cell performance.

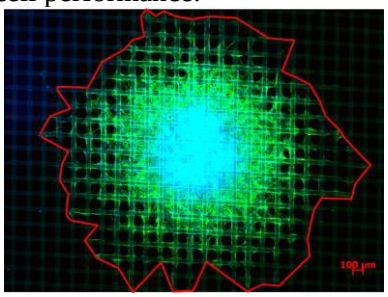

Fig. 1: Fluorescence images of reaggregate cultured of NHDF on net fabrics PET 42/105 after 7 days in culture (green: F-Actin, blue: DAPI stained). Red line: the outgrowth area

REFERENCES: [1]Hutmacher D.W. (2000) Biomaterials **21**(24): 2529-2543, [2]Sanders J. E., Lamont S. E., et al. (2005) Biomaterials **26**(7): 813-818, [3]Sun T., Norton D., et al. (2007) Biotechnol Bioeng. **97**(5): 1318-1328

ACKNOWLEDGEMENTS: The work is supported by The Faculty of Materials Science & Engineering, WUT and Empa-Poland PhD School.

BIOACTIVE ROOT CANAL FILLING MATERIALS

D. Mohn[1], M. Zehnder[2], C. Bruhin[1], T. Imfeld[2], W.J. Stark[1]

[1] *Department of Chemistry and Applied Biosciences, ETH Zurich, 8093 Zurich, Switzerland*
[2] *Department of Preventive Dentistry, Periodontology, and Cariology, University of Zurich, Center of Dental Medicine, 8032 Zurich, Switzerland*

INTRODUCTION: In the age of biomaterials it is somewhat surprising that dentists, especially endodontists, still relate on ancient materials and concepts to fill a root canal. Up to now a successful filling includes a bioinert core material and a sealer that is normally irritating tissue. Recent publications have challenged this concept by using phosphate based glasses as composite fillers [1] for the core material. The here presented work describes the incorporation of bioactive glass into a polymeric matrix for an improved root canal filling. The inorganic filler component served as active material using the bioactivity of the nanoparticulate glass particles to provide a seal without the use of an extra sealer.

METHODS: Bioactive glass (BG) nanoparticles were produced by flame-spray synthesis [2] and combined with polyisoprene (PI) or polycaprolactone (PCL) via solvent casting in different weight ratios [3]. The surface morphology of as prepared composites was investigated with a scanning electron microscope (SEM) and the water contact angle was measured to determine the wettability. In vitro bioactivity tests were carried out using simulated body fluid (SBF) and analyzed with SEM and X-ray diffraction. Dye penetration in standardized and filled root canal training blocks was tested during 2 days against commercial samples which contained PI and PCL as matrix, respectively.

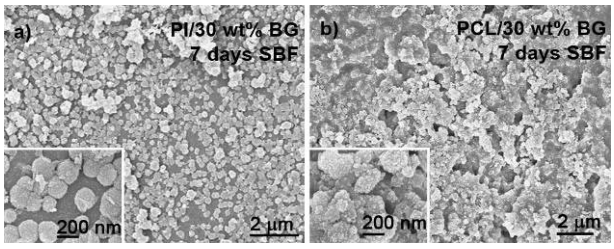

Figure 1: SEM images of PI/30 wt% BG (a) and PCL/30 wt% BG (b) composite samples after immersion in SBF for 7 days showing hydroxyapatite growth.

RESULTS: The water contact angle of PCL composites decreased with increasing amount of bioactive glass nanoparticles while for PI samples hardly any change could be observed. SEM images corroborated these findings due to the absence of a nanostructured surface topography of PI samples. However, both composite systems showed hydroxyapatite growth (Figure 1). Dye penetration revealed that commercial PI samples had the highest leakage while adding BG to the pure polymer prevented leakage completely (Figure 2).

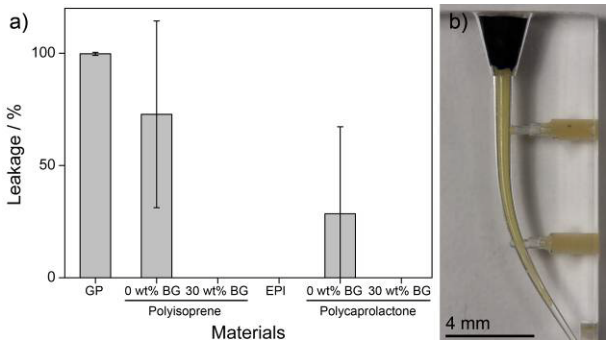

Figure 2: a) Leakage of root canals filled with commercial samples (GP: Gutta-Percha and EPI: Epiphany) and the corresponding composite. b) Filled root canal with PI/30 wt% BG and the dye on top.

DISCUSSION & CONCLUSIONS: Although the incorporation of BG nanoparticles showed no nanoparticle exposure at the surface of PI composite systems, these composites showed a faster hydroxyapatite growth after immersion in SBF than PCL composites. The faster growing was clearly visible on SEM images (Figure 1). Furthermore, both composite systems with BG prevented dye leakage completely. A possible explanation could be the absorption of dye and rapid expansion of the particles and thus a marginal adaptation to the canal wall. Incorporation of bioactive glass fillers in polyisoprene and polycaprolactone made the resulting nanocomposite materials bioactive and improved their immediate sealing ability.

REFERENCES: [1] A. Alani, J.C. Knowles et al. (2009) *Dent. Mater.* **25**:400-10. [2] T.J. Brunner, R.N. Grass et al. (2006) *Chem. Commun.* **13**:1384-86. [3] D. Mohn, C. Bruhin et al. (2010) *submitted*.

ACKNOWLEDGEMENTS: Financial support by the Department of Preventive Dentistry, University Zurich is kindly acknowledged.

In vitro biocompatibility of synthetic mussel adhesive peptides

Y. Morán[1], B. Saldamli[1,2], V. Hoffmann[1], M. Kozielec[3], K. Rischka[3], R.Sader[1]

[1] *Clinic for Oral Cranio- Maxillofacial and Facial Plastic Surgery, Frankfurt*
[2] *Clinic of Orthopaedics and Traumatology, Technical University Munich, Munich*
[3] *Fraunhofer Institute for Manufacturing Technology and Applied Materials Research (IFAM), Bremen.*

INTRODUCTION: Due to its strong underwater adhesion, the byssus plaque of the common blue mussel *Mytilus edilus* has attracted scientific and commercial attention. Studies with purified mussel adhesive proteins have pointed to the potential use of Mytilus edilus foot protein-1 (Mefp-1) as an adhesive for soft tissues, however with certain limitations for clinical use [1]. On the other hand, the commercially available biocompatible recombinant Mefp-1 adhesive does not exert comparable strength to the natural protein [2]. Molecular biomimetitcs is an alternative approach to obtain synthetic mussel adhesive proteins. In previous studies hybrid systems containing Mefp-1 decapeptides and polyethylene glycol have shown good adhesive and cohesive properties [3]. Aim of this study was to investigate the biocompatibility of synthetically produced Mefp-based peptides *in vitro*.

METHODS: The synthetic mussel peptides pMefp-1, pMefp-1-Hema and Mal-pMefp-1 were produced by solid-phased peptide synthesis at IFAM, Bremen. The biocompatibility was assessed according to the ISO 10993-5 for testing biomaterials. L929 mouse fibroblasts (DSMZ) were inoculated in 96-well plates (BD Falcon) at a density of 1×10^4 cells/well and cultured in DMEM with 10 % FCS at 37 C˚, 5% CO_2. The aqueous peptide solutions were sterilized by filtration (0.2 µm pore size) and supplemented to the cell cultures at final concentration of 0.05% [w/w]. For the positive control 0.1% Triton®X-100 was added to the cell culture. Cells cultured without any additive served as a negative control. After 24 h cell viability was measured using the WST-1 reagent. Three independent test runs were performed in triplicate. Graphs and statistical analysis were made with GraphPad Prism® and analyzed with the Bonferroni multiple comparison tests.

RESULTS: The addition of the synthetic peptides pMefp-1, pMefp-1-Hema and Mal-pMefp-1 at the concentration 0.05% to the cell culture medium resulted in a slight decrease of the cell viability. No significant difference was found between the three pMefp-1 variants. Furthermore there was no neither of the pMefp-1 showed statistically significant difference when compared to the negative control ($p>0.05$).

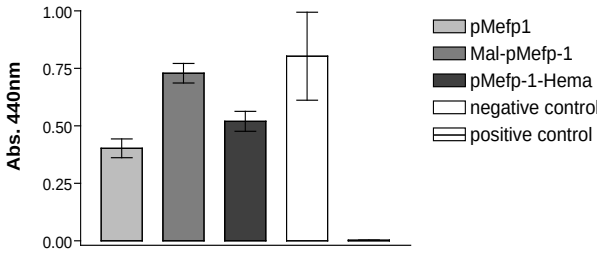

Fig. 1: Viability of L929 cells measured by the WST-1 assay after 24 h exposure to synthetic mussel adhesive peptides. (Mean values of 3 independent experiments).

DISCUSSION & CONCLUSIONS: Hybrid systems containing Mefp-1 based peptides in combination with synthetic polymers, synthesized at Fraunhofer IFAM by solid-phase peptide synthesis, have displayed improved tensile and shear strength compared with pure acrylate systems [4]. In this study the synthetic mussel peptides pMefp-1, pMefp-1-Hema and Mal-pMefp-1 exhibited good biocompatibility. These peptides as a Mefp1-based hybrid polymer followed by further functionalization offer new perspectives for the production of soft tissue adhesives. Such biomimetic inspired adhesives are especially interesting for dental implantology, where the soft tissue seal around implants is still a problematic issue.

REFERENCES: [1] L. Ninan, J. Monahan, R. L. Stroshine, et al (2003) *Biomaterials* **24**:4091–4099. [2] G.H. Silvermann and F.F. Roberto (2007) *Mar Biotechnol* **9(6)**:661-81. [3] B.P. Lee, J.L. Dalsin, B.P. Messerschmith (2002) *Biomacromolecules* **3(5):**1038-47. [4] I. Grunwald, K. Rischka, S. M. Kast, et al (2009) *Phil. Trans. R. Soc*. **367**:1727-47.

ACKNOWLEDGEMENTS: Financial support by the BMBF under grant DLR 01EZ0843 is kindly acknowledged.

Inhibition of Dentin Biodegradation Using Biologically Active Compounds and TiF_4

M. Özcan [1], M. Dundar[2], E. Comlekoglu[2]

[1] University of Zurich, Clinic for Fixed and Removable Prosthodontics and Dental Materials Science Dental Materials Unit, Zurich, Switzerland. [2] Ege University, Department of Prosthodontics, Izmir, Turkey.

INTRODUCTION: Dental profession is becoming minimal invasive with the use of adhesive promoters. However, biodegradation occurs over time especially in the hybrid layer due to denaturation of the denuded and unfilled collagen fibers under or inside the hybrid layer by the host-deriven proteinase enzymes, matrix metalloproteinases such as MMP-2 and MMP-9 and water. Caffeic acid phenethyl ester (CAPE) is a biologically active ingredient of propolis known with its antioxidant, anti-inflammatory, and carcinostatic activites [1] and Titanium tetrafluoride (TiF4) reduces demineralization of dental hard tissues [2]. The objectives of this study were a) to evaluate the effect of CAPE and/or TiF_4 on the microtensile bond strength (MTBS) of three adhesive cements based on 4-META, MDP and Bis-GMA and b) to assess nanolakage patterns at the adhesive interface.

METHODS: Eighty-four (N=84) human third molars stored in %0.1 thymol-saturated isotonic saline at 4°C, were randomly divided into 3 groups. Three adhesive cements with different curing modes were adhered onto the prepared dentin (n=28 per group). Each cement group was further randomly divided into 4 subgroups of surface treatments: TiF_4 (n=7), CAPE (n=7), TiF_4+CAPE (n=7). Non-conditioned teeth per luting cement group acted as control (n=7). Ceramic blocks (8x8x6 mm) were adhered onto the prepared dentin surfaces. The specimens were then thermocycled (x1500, 5-55^{o}C, 20 s). Each tooth was sectioned perpendicular to its longitudinal axis under water-cooling and beams (1x1 mm) were obtained for the MTBS test (1 mm/min). Failure modes were evaluated under light microscope (x40) and SEM and nanoleakage under TEM.

RESULTS: The effect of cement type on MTBS (MPa) was significant with Bis-GMA and 4-META presenting higher values (15.7±3.4, 14.9±3.9, respectively) than that of MDP (10.5±3.2) ($p<0.05$) (ANOVA, Tukey`s test). For all cement groups, the MTBS values of the experimental chemical agent groups (CAPE: 12.9±2.2 and TiF4: 12.9±3.8, respectively) were lower than those of the control groups. Interaction terms between dentin treatment and luting resin were significant ($p<0.05$). The failure mode were mainly mixed (cohesive and adhesive) for Bis-GMA (21/36) and 4-META (17/36). While TiF_4 treatment alone could not prevent nanoleakage at the hybrid layer, nanolakage patterns were significantly improved with the use of CAPE. Combined use of TiF_4+CAPE was less effective.

DISCUSSION & CONCLUSIONS: The experimental chemical agent based on CAPE may have potential use in adhesive promoters for minimal invasive dentistry.

REFERENCES: [1]Jin UH, Chung TW, Kang SK, Suh SJ, Kim JK, Chung KH, Gu YH, Suzuki I, Kim CH (2005) Caffeic acid phenyl ester in propolis is a strong inhibitor of matrix metalloproteinase-9 and invasion inhibitor: Isolation and identification. *Clin Chim Acta* **362**:57-64. [2]Schlueter N, Ganns C, Mueller U, Klimek J (2007) Effect of titanium tetrafluoride and sodium fluoride on erosion progression in enamel and dentine in vitro. *Caries Res* **41:**141-45.

ACKNOWLEDGEMENTS: Part of this study was granted by European Federation for Conservative Dentistry in 2009.

Ceramic Granules Coated with Fibrin Sealant as a Scaffold for Perfusion Bioreactor in Bone Tissue Engineering

E. Piccinini[1], D. Wendt[1], A. Scherberich[1], I. Martin[1]

[1]Institute for Surgical Research & Hospital Management, University Hospital Basel, Basel, Switzerland

INTRODUCTION: The need for cellularized osteogenic grafts that could induce or accelerate bone regeneration is often conflicting with the heterogeneity of shape, volume and position of the bone defects. Although this hurdle could be overcome by using granulated ceramic materials as fillers, the difficulties of seeding and expanding bone marrow derived human mesenchymal stromal cells (BMSC) on small size granules were so far a challenge for bone tissue engineering approaches. Reasoning that a fiber network may promote a better cell retention on ceramic surfaces and in the gaps between the granules, this study aimed at assessing the feasibility of manufacturing osteogenic grafts with enhanced cell retention efficacy by seeding and culturing BMSC on ceramic granules coated with lyophilized fibrin sealant Tisseel® in an active perfusion bioreactor system.

METHODS: TricOS® ceramic granules (60% Hydroxyapatite (HA) and 40 % beta Tricalcium phosphate (β-TCP), dimensions 1-2 mm) were placed in a cylindrical basket (2cm^3), covered with Tisseel® fibrin glue, and then lyophilized by Baxter AG (Vienna, Austria). The basket was then loaded into the perfusion bioreactor. Subsequently, a suspension with 120 millions of freshly isolated bone marrow nucleated cells, containing approximately 15.000 CFU-f, was injected into the bioreactor and cultured in α-MEM supplemented with dexamethasone, ascorbic acid and FGF-2. Medium change was performed twice a week. After 19 days of *in vitro* culture, the basket was extracted, divided in fractions and assayed for viable cells distribution (MTT), Scanning Electron Microscopy (SEM) and histological stainings such as Hematoxylin and Eosin (HE) or Van Gieson (VG). Scaffold portions were implanted subcutaneously in nude mice for 8 weeks, and assayed histologically for bone formation after explantation.

RESULTS: After 19 days in vitro, viable cells densely populated the scaffold as assessed by MTT staining (*Fig.1a*). Stained cells were located directly on the granules and also in the fibrin sealant between the granules. Scaffold colonization and matrix deposition were confirmed by SEM (*Fig.1b*) and H&E (*Fig.1c*), showing that cells adhered on exposed granule surfaces and on pore walls.

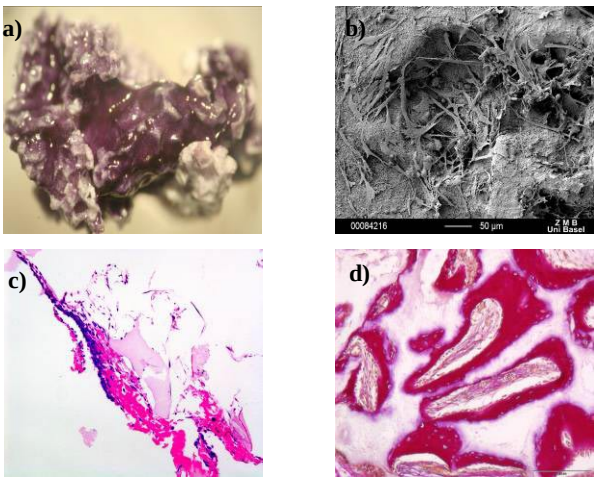

Fig.1: Scaffolds after in vitro culture (a, b ,c) and in vivo implantation (d). a) MTT staining of viable cells; b) SEM picture of a granule surface; c) HE staining on a scaffold section; d) bone formation evidenced by VG staining after explantation.

After explantation, scaffold samples showed extensive bone formation as assessed by VG staining (*Fig.1d*); moreover, the presence of osteocytes with a ramified morphology embedded in lacunae and lining osteoblasts in bone forming areas indicated that seeded cells acquired an osteogenic committment.

DISCUSSION & CONCLUSIONS: In this work we demonstrated that freshly isolated BMSC can be seeded and entrapped on ceramic granules with lyophilized fibrin sealant, ultimately leading to bone formation when cultured inside a perfusion bioreactor. The use of pre-cast scaffolds with lyophilized fibrin simplified the seeding procedure and reduced contamination risks and operator variability. Further experiments will examine the possibility to use the scaffold as an off-the-shelf product for a bioreactor-based streamlined approach in clinically-oriented applications.

ACKNOWLEDGEMENTS: Authors would like to thank Andreas Goessl from Baxter® for kindly manufacturing and providing the scaffolds, the ZMB (Zentrum für Mikroscopie) in Basel for SEM images, and Prof. G. Jundt and his group in the Department of Pathology for sectioning and staining the samples.

The Effect of Plasma Surface Modification of PEEK – Parallel Studies of Cytocompatibility and Bacterial Adhesion

A.H.C. Poulsson[1], E.T.J. Rochford[1,2], T.F. Moriarty[1], R.G. Richards[1,2,3].

[1]AO Research Institute, Davos, CH. [2]Aberystwyth University, UK. [3]Cardiff University, UK.

INTRODUCTION: Polyetheretherketone (PEEK) has bulk properties such as radiolucency, high strength and good wear resistance which are advantageous in medical devices. However, an intrinsic problem for many polymers including PEEK is their low surface energy which can limit eukaryotic cellular adhesion. Higher energy surfaces are known to promote rapid cell adhesion[1]. This study investigates increasing the surface energy of PEEK by oxygen plasma treatment to improve the adhesion and functionality of human primary osteoblast-like (HOB) cells, and the affect of this surface treatment on the adhesion of clinically relevant bacteria.

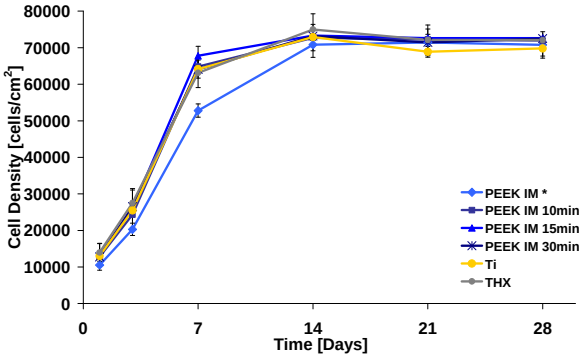

Figure 1: HOB cell adhesion to treated IM PEEK, Ti and THX was significantly higher than to untreated PEEK IM.

METHODS: Discs of Machined (PEEK M) and injection moulded (PEEK IM) PEEK Optima™ (Invibio), Thermanox (THX) (Nunc) and standard medical grade titanium (Ti) (ISO 5832/2 Synthes) were used in this study. The PEEK was exposed to oxygen plasma (EMITECH RF). Surface analysis was performed by XPS, contact angle (CA), AFM and SEM. HOB cells were cultured in mineralisation media α-MEM (0.1μM dexamethasone and 10mM β-glycerophosphate) over the 28d experiments. Cell function was assessed by ALP activity, qPCR, Alizarin red S staining, SEM and alamarBlue™ assay. Bacterial suspensions of clinical isolates of *S. epidermidis* (138 and BK1) and *S. aureus* (V8189-94 and JAR) in PBS were dispensed into a custom made adhesion chamber at $1x10^7$cfu/ml, containing the sample discs for 2.5h (37°C, 125rpm). Miles and Misra's[3] method was used to obtain total viable counts. SPSS v16.0 was used for statistical analysis.

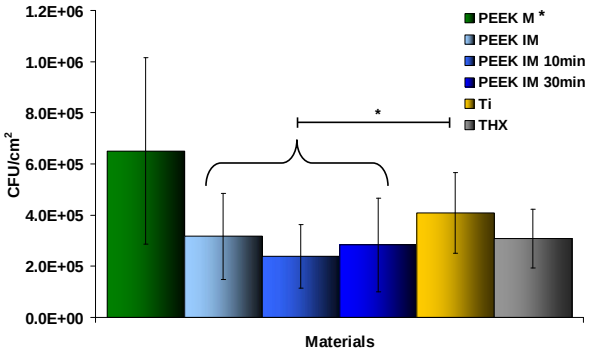

Figure 2: Adhesion of S. epidermidis 138 to PEEK M, PEEK IM and PEEK IM 10min and PEEK IM 30min, Ti and THX.

RESULTS: Surface characterisation by XPS of untreated PEEK showed ~11 atom% surface oxygen. Analysis of the plasma treated PEEK showed the surface oxygen to increase with longer treatment times up to ~16 atom% after 30min treatment, and an increase in surface energy was confirmed by CA. HOB cell confluence was reached on the treated PEEK IM and Ti, THX surfaces between 7-14d while the untreated PEEK IM surfaces confluence was only reached after 14d (Fig 1). The adhesion of *S. epidermidis* to the control materials corresponded primarily to topography, with the average bacterial adhesion increasing with increasing surface roughness. The bacterial adhesion increased from $3.08x10^5$ cfu/cm^2 on the smoothest surface, THX, to $6.51x10^5$ cfu/cm^2 on the roughest surface, PEEK M (Fig 2). There was no significant difference between bacterial adhesion to the treated PEEK IM compared to the untreated PEEK IM. **DISCUSSION & CONCLUSIONS:** Increasing the surface energy of the PEEK surfaces by oxygen plasma treatment has been found to aid the adhesion, proliferation and mineralisation of HOB cells *in vitro*. Preliminary results indicate that the adhesion of *S. epidermidis* 138 to injection moulded PEEK is not significantly altered by increasing surface energy. These initial findings suggest that surface modification of PEEK to increase osseointegration does not influence the vulnerability of the material to bacterial adhesion.

REFERENCES: [1]Kasemo, B. Surf. Sci. 500, 656, 2002. [3]Miles, A.A. and Misra, S.S. J Hygiene 38, 732-749. 1938. **ACKNOWLEDGEMENTS:** PEEK discs and financial contribution by Invibio Ltd. Ti discs from Synthes Inc.

Single stem cell fate – influence of dimensionality on adipogenesis

M.Rottmar[1], V.Vogel[2], K.Maniura-Weber[1]

[1] *Empa, Lab for Materials Biology Interactions, St.Gallen Switzerland.*
[2] *ETH, Biologically Oriented Materials, Zurich, Switzerland*

INTRODUCTION: The regulation of biological processes such as proliferation and differentiation is to a large degree connected to cell shape[1]. Altered cell morphology correlates with a number of changes in gene expression profiles. These include but are not limited to up- or down-regulation of proteins involved in proliferation, ECM production, cellular signalling or differentiation[2]. This possible relationship is therefore of great interest for tissue engineering and cell based sensors as well as for the understanding of basic stem cell biology.
The development of distinct cell types from multipotent precursor cells is thought to occur in a two-phase process, comprising the commitment of a cell to a specific lineage, still retaining a certain degree of plasticity and interconversion potential, and terminal differentiation to become a specialized functional cell[3]. Encompassing a well organized series of events the gradual process of differentiation such as for example adipogenesis or osteogenesis, can be followed by monitoring different marker proteins being expressed at various time points.

Adipogenic differentiation generally requires a high cell density but has been observed with single cells restricted to small 2D fibronectin patterns[1]. However, the cultivation of most cell types on planar surfaces is not optimal as it does not recapitulate the *in vivo* situation[4]. The aim of our project is to monitor the fate of single mesenchymal stem cells (MSCs) in quasi 3D microwells. With the microwell platform various physical parameters of the cell environment can be controlled thus enabling the investigation of dimensionality-, substrate stiffness- and cell shape-related effects on adipogenesis and stem cell (de)differentiation in general.

METHODS: Human bone marrow stromal cells (HBMC) were isolated from bone marrow samples and were cultivated in expansion or adipogenic medium. To monitor adipogenesis cells were immunohisto-chemically stained against peroxisome proliferator-activated receptor gamma (PPARγ) or stained for OilRed O to detect differentiation. The 3D microwells were produced by standard microfabrication techniques in silicon followed by thin film replica molding in PDMS. The wells were functionalized with fibronectin whereas the chip surface was passivated to prevent cell attachment[5].

RESULTS: Stainings of lipid droplets with OilRed O showed that with increasing cell seeding density more cells differentiate into adipocytes (Fig.1). Also, cells are capable of following the pathway of adipogenic differentiation when cultivated within 3D microwells under the chosen conditions (Fig. 2).

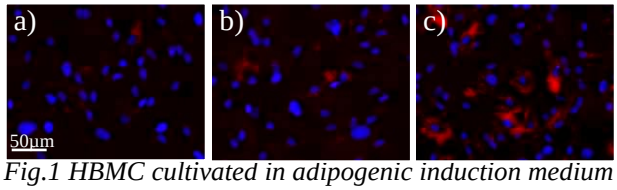

Fig.1 HBMC cultivated in adipogenic induction medium for 10 days at a density of a) 5'000 b) 15'000 or c) 25'000 cells/cm^2 before staining for lipid droplets (red) and nuclei (blue)

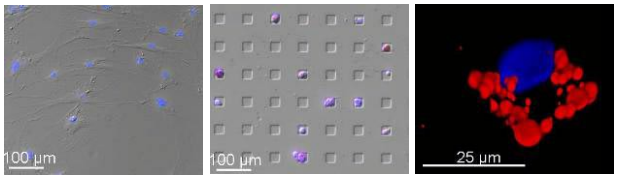

Fig.2 HBMC cultivated in adipogenic medium for 7 days on a) PDMS beside or b) in square shaped microwells before staining for lipid droplets (red) and nuclei (blue) c) 3D- reconstruction of a single cell shown in b)

DISCUSSION & CONCLUSIONS: Adipogenic differentiation of MSCs usually requires high density cultures. In microwells however, adipogenesis was reproducibly observed with single cells. Primary results therefore suggest that the microwell platform is efficient to independently study the effects of different physical cues (dimensionality, substrate stiffness, cell shape) compared to chemical cues on lineage commitment of single stem cells.

REFERENCES: [1] McBeath, R. et al. *Developmental Cell* 6, 483-495 (2004). [2] Dalby, M. et al. *Eur Cell Mater* 9, 1-8 (2005). [3] Oreffo, R.O.C et al. *Stem Cell Rev* 1, 169-78 (2005) [4] Dunn, J.C. et al. *FASEB J.* 3, 174-177 (1989) 5 Rottmar, M. et al. *J Mater Sci Mater Med.* (2009) DOI 10.1007/s10856-009-3926-7

ACKNOWLEDGEMENTS: We are indebted to Prof. Marcus Textor and his group at ETH Zürich for sharing their knowledge on the microwell fabrication technique. The present study is supported by CCMX Matlife (CH).

Biodegradable Fe-based alloys for medical applications: Design strategy and degradation characteristics

M. Schinhammer, A.C. Hänzi, F. Moszner, J.F. Löffler, P.J. Uggowitzer

ETH Zurich, Laboratory of Metal Physics and Technology, Zurich, Switzerland.

INTRODUCTION: Interest in biodegradable metals for use as temporary implant material in vascular intervention and osteosynthesis increased over the past few years. It has been found that in certain cases degradable implants may overcome some of the restrictions of permanent devices, such as prolonged physical irritation and chronic inflammation. Besides magnesium, iron is another interesting candidate for use as biodegradable implant material. Preliminary studies have already shown the potential of iron for degradable medical applications. However, because of the very low degradation rate of pure iron under physiological conditions, such implants reveal reactions rather similar to those found in permanent applications.

This contribution presents a design strategy deployed in developing new Fe-based alloys with tailorable microstructural, electrochemical and mechanical properties meeting the requirements of temporary implants, in particular those of cardiovascular stents. From a medical point of view degradation period over 12–24 months would be advisable for such applications.

DESIGN STRATEGY: Previous studies revealed not only the potential of Fe-based alloys as biodegradable implant material but also emphasized the need to increase the degradation rate to meet the requirements of temporary stent applications. The here-presented design strategy aims at both an increase in the degradation rate and an improvement in the mechanical properties with respect to currently known Fe-based alloys.

The alloy development approach takes into account two criteria which influence the corrosion susceptibility of the metal: (1) the addition of less noble alloying elements within the solubility limit in Fe to reduce the degradation resistance of the Fe matrix; and (2) the addition of noble alloying elements to generate small and finely dispersed intermetallic phase (IMP) particles that act as cathodic sites towards the Fe matrix, inducing microgalvanic corrosion and thereby accelerating the degradation of the material. Based on metallurgical and toxicological considerations manganese was found suitable to pursue criterion (1) as Mn lowers the standard electrode potential of the Fe–Mn alloys. Taking metallurgical, electrochemical, toxicological and processing related aspects into account, palladium was chosen as suitable alloying element to pursuit criterion (2). It is noteworthy that only small quantities (less than 1 at.% of Pd) are considered to fulfill the requirements regarding the processing of the alloys and their biocompatibility: given the small weight of a coronary Fe stent (≈20 mg), its relatively long degradation period, and the low Pd content in the alloys suggested here, the Pd content is not expected to be problematic.

METHODS: The alloys were prepared by casting under argon atmosphere, forging, solution heat treatment and aging. The microstructure was investigated using optical microscopy, scanning and transmission electron microscopy and X-ray diffraction. The degradation performance of the alloys was evaluated by immersion testing in simulated physiological media and using electrochemical impedance spectroscopy (EIS).

RESULTS & DISCUSSION: The alloys produced according to the design strategy revealed interesting microstructural, mechanical and electrochemical properties: immersion testing and EIS in simulated physiological media showed an increased degradation rate of the newly developed alloys compared to pure Fe. The alloys developed feature attractive mechanical properties, i.e. high strength at reasonable ductility values, and by means of appropriate heat treatments these properties can be adjusted.

CONCLUSIONS & OUTLOOK: The design approach presented in this study relies on the controlled modification of the microstructure of iron by suitable alloying and appropriate heat treatment parameters. The newly developed alloys show an enhanced degradation rate and an attractive mechanical performance underlining the high efficiency of the design strategy presented here. The design strategy offers the possibility to tailor the alloy's characteristics according to the requirements of specific degradable implant applications.

Regarding the promising results presented in this study, future work will focus on the detailed characterization of the alloys as well as the evaluation of their *in vitro* cytocompatibility. Animal studies will be carried out to assess the biocompatibility and performance of the alloys *in vivo*.

Characterization of some composites ALG-HA potentially used as bone regeneration scaffolds

Stefanescu Ileana[1], Antoniac Iulian[1], Stancu I.C.[1] , Cotrut C.[1], Vranceanu D.[1]
[1]*University Politehnica of Bucharest, Splaiul Independentei 313, sector 6, Bucharest, Romania*

INTRODUCTION: Sodium alginate (ALG) is extracted with a diluted alkali solution from marine brown algae and is not a random polysaccharide, but depending on the algae source, consists of blocs of similar and strictly alternating residue (i.e. MMM, GGG, GMGMGM), each of which has different conformational preferences and behaviours. ALG is soluble in aqueous solutions and forms stable gels at room temperature in the presence of non-cytotoxic concentrations of certain bivalent cations (i.e., Ca^{2+}) through ionic interaction between G acid groups. This leads to 3D structures, often with viable cells embedded in the gel by cross-linking in non-cytotoxic conditions.

Nafcillin, is a semi-synthetic antistaphylococcal penicillin, highly effective in penicillinase-producing staphylococcal infections, in which the activity is mainly created through steric hindrance. Unlike penicillin, ampicillin, or the extended-spectrum penicillins, nafcillin resists hydrolysis by penicillinase; therefore, along with other agents in the same group (e.g., oxacillin, dicloxacillin), this antibiotic is active against penicillinase-producing *Staphylococcus aureus*. In the present work, ALG-hydroxyapatite composites have been created as cross-linkable materials physically loaded with nafcillin. The drug-release efficiency was explored by UV-VIS spectroscopy. These materials are intended as bone fillers presenting, besides the incorporated drug, the advantage of low-invasive delivery in the bone-defect through injection, followed by an improvement of the mechanical strength due to *in vivo* Ca^{2+} cross-linking.

METHODS: ALG solution (2% wt%) in physiologic saline (0.9% NaCl) was mixed with different concentrations of hydroxyapatite (HA) powder: 5%, 10%, 50%, 200% and 500% (wt%). The phase distribution of the inorganic filler in the organic matrix was evaluated through scanning electron microscopy (SEM). The rheograms have been drawn to control the injectability of the formulations.

The drug release has been performed using cross-linked composites microbeads loaded with 10 and, respectively, 20% (wt%) antibiotic. The beads have been cross-linked in $CaCl_2$ (50mM in saline). They have been rinsed with saline and then suspended in saline. The supernatant has been systematically analysed with respect to nafcillin release in time; this was monitored as specific absorbance at 330 nm over time. The end of the release, as obtained through UV-VIS, was confirmed through FT-IR.

RESULTS: Five composites formulations have been prepared and then loaded with nafcillin (two different ratios: 10 and 20% wt). The HA has been homogeneously distributed in the composites, as shown in figure 1. Increasing the inorganic filler ratios has lead to increasing viscosity of the composites, the formulations remaining injectable.

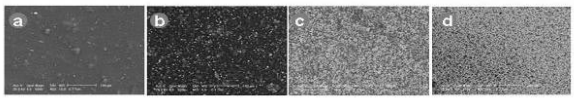

Fig.1. SEM appearance of the ALG-HA composites: a) 5% HA, b) 10% HA, c) 200% HA, d) 500% HA.

The inorganic filler content has proved to play an important role in the drug release enhancing the phenomenon.

DISCUSSION & CONCLUSIONS: This work reports the potential of ALG-HA composites to be used as in situ cross-linkable bone regeneration scaffolds deliverable through minimally invasive surgery (injection). Nevertheless, the bone healing process could be sustained through progressive localized antibiotic release. The release kinetics as well as the mechanical properties of the resulting scaffolds are controllable through the balance organic/inorganic. Nevertheless, the in situ cross-linking of the ALG improves the stability of the materials and the biomechanical performance.

REFERENCES: [1]Swayampakula Kalyani, Biduru Smitha, Sundergopal Sridhar, Abburi Krishnaiah, *Pervaporation separation of ethanol–water mixtures through sodium alginate membranes*, Desalination, Volume 229, Issues 1-3, 15 September 2008, Pages 68-81; [2] S. Miyazaki, A. Nakayama, M. Oda, M. Takada, D. Attwood, *Drug release from oral mucosal adhesive tablets of chitosan and sodium alginate*, International Journal of Pharmaceutics, Volume 118, Issue 2, 16 May 1995, Pages 257-263

Deposition of Composite Layers made from Hydroxyapatite and Silver Nanoparticles

I. Stefanescu[1], D. Bojin[1], I. Antoniac [1]

[1] *University "Politehnica" of Bucharest, Faculty of Materials Science and Engineering*

INTRODUCTION: In the last years, the deposition of bioactive coatings on metal implants has become a widespread technique in medical applications. Bioactive ceramic materials are widely used as bone substitutes, among these; a particular attention was paid to hydroxyapatite (HA) because of its outstanding properties. One of the most important ways of using hydroxyapatite is submission of coatings on bioinert metal supports. These depositions have a number of key functions. First, they allow a stable fixation of the implant in bone and promote bone tissue regeneration. However hydroxyaptite layers deposited on metal substrates do not give a solution against the occurrence of pathogens and inflammatory reactions. High risk of infection after surgery and antimicrobial properties of silver have increased interest in research to identify a method for submission of silver nanoparticles on the surface of bioactive materials or in their composition.

METHODS: The aim of this study was to obtain a composite biomaterial that summed hydroxyapatite properties - high biocompatibility, facilitation of bone regeneration cells formation and antibacterial properties of silver, through the integration of Ag nanoparticles in HA layers. HA coatings were deposited on the metallic support of Ti6Al4V by two methods, chemical and pulsed laser deposition (PLD). Composition, morphology and layer structure were investigated with electronic microscopy ESEM, EDS and X ray diffraction (XRD). In order to obtain antibacterial properties, we have been deposited on both surfaces, Ag nanoparticles from suspension. Ag nanoparticles were obtained through a sonochemical method and their size and shape were investigated using transmission electron microscopy (TEM).

RESULTS: HA coatings obtained by chemical method consists of spherical granules with high porosity (Fig. 1)

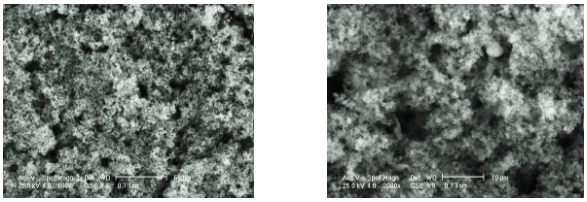

Fig. 1: SEM micrographs of HA coatings obtained after chemical deposition at lower magnification 500X (left) and higher magnification 2000X (right).

and the coatings made through pulsed laser deposition (PLD) (Fig. 2) are more compact excepting the cracks, arisen from the application of recrystallization heat treatment.

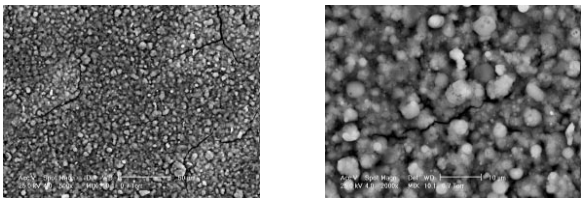

Fig. 2: SEM micrographs of HA coatings obtained after PLD deposition at lower magnification 500X (left) and higher magnification 2000X (right).

After the formation of the coatings we continued with the deposition of the Ag nanoparticles, which after or during the deposition, formed a dendritic network on the samples surfaces (Fig. 3).

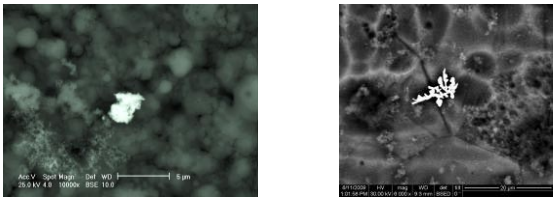

Fig. 3: Secondary and backscattered electrons images representing morphology and composition of HA surface layer by chemical deposition (left) and PLD (right), and the lighter areas representing Ag nanoparticles (clusters).

DISCUSSION & CONCLUSIONS: Following our research we believe that the best method for obtaining the composite layer is the formation of HA through chemical method, since it enables interruption of layer growth process, while silver nanoparticles are deposited through physical methods, whenever we want, without hindering the growth of the layer. Thus bacteriostatic activity is active throughout the duration of the layer.

REFERENCES: [1] Oonishi H., Yamamoto M., Tsuji E., *Bioceramics 15*, Trans Tech. Publications, Uetikon-Zurich (2003), p. 735.
[2] Kreibig U., Vollmer M. 1995 *Optical Properties of Metal Clusters* (Springer Series in Material Science vol 25) (Berlin: Springer).

Light-curable bioactive polymeric composite glues for bone defect treatment

A.Stepuk, O.D.Schneider, D.Mohn, W.J.Stark

Institute for Chemical and Bio-Engineering, ETH Zurich, Zurich, Switzerland.

INTRODUCTION: Recent research on bone implant materials targets combination of resorption and sufficient mechanical properties [1]. Photopolymerizable acrylic cements [2] possess high mechanical properties and show good biocompatibility. However a major drawback is the difficulty to set them *in vivo*. The current work represents Heliobond® adhesive, consisting of bisphenol A diglycidyl methacrylate and Tri(ethylene glycol) dimethacrylate (BisGMA/TEGDMA), used as a matrix and tricalcium phosphate (TCP) nanoparticles as filler composites. So far, this study describes the effects of embedding TCP nanoparticles in light-curable resin and its influence on bioactivity and bone adhesion strength.

METHODS: Amorphous TCP nanoparticles were prepared by flame spray synthesis [3]. The mixtures of polymer and TCP nanoparticles were used as precursors for composite and cured by blue light (λ = 450 nm) in different time periods (15 to 30 seconds). The polymeric resin was loaded with 0 and 20 wt. % TCP fillers. Composites were mixed manually with a spatula and afterwards were molded in forms of platelets (10x80x0.5 mm) for *in vitro* degradation tests and cylinders (9x4.5 mm) for mechanical testing. The adhesion of pure polymer and Heliobond®/TCP composite on cow hip bone surface was designed to maintain "close to in vivo" conditions (Fig. 1).

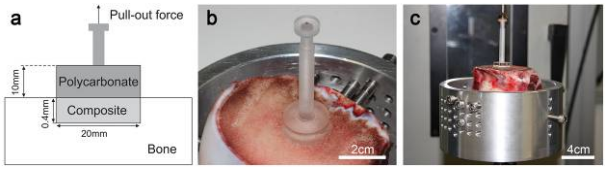

Fig. 1: Adhesion to bone: (a) Schematic test setup. (b) Image of a glued polycarbonate rod on a fresh cut cow hip bone after light-curing of the sample. (c) Pull-out test in a conventional testing machine.

RESULTS: *In vitro* bioactivity tests of pure adhesive polymer and 20 wt. % containing TCP composites showed both degradation and hydroxyapatite deposition. X-ray analysis of Heliobond®/TCP composite after storing in SBF solution for 14 days showed formation of hydroxyapatite (HAp) layer (Fig. 2a). Scanning electron microscopy images (Fig. 2b) show deposition of needle-shaped HAp crystals formed on the surface of composite scaffolds.

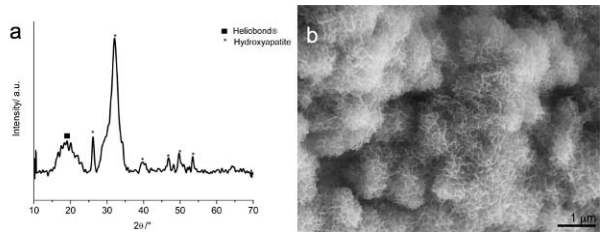

Fig. 2: (a) XRD of Heliobond®/TCP after 14 days setting in SBF. (b) SEM of sample Heliobond®/TCP after 14 days in SBF.

Pure polymeric composites resulted in a mass loss of 7 wt. % after two weeks immersion in SBF (Fig. 3a). By embedding TCP nanoparticles in the polymer matrix, the water uptake could be increased (Fig. 3b), the shrinkage reduced and therefore these factors improved mechanical reliability.

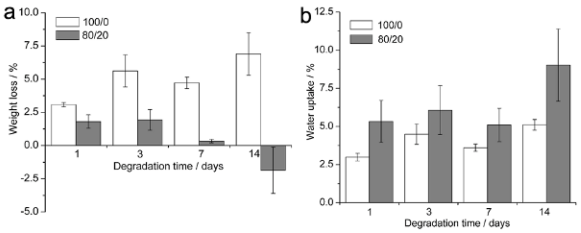

Fig. 3: (a) Weight loss and water uptake (b) of different Heliobond®/TCP composites as a function of degradation time in simulated body fluid.

Compressive strength measurements demonstrated stiffness and elasticity of the material comparable to natural bone. Incorporation of 20 % wt. reactive TCP nanoparticles improved adhesion to bone in close to *in vivo* conditions.

DISCUSSION & CONCLUSIONS: BisGMA/TEGDMA polymeric composites filled with TCP nanoparticles showed rapid *in vitro* biomineralization after immersion in simulated body fluid, high mechanical properties and enhanced adhesion to bone tissue, which could potentially apply them as *in vivo* light-curing biomaterials [4].

REFERENCES: [1] J.L. Ifkovits , J.A. Burdick (2007) *Tiss Eng* **13**: 2369-85. [2] J.N.R. O'Donnel et al. (2008) *J Bioact Compat Polym* **23:** 207-226. [3] S. Loher, W.J. Stark, M. Maciejewski et al. (2005) *Chem Mater* **17**:36-42. [4] O.D. Schneider, A. Stepuk, D. Mohn, N. Luechinger, K. Feldman, W.J. Stark (in press) *Acta Biomater*.

Piroxicam loaded PLGA microspheres for portal vein embolization

Z. Tadic[1)], K. Lehmann[2)], R. Graf[2)], B. Gander[1)]

[1)] *Institute of Pharmaceutical Sciences, ETH Zürich, 8093 Zürich;*

[2)] *Dept. of Visceral Surgery, University Hospital Zürich, 8091 Zürich, Switzerland.*

INTRODUCTION: Portal vein embolization (PVE) can improve patient safety prior to liver surgery by inducing liver hypertrophy[1]. PVE causes atrophy of the occluded part of the liver and this in turn mediates hypertrophy of the healthy liver, the remnant after surgery. As a drawback, PVE induces an inflammatory response at the site of occlusion due to the use of foreign material, and thereby affects contralateral regeneration[2].

In the present study, the goal was to produce biodegradable microspheres of adequate size and loaded with the anti-inflammatory drug piroxicam (PX). We hypothesize that the release of an anti-inflammatory drug at the site of occlusion will lower or suppress the inflammatory response, reduce trapping of macrophages, and thereby afford enhanced contralateral proliferative activity in the healthy liver lobes.

METHODS: Piroxicam was microencapsulated into poly(lactic-co-glycolic acid) (PLGA) microspheres by solvent evaporation from o/w-emulsion. The preparation method was optimized to achieve a therapeutically useful particle size range of 100-300 µm. Drug content was analyzed spectrophotometrically after dissolving the microspheres in DMSO. Drug release was measured at 37°C in phosphate buffered saline (pH 7.4) supplemented with 0.5% polysorbate 20 and 0.05% sodium azide. Drug concentration was assayed spectrophotometrically.

RESULTS: Under optimized process conditions, the yield adequately sized (100-300 µm) PLGA microspheres ranged from 15 to 30% and increased with higher drug content. The encapsulation efficiency for piroxicam was most satisfactory, even at very high drug content (*Table 1*).

Table 1 Content and encapsulation efficiency of piroxicam in PLGA microspheres

Theoretical drug content [% of piroxicam in microspheres]	Analyzed drug content [µg piroxicam / mg microspheres]	Loading efficiency [%]
10	81.4 ± 7.2	81.4 ± 7.2
20	172.2 ± 4.8	86.1 ± 2.4
30	284.7 ± 9.3	94.9 ± 3.1
40	373.2 ± 11.2	93.3 ± 2.8

The kinetics of drug release varied with the drug content (*Fig. 1*). Drug release was delayed from microspheres loaded with 8% drug, sustained when the drug content was 17% and immediate and complete at loadings of 28% and higher.

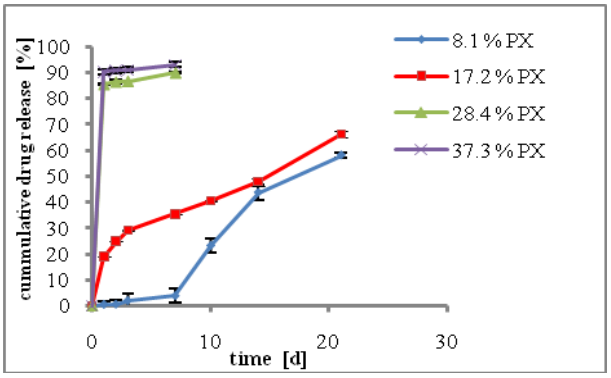

Fig. 1: Drug release from PLGA microspheres as a function of drug content in the microspheres.

DISCUSSION & CONCLUSIONS: The high loading efficiency achieved with piroxicam must be ascribed to the hydrophobic nature of the drug, which affords a high affinity to the organic polymer phase in the microencapsulation process. The obviously strong molecular interaction between piroxicam and PLGA resulted also in a rather slow drug release at a drug content of up to 17%. Higher drug loadings (28 and 37%) produced an important burst release during the first day, which must be ascribed to the high porosity the high drug content must have created in the PLGA matrix. Through this porosity, the surface for molecular interactions was substantially lowered. Thus, the release kinetics of the anti-inflammatory drug piroxicam can be controlled by varying its content in the microspheres. For the planned use for PVE in a rat model, the microspheres should release the drug constantly, over a prolonged period of time. Since in rats, liver regeneration is completed in two weeks, this duration will be readily achievable through further optimizing the drug loading.

REFERENCES: [1] E.K. Abdalla, M.E. Hicks and J.N. Vauthey, (2001) *Portal vein embolization: rationale, technique and future prospects*, British Journal of Surgery **88**, pp 165-175. [2] K. Furrer, Y. Tian, T. Pfammatter, W. Jochum, A. M. El-Badry, R. Graf, and P.A. Clavien, (2008) *Selective Portal Vein Embolization and Ligation Trigger Different Regenerative Responses in the Rat Liver*, Hepatology **47**(5), pp 1651-1623

N-dimensional PEG hydrogel - block copolymer scaffolds for controlled mouse stem cell differentiation

Shadi Taghavi[1], Conlin Oneil[1], J.A. Hubbell[1]

[1] *Laboratory for Regenerative Medicine & Pharmacobiology, EPF Lausanne, Lausanne, Switzerland*

INTRODUCTION: N-dimensional PEG-based hydrogels are here described where block copolymer micelles formed from poly(ethylene glycol)-bl-poly(propylene sulfide), (PEG-PPS), with PEG terminal pyridyl disulfide groups are incorporated into multi-arm PEG vinylsulfone / dithiothreitol (or peptide matrix metalloproteinase substrate) hydrogel matrix. This type of gel allows for the encapsulation and controlled release of hydrophobic small molecules which can alter the behavior of cells either incorporated into or adsorbed onto the hydrogel. Here we use retinoic acid as a model compound as it induces mouse embryonic stem cells to differentiate into neuronal cells. Further, the hybrid block copolymer PEG scaffold allows for control of the viscoelastic properties of the hydrogel, potentially allowing for a more dynamic matrix which may more closely mimic natural tissue mechanical properties. Here we describe the encapsulation and in vitro release of retinoic acid from PEG-PPS micelles, the viscoelastic properties of micelle-PEG hydrogels and the initial experiments with embryonic stem cells in vitro.

METHODS:

- Micelles fabrication[1]
- Micelles characterization: DLS, Ellman's assay,
- In vitro release of Retinoic acid[2]
- Cell Culture [3]
- Hydrogel fabrication[4]
- Quantification of hydrogels mechanical properties

RESULTS:

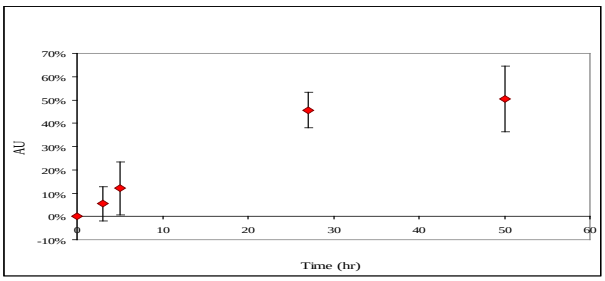

Fig. 1. In vitro release of Retinoic acid.from PEG-PPS micelles

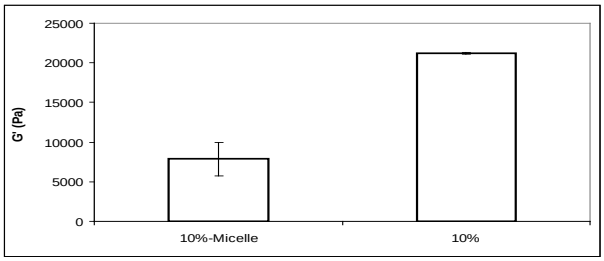

(a)

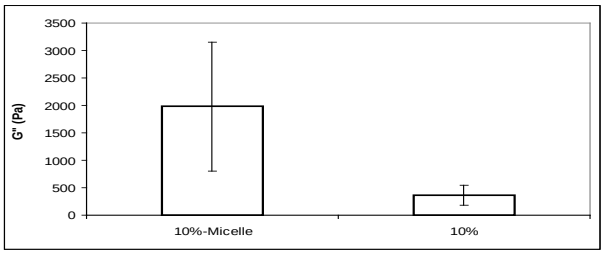

(b)

Fig. 2. G'(a) and G'' (b) for 10% Hdrogels with and without PEG-PPS micelles

Figure 1 shows the in vitro release of Retinoic acid from PEG-PPS micelles. Figure 2 is the rheology study on 10% hydrogel forming in presence of micelles with PEG terminal pyridyl disulfide groups (a) and without micelles (b).

DISCUSSION & CONCLUSIONS: Retinoic acid is successfully encapsulated and released in PEG-PPS micelles. In vitro study showed that less than 50% of Retinoic acid is released in third day. Using PEG-PPS micelles, with PEG terminal pyridyl disulfide groups in multi-arm PEG hydrogel, decreases the elastic modulus of the hydrogel whereas increases the viscous modulus of that.

REFERENCES: [1] D.V. Molecular Pharmaceutics 5 (2008) 632-642, [2] C. P. O'Neil, Journal of Controlled Release 137 (2009) 146-151, [3] R. L. Capenedo Biomaterials 30 (2009) 2507-2515. [4] M. P. Lutolf, Nature 462 (2009) 433-441.

ACKNOWLEDGEMENTS: We appreciate Matthias Lutolf and LSCB members for their help and supports.

FAILURE MECHANISMS OF DLC COATED JOINT REPLACEMENTS

K.Thorwarth[1], U. Müller[1], G. Thorwarth[3], C.V. Falub[2], M. Stiefel[1], Ch. Affolter[1], B. Weisse[1], C. Voisard[3] and R. Hauert[1]

[1]EMPA, Swiss Federal Laboratories for Materials Testing and Research, CH-8600 Dübendorf.

[2] ETH Zürich, Solid State Physics Laboratory, CH - 8093 Zürich.

[3] Synthes GmbH, CH - 4513 Langendorf.

INTRODUCTION: Diamond Like Carbon (DLC) is a very promising coating material to improve biomechanical properties of articulating implants due to its extreme hardness, chemical inertness, wear resistance and biocompatibility [1]. Although in several instances, DLC - coated implants were tested with particular regard to film delamination under different conditions, many implanted medical devices like joint replacements have failed due to coating delamination after a few years. Slow delamination, in the order of a few µm/year, is very difficult to detect but can lead to a complete failure of the coating after a sufficient time in vivo. To give a reliable adhesion lifetime prediction for DLC coated implants, a thorough estimation of all potential failure mechanisms is of particular importance. Beside mechanical failure, other delayed interface crack growth mechanisms also have to be considered, especially hydrogen embrittlement, galvanic, crevice, and pitting corrosion as well as stress corrosion cracking (SCC).

METHODS: Ball-on-socket implants made from CoCrMo were coated with DLC using a Plasma Activated Chemical Vapour Deposition (PACVD) method with acetylene (C_2H_2) as process gas. These implants were tested in a joint simulator setup [2] running in synovial testing fluid (Thermo Scientific Hyclone®). Beside these test implants, also 2 series of explants retrieved after 2 and 8 years in vivo which failed due to coating delamination, were investigated to analyze the failure mechanism. Different analytical (FIB; XRD; EDX) and imaging methods (SEM; TEM) were used to determine and understand the main causes of failure.

RESULTS: Beside mechanical failure, which can easily be detected in simulator tests, different corrosion processes at the interface between the DLC coating and the substrate are most reasonable for film delamination (see figure 1). Here, the coating delamination is controlled by SCC and crevice corrosion (CC) mechanisms since they show strong dependence on stress and environment. We present new methods to determine three pertinent failure mechanisms, in detail stress corrosion cracking, crevice corrosion (CC) and mechanical failure of coated implants, especially in respect to long term delamination. In the case of SCC it will be shown that SCC may occur in a few nanometer thin reactively formed interface layer. Under certain conditions also crevice corrosion occurs.

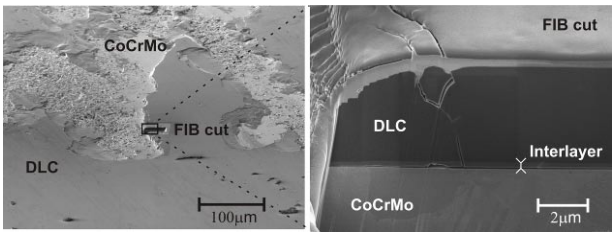

Fig. 1: SEM picture of a local defect on a DLC coated implant (left) and enlarged FIB transversal cut showing the interface crack (right).

DISCUSSION & CONCLUSIONS: Important failure mainly occurred due to CC of the adhesion promoting interlayer or due to a reactively formed interface material susceptible to SCC, where slow crack propagation occurs in corrosive media such as body fluid. We found testing in saline solutions to be insufficient, as proteins play an important role, especially as they may provide CC-conditions. Simulator testing shows that mechanical failure is mainly caused by third body wear involving wear particles.

REFERENCES: [1] R. Hauert (2008), in *Tribology of Diamond-Like Carbon Films: Fundamentals and Applications* (eds. C. Donnet and A. Erdemir) Springer, p. 494.

[2] G. Thorwarth, C.V. Falub, et al. (2009), Acta biomat. (Article in Press DOI: 10.1016/ j.actbio. 2009.12.019)

ACKNOWLEDGEMENTS: Financial support from the Swiss Commission for Technology and Innovation (CTI) and Synthes GmbH is gratefully acknowledged.

Disposable Polymeric Micro-Cantilever Arrays for Biomedical Applications

P. Urwyler[1,3], O. Haefeli[2], H. Schift[1], J. Gobrecht[1,2], and B. Müller[3]

[1]*Paul Scherrer Institute, Villigen, Switzerland.* [2]*University of Applied Sciences Northwestern Switzerland, Windisch, Switzerland.* [3]*Biomaterials Science Center, University of Basel, Switzerland.*

INTRODUCTION: Micro-fabricated cantilevers, similar to those used in scanning probe microscopes, have become increasingly popular as transducers in chemical and biological sensors. In the field of biomedicine, silicon-based micro-cantilevers are applied but they are often too expensive for single usage. Polymer materials offer tailored physical and chemical properties including biocompatibility that can be combined with low-cost mass production. We have established the injection molding technique to fabricate different polymer cantilever arrays with dimensions in the micrometer range to be functionalized and calibrated for applications in biomedicine.

METHODS: The development and fabrication of disposable polymeric micro-cantilever arrays, as shown in Fig. 1, is based on thermal injection molding. The injection molding, well established on the millimeter scale and above, is adapted to the micrometer scale. The mold is rapidly heated so that the melt isothermally fills the cavity. Such a processing allows working within the standard injection molding cycle timeframe. The isothermal process facilitates the complete filling of high-aspect-ratio micro-cavities with a variety of polymer materials.

RESULTS: Micro-cantilever arrays (see Fig. 1) made of cyclic olefin copolymers (COC), polyoxy-methylen copolymers (POM-C), polypropylene (PP), and polyvinylidenfluorid (PVDF) were successfully injection molded. High performance polymers such as polyetheretherketone (PEEK) are conceivable, but have special processing conditions like elevated temperature requirements.

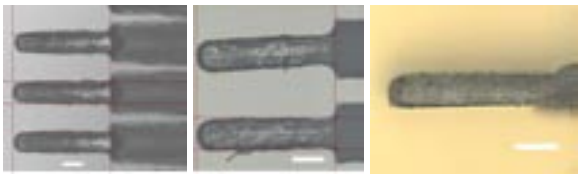

Fig. 1: Injection molded 100 µm-wide COC (left), POM (center) and PP (right) cantilevers. Scale bars 100 µm

The micro-cantilevers were flat enough to be characterized directly using the atomic force microscope (AFM). The resonance frequencies of selected cantilevers are summarized in Table 1. The heat tests, performed using the Cantisens® Research platform (see Fig. 2), shows the proper behavior of the cantilevers.

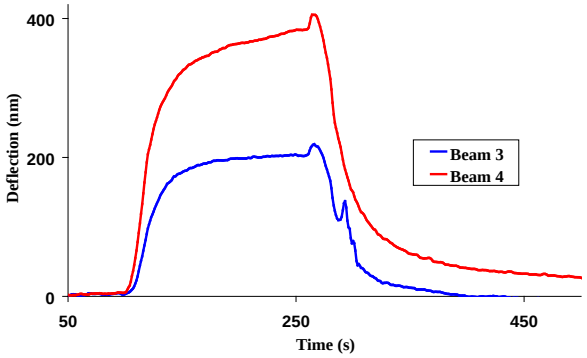

Fig. 2: Heat test from 22 to 32 °C with injection-molded PVDF cantilevers. (Beam 3 – deflection 200 nm, beam 4 – deflection 375 nm).

Table 1: Micro-cantilever resonance frequencies

Material Beam No	Theoretical	Experimental (AFM)
PVDF 1	43 kHz	79.27 kHz
PVDF 2		79.00 kHz
PVDF 3		79.05 kHz
PP 1	53 kHz	78.7 kHz
PP 2		78.9 kHz
PP 3		78.6 kHz

CONCLUSIONS & OUTLOOK: This work presents injection molding of polymeric micro-cantilevers with an aspect ratio as large as 10. The heat tests and the preliminary biochemical thiol-tests suggest that cantilevers are mechanically compliant for usage in biochemistry and biomedicine. The cantilever array sensors will support the selection of advanced surface-modified substrates and medical implant surfaces. Here, we foresee the measurement of contractile cell forces as described earlier.[1]

REFERENCES: [1] J. Köser, J. Gobrecht, U. Pieles, B. Müller (2008) *Eur. Cells Mater* **16**:38.

ACKNOWLEDGEMENTS: This activity is funded by the Swiss Nanoscience Institute through the applied research project DICANS, a collaborative initiative between the BMC, PSI, FHNW and Concentris GmbH. We thank the members from the LMN-PSI, INKA, FHNW (IKT, IPPE), EMPA (K. Jefimovs) for their technical assistance.

Functionalized magnetic nanoparticles used for drug delivery in knee injuries

Vranceanu Diana[1], Antoniac I.[1], Laptoiu D[2]., Corobea C.[3], Stefanescu I.[1]

[1]University Politehnica of Bucharest, [2] Colentina Clinical Hospital Bucharest, [3] ICECHIM Bucharest.

INTRODUCTION: Aside from the small size and low toxicity to humans, magnetic nanoparticles can be transformed through an external magnetic field gradient, penetrating deep into the human tissue. In this way, controlled transport of drugs to target sites can be achieved. Magnetically controlled viscosupplimentation is a new bioactive treatment concept, combining the demonstrated effects of intraarticular therapy with a new support system.

METHODS: S-type magnetite nanoparticles were synthesized by co-precipitation process in alkaline catalysis by Massart adaptation process.The particles were analyzed in colloidal phenomena both in dispersion environment (water) and solid. Subsequently, magnetic particles were synthesized covered by the "layer by layer" with chitosan and hyaluronic acid. DLS and Zeta Potential Analysis confirmed the deposit layers of chitosan and hyaluronic acid. Indirect confirmation of the deposit properties was made by DLS analysis, FTIR and SEM.

RESULTS: The presence of chitosan allows the load change electric particle surface (the tasks negative to positive charges). Using this principle further selectivity based applications can be developed. Chitosan coating based allows an advanced stabilization of particulate in dispersion medium, but also eliminates the phenomena of strong aggregation in the solid phase.

The spectrum of magnetic chitosan nanoparticles show OH and NH2 characteristic peaks of chitosan groups at 3200-3600 cm $^{-1}$ and 1520-1790 cm $^{-1}$

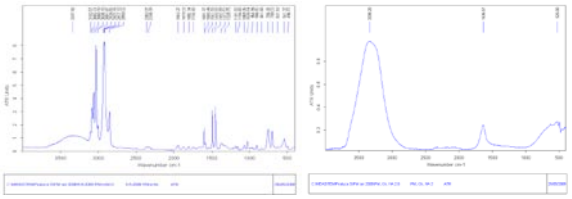

a) *b)*

Figure 1. FTIR spectrums ; a) coated magnetic nanoparticles with chitosan , b) coated magnetic nanoparticles with chitosan and HA.

SEM analysis SEM analysis showed the presence of two main morphological forms. They have a near spherical morphology in both cases.

a) *b)*

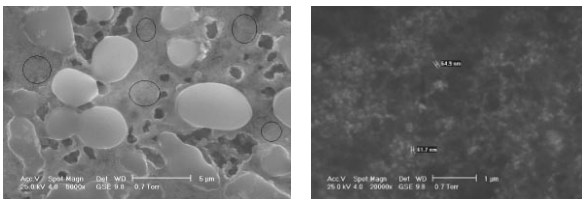

Figure 2. SEM images a) magnetic nanoparticles, b)coated magnetic nanoparticles with chitosan

Hyaluronic acid may play a complementary role positive to stabilize the particles coated with first layer (chitosan). Excess hyaluronic acid but may cause colloidal aggregation phenomena.

DISCUSSION & CONCLUSIONS: Particles with two coatings (type magnetite – chitosan – hyaluronic acid), have the best stability, the narrowest distribution, most positive charge potential and the lowest tendency colloidal aggregation. Further study may exploit opportunities of optimization of synthesis for the design of certain size or surface properties on mathematical modeling, and direct use of the particles as drug carriers, particles for medical imaging, coatings field for magnetic sensor system type/biological markers.

REFERENCES: [1] Frey NA, Peng S, Cheng K, Sun S. *Magnetic nanoparticles: synthesis, functionalization and applications in bioimaging and magnetic energy storage.* Chem Soc Rev. 2009 Sep; 38(9):2532-42, Epub 2009 Jun 23.; [2] Xie J, Huang J, Li X, Sun S, Chen X. *Iron oxide nanoparticle platform for biomedical applications.* Curr Med Chem. 2009;16(10):1278-94; [3] Du L, Chen J, Qi Y, Li D, Yuan C, Lin MC, Yew DT, Kung HF, Yu JC, Lai L. *Preparation and biomedical application of a non-polymer coated superparamagnetic nanoparticle.* Int J Nanomedicine. 2007;2(4):805-12.

ACKNOWLEDGEMENTS: This work was financial supported by CNMP within the PN II project nr: 42-132/01.10.2008, acronym ARTROMAG.

Corrosion resistance of Zr based coatings for medical applications

D.M.Vranceanu[1], C.M.Cotrut[1], I.Antoniac[1]

[1]*Politehnica University of Bucharest, Romania.*

INTRODUCTION: Various inorganic coatings are used to protect the metallic structures from electrochemical corrosion for many years, but their applications in biomedical fields are severely limited because of mechanical degradation. In recent years, there has been a growing interest in the use of PVD method for deposition inorganic protective coatings on a wide variety of biomedical implants. This paper reports the characterization of single layer ZrCN and alternate Zr/ZrCN multilayered coatings, with low and high carbon content, deposited by magnetron sputtering technique. The influence of the carbon content on the corrosion resistance of the coatings in artificial physiological solution (APS) was analyzed.

METHODS: The thin films were deposited by the reactive magnetron sputtering method [1], in a N_2 + CH_4 gas mixture using a metallic Zr cathode (purity 99.9%). For the Zr/ZrCN structure, the reactive gas was periodically introduced/evacuated in/from the deposition chamber for predetermined durations. The overall thickness of all coatings was ~ 1.2 μm. The substrate material used was Ti6Al4V alloy that was cut to yield 45×30×5 mm specimens. The recognition of elemental constituents of the film, surface morphology and hardness were investigated by energy dispersive X-ray (EDX) spectroscopy attached to the scanning electron microscope, SEM and Vickers microhardness test. The corrosion behavior of the coated and uncoated samples at 25^0C was assessed using electrochemical tests. The solutions used were NaCl – 8.44 g/l, Na HCO3 – 0.35 g/l, NaH2PO4 – 0.06 g/l, Na $H_2PO_4 \cdot H_2O$ – 0.06 g/l with a pH=7.4. A saturated calomel electrode (SCE) was used as reference electrode. The potentiodynamic polarization technique was used to detect any tendency of the samples to passivity. For the potentiodynamic polarization, the potential range used to produce the curve is broad, ranging from −3 to 3 V. The scan rate being used in this paper was 0.16 mV/s. The corrosion current densities and critical current for passivation obtained were used to explain the corrosion resistance of the coating.

RESULTS: The EDX spectra of ZrCN single layer is shown in Fig. 1. The EDX spectra show peaks corresponding to elements that are present in the film and the substrate. It can be noticed that no peak corresponding to any impurity element, other than those supposed to be present in ZrCN film, is found in EDX spectrum. The result of the SEM analyses is presented in figure 1 for the Zr/ZrCN coating. The surfaces are smooth and only few defects can be observed. The hardness of the multilayers was found to be lower than that of the ZrCN film (30÷34 GPa for ZrCN and 24÷28 GPa for Zr/ZrCN).

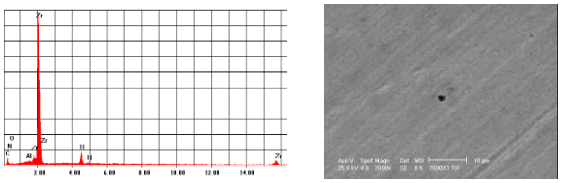

Fig. 1: EDX spectra of ZrCN coating (left) and SEM image of Zr/ZrCN coating (x2000) (right).

The best corrosion resistance was measured for the multilayered coating with high carbon content (Zr/ZrCN-1). The measured decrease of the corrosion currents indicates that the coatings improved the corrosion resistance over the Ti6Al4V substrates.

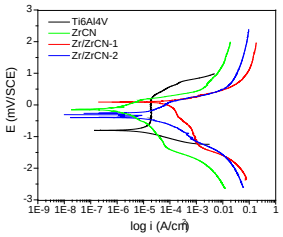

Fig. 1: Potentiodynamic polarization curves.

DISCUSSION & CONCLUSIONS: As compared with the uncoated Ti6Al4V alloy substrates, all the thin films proved superior corrosion resistance and mechanical properties. The Zr/ZrCN multilayer coatings with high carbon content showed the best corrosion resistance in comparison with the monolayers. In conclusion, ZrCN film proved their capability to improve the mechanical and anticorrosive properties of the Ti6Al4V substrates.

REFERENCES: [1]M.Braic, M.Balaceanu, A.Purice, F.Stokker-Cheregi, A.Moldovan, N.Scarisoreanu, G.Dinescu, A.Dauscher, M.Dinescu (2006) *Surf. Coat. Technol.* **200**: 6505.

ACKNOWLEDGEMENTS: The work was supported under the Romanian R&D Project Coat4Joints 72-180.

The development of a Triple-Celltype-System (TCS) that mimics the bone environment to study cell-cell-cell interactions/competition and biocompatibility

Frederik Wein, Ursina Tobler, Claudia Brose, Jean-Pierre Kaiser and Arie Bruinink
MaTisMed, Materials-Biology Interactions Lab EMPA – Swiss Laboratory of Material Testing and Research, St Gallen, Switzerland

INTRODUCTION: The successful treatment of bone defects and non-union fractures with implants depends on its osteo-integrative characteristics. An appropriate bone implant surface supports mesenchymal stem cell (MSC) proliferation and induces differentiation towards the bone forming lineage. The majority of current in vitro efforts to optimize implant surfaces is based on one single cell type. Under physiological conditions a variety of different cell types are competing to contact and colonize the implant surface. Two of the most numerous and important cell types in the bone environment are fibroblasts and cells of the osteoblast lineage. Each of those mutually affects the state of differentiation and functionality of the other cell type and these interactions play a defining role in the fate of the implant [1]. Numerous studies emphasize vascularisation and by that the supply of oxygen and nutrients as a limiting factor for the bone forming cells to thrive. Bone cells are known to influence vascularization. Therefore, to mimic the *in vivo* situation more appropriate we assume the inclusion of endothelial cells to be crucial . The aim of the present study is to assign the physiological cell competition to two and three dimensional in vitro conditions in order to facilitate new insights into osteointegrative properties of biomaterials. Therefore, addressing the first hurdle of a human TCS we developed a common culture medium (TCS-medium) for primary osteoblasts, fibroblasts and endothelial cells.

METHODS: Primary human abdominal fibroblasts (HAFs) originated from a biopsy of adult abdominal skin. Primary human microvascular endothelial cells (HMVEC) were purchased from Lonza and primary adult human bone cells were obtained by cultivating trabecular bone pieces from adult patients. Cells growing out of the bone pieces were defined as HBC. Only HBC cells of the first two passages were used for the experiments. To distinguish the three types, cells were labelled prior to seeding with an unspecific membrane dye Vybrant™ (DiI/D/O) [2]. HAF were routinely cultured in DMEM with 10% FCS and 1% PSN while HMVEC expansion medium was purchased from Lonza and HBC were expanded in modified αMEM, 10% FCS, 1% PSN and 1 ng/ml FGF2. FACS analyses have been performed with all cell types using Human bone, ALP (clone B4-78; Dev. Hybridoma Bank), CD31 (clone WM-59, Sigma), VEGFR2 (clone KDR-1, Sigma) and the secondary antibody IgG (H&L) Alexa488 (Molecular Probes).

RESULTS: The expression of lineage surface markers have been analysed by flow cytometry for HBC, HMVEC and HAF. HBC expressed bALP in the TCS-medium on a higher level (93%±1.81) than in the expansion medium (23%±3.83). 98%±0.44 and 94%±3.87 of all analysed HMVEC expressed endothelial cell markers (CD31 and VEGFR2) in expansion and TCS-medium conditions whereas HAF remained negative for all tested lineage markers. Each cell type was cultured for 7 days in expansion and TCS-medium prior analyses (n=3). Fluorescence microscopy showed that each cell type could be distinguished by the vital dyes (red, green, yellow) until 7 days after labelling. First experiments imply that the TCS-medium supports proliferation, differentiation, and a normal morphology.

DISCUSSION & CONCLUSIONS: The common TCS-medium conditions have proven to maintain endothelial cell markers on HMVEC and simultaneously induce osteogenesis solely in HBC and not in primary fibroblasts. These qualities allow the study of competing cell interactions. First experiments indicate the technical feasibility to analyze proliferation, differentiation and spatial distribution of each of the co-cultured cells via FACS and microscopy. In future, these features will be analyzed with respect to the given substrata. The TCS embodies a great opportunity to study cell-cell and cell-material interaction in a way that mimics the in vivo bone microenvironment.

REFERENCES: [1]B. Ogiso, F.J. Hughes, A.H. Melcher et al (1991) *J Cell Physiol* 146:442-50. [2]J.P. Kaiser and A. Bruinink (2004) *J Mater Sci: Mater Med* 15:429-35.

ACKNOWLEDGEMENTS: This work has been supported by EC FP7 Magister NMP-2007-4.2.3.-1

Two-Dimensional Morphological Gradients for Cell Biology

C. Zink, L. Clasohm, N. D. Spencer

ETH Zurich, Department of Materials, Laboratory for Surface Science and Technology, Switzerland

INTRODUCTION: Surface roughness plays an important role in contact-related phenomena, such as tribology or adhesion. Also, roughness plays a crucial role in the biological response to a surface, i.e. cell adhesion, morphology, proliferation and differentiation. Two methods were developed in our lab to create morphological gradients on a micrometre and on a nanometre scale. Additionally a combination of the two is used to create two-dimensional orthogonal roughness gradients varying in feature size along the two axes.

METHODS: Micro-featured gradients can be produced by using a two-step process: First aluminium substrates are sandblasted, followed by gradually polishing the rough surface with a chemical polishing solution. Cell experiments with these gradients have shown that with increasing roughness, rat calvarial osteoblasts (RCO) have a significantly higher proliferation rate[1].

The nanoparticle-density gradient can be fabricated by kinetically controlled adsorption of negatively charged silica particles onto a positively charged, polyethylene-imine-(PEI) coated substrate. A subsequent sintering process results in a firm attachment of the particles and the removal of the PEI. RCO cell experiments on these gradients showed a significant decrease in proliferation with increasing particle density on the surface[2].

To combine these two techniques, an alumina replica of the micro-featured gradient is made in order to withstand the high temperatures required during the particle-attachment process.

RESULTS: Figure 1 shows an SEM micrograph of an alumina replica with silica nanoparticles attached to it at a very high density. The two different roughnesses can clearly be distinguished: The nanoparticles add roughness in the nanometre length scale and the alumina grains, along with the waviness of the substrate, add features in the micrometre range.

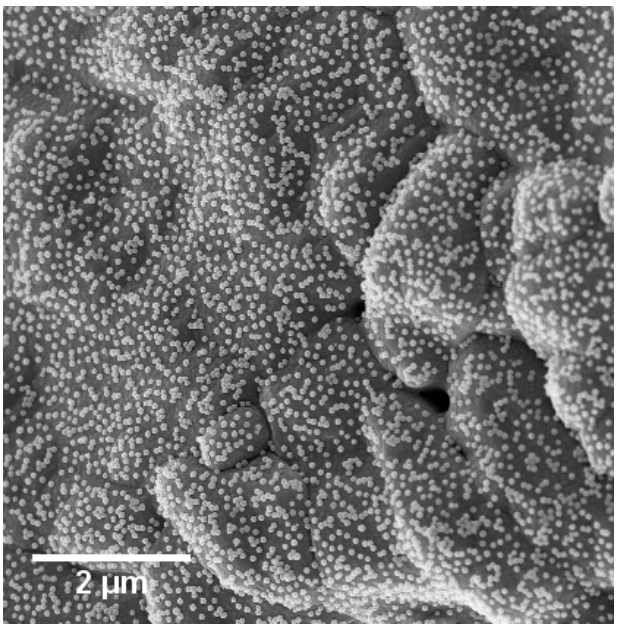

Fig. 1: SEM micrograph of silica nanoparticles on alumina roughness gradient.

DISCUSSION & CONCLUSIONS: These newly created, two-dimensional gradients are an excellent choice to study the influence of surface roughness on cell behaviour. They not only cover features from the nano- to the micrometre length scale, but also numerous combinations of the two.

REFERENCES: [1]Kunzler T. P., Drobek T., Spencer N. D., Applied Surface Science, 253 (2006) 2148-2153, [2]Huwiler C., Künzler T. P., Textor M., Vörös J., N. D. Spencer, Langmuir, 2007, 23 5929-5935

ACKNOWLEDGMENTS: Generous financial support from Straumann AG is gratefully acknowledged.

Stress evaluation in major connectors of maxillary removable partial dentures

F. Topala[1], L. Sandu[1], S. Porojan[1], N. Faur[2]

[1] *"V. Babes" University of Medicine and Pharmacy Timisoara, Romania.*
[2] *Politehnica University Timisoara, Romania.*

INTRODUCTION: Designs of removable partial dentures are suggested to affect the abutment teeth during functions [1-3]. The purpose of this study was to determine the minimum major connector dimensions of maxillary major connectors achieved for Kennedy class I edentations that would provide adequate functional strength by finite element analysis.

METHODS: Experimental Co-Cr major connectors with different widths (10 - 15 mm at the midline) were modeled. The geometrical models of telescopic retained connectors were generated using Rhinoceros (McNeel North America) NURBS (Nonuniform Rational B-Splines) modelling program for a maxillary Kennedy class edentation. The thickness was maintained constant at 1 mm for all cases. In building the finite element model, the characteristics of the Co-Cr alloy used for the framework were entered into the computer program. Vertical displacements of 0.5 mm were applied at the distal ends of the ridges, to simulate the displacement of the connector toward the ridge, while the mesial ends at the connection with the outer double crowns were fixed in all directions. Considering that the displacement value used was those that appear normally during mastication, it was sufficient to limit the study at this value. A three-dimensional finite element analysis software ANSYS (Ansys Inc., Philadelphia, USA) was used for the study of structural simulations. The finite element models were developed by dividing the model into 1879 elements, connected at 4216 nodes. Rigidity tests were performed by measuring relative displacements and von Misses stresses generated under simulated compressive loads.

RESULTS: Results were displayed as colored contour plots to identify regions of different stress and displacement values. Stresses under displacement loading simulating vertical forces were located near the palatal surface of the secondary crowns in all cases (Fig. 1). For the experimental models taken into the study the maximal equivalent stresses varried within 24.64%. The variations increased with the increasing of the width and became insignificant for over 14 mm in width. The maximal displacements were registered at the distal ends of the ridges (Fig. 2).

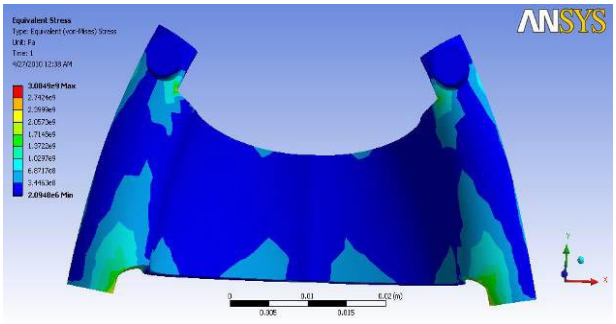

Fig. 1. Stress distribution in the major connector.

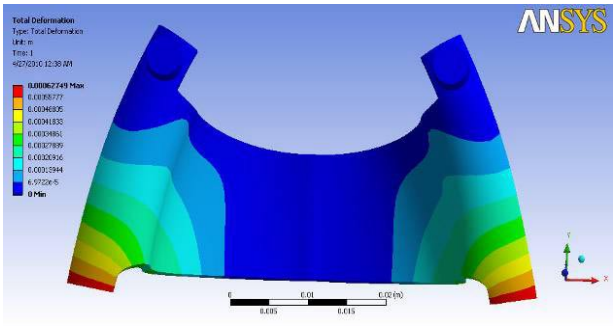

Fig. 2. Displacement in the major connector.

DISCUSSION & CONCLUSIONS: This in vitro study demonstrated that only stresses of the maxillary palatal plates were influenced by the width, with high values located near the secondary crowns. The displacements were not influenced by the width of the major connectors.

REFERENCES: [1] H. Itoh, K. Baba, K. Aridome, D. Okada, A. Tokuda, A. Nishiyama, H. Miura, Y.Igarashi (2008) *J Oral Rehabil* 35(11):810-5. [2] T.E. Pienkos, W.J. Morris, P.M. Gronet, S.M. Cameron, S.W. Looney (2007) *J Prosthet Dent* 97(5):299-304. [3] K. Aridome, M. Yamazaki, K. T. Baba, T. Ohyama (2005) *J Prosthet Dent* 93(3):267-73.

ACKNOWLEDGEMENTS: This study was supported by the Grant ID_1264 from the Ministry of Education and Research, Romania.

In vitro study on internal fits of crown frameworks achieved by different technologies

S. Porojan, L. Sandu, F. Topala, D. Pop, A. Podariu

"V. Babes" University of Medicine and Pharmacy Timisoara, Romania.

INTRODUCTION: Prouving to be competitor to classic framework materials, like dental alloys, new sophisticated materials and dedicated systems were developed in order to be introduced in dental technology. The internal accuracy is a main factor that influences the long-term reliability of a crown framework. The objective of the study was to make investigations regarding adaptation discrepancies for single tooth restorations obtained through conventional and alternative proceedings.

METHODS: The studies were centered on metallic crown frameworks obtained through melting – casting classical procedure, ceramic frameworks obtained through pressing, ceramic crown frameworks obtained through combined procedure of classical modeling and CAM, and ceramic crown frameworks obtained using CAD/CAM procedure. In this way, it was desired to introduce innovative working methods in order to determine some investigation parameters and establish the discrepancies of classical and alternative obtained restorations. Therefore sixteen maxillary molar dies were fabricated with two different preparation designs: chamfer, and 1 mm thick shoulder. Internal adaptation was evaluated by measuring the internal space width using a test-fit silicone paste.

RESULTS: Significant differences in terms of internal discrepancies were observed only between the restorations with different preparation designs for the metallic and ceramics obtained through pressing. For those the fit on shoulder preparations is 40% better than those on chamfer.

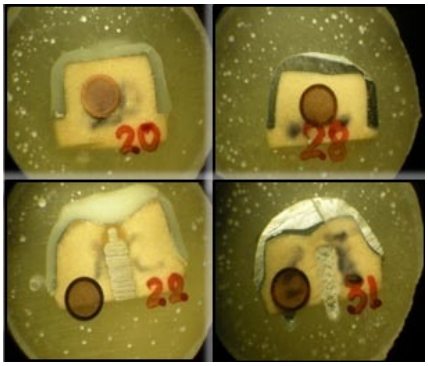

a *b*

Fig. 1: Fit evaluation for: a. pressed ceramics and b. metallic frameworks.

For the restorations obtained by CAD/CAM the fit in the angle between the shoulder and the axial surfaces represented a problem.

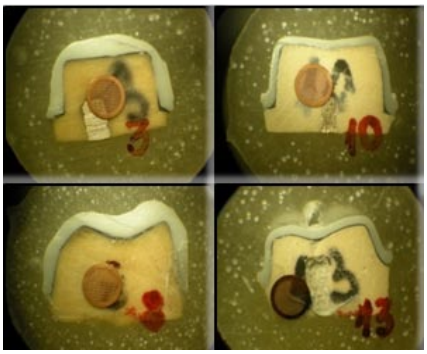

a *b*

Fig. 1: Fit evaluation for CAM frameworks obtained by: a. Wax-up/CAM and b. CAD/CAM.

DISCUSSION & CONCLUSIONS: The applicative individualization and reproduction of design parameters constitute a challenge in the technology and therewith the goal of the experimental researches. Based on the results of this study, it could be concluded that a shoulder preparation is highly recommended whenever possible. Only for CAM obtained restorations the chamfer is a similar alternative from internal fit point of view.

REFERENCES: [1] M.A. Al-Rabab'ah, T.V. Macfarlane, J.F.McCord (2008) *Eur J Prosthodont Restor Dent* 16(3):109-15. [2] T. Nakamura, H. Tanaka, S. Kinuta, T. Akao, K. Okamoto, K. Wakabayashi, H.Yatani (2005) *Dent Mater J* 24(3):456-9. [3] K.B. Lee, C.W. Park, K.H. Kim, T.Y.Kwon (2008) *Dent Mater J* 27(3):422-6.

ACKNOWLEDGEMENTS: This study was supported by the Grant ID_1264 from the Ministry of Education and Research, Romania.

Numerical investigation of telescopic retained mandibular overdentures

L. Sandu[1], F. Topala[1], S. Porojan[1], N. Faur[2], A. Podariu[1]

[1] *"V. Babes" University of Medicine and Pharmacy Timisoara, Romania.*
[2] *Politehnica University Timisoara, Romania.*

INTRODUCTION: The telescopic overdenture is one possible solution for prosthetic rehabilitation for a partially dentate arch with few remaining teeth. Dentures supported by telescopic crowns are an alternative for snap or bar retained dentures [1-3]. The system of double crowns consists of the male component of attachment, patrix or inner crown, which is cemented to the abutment tooth, and the female component of attachment, matrix or outer crown, which is the removable part of the attachment [4]. The finite element analysis was conducted to assess the effect of the conical double crowns taper on the stress distribution in the fixed and removable frameworks.

METHODS: The 3D models of two mandibular canines were modelled using literature data. The abutment teeth were prepared with different tapers (between 4 and 10 degree), to allow comparing the influence of the taper on stress distribution in the attachment components. The overdenture framework was connected to the outer crowns of the canines. The geometrical models were generated using Rhinoceros (McNeel North America) NURBS (Nonuniform Rational B-Splines) modelling program. The finite element models were obtained by importing the solid models into ANSYS finite element analysis software (Ansys Inc., Philadelphia, USA). All the nodes on the external surface of the teeth roots were constrained in all directions. A displacement of 0.5 mm was applied on the distal end of the removable framework, to simulate the displacement toward the ridge during functions. Von Misses equivalent stresses were calculated in the double crowns and removable framework in condition of varying preparation angles of the teeth.

RESULTS: The maximal equivalent stress values were not significantly different for the investigated preparation angles. Only the distribution of the stresses varied, stress areas increased with the increase of the angle. Stresses were located in the cervical part of the inner crowns (Fig. 1), mesial and distal, and distal the outer crowns in the removable framework (Fig. 2).

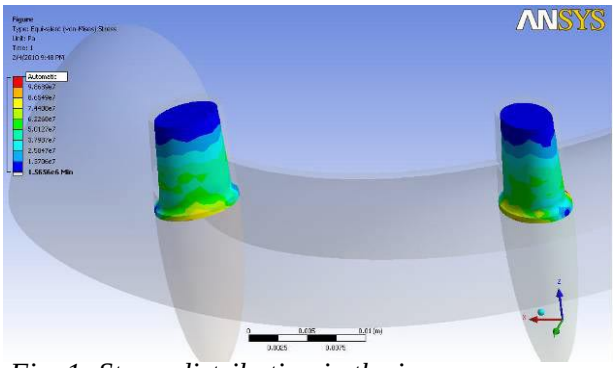

Fig. 1: Stress distribution in the inner crowns.

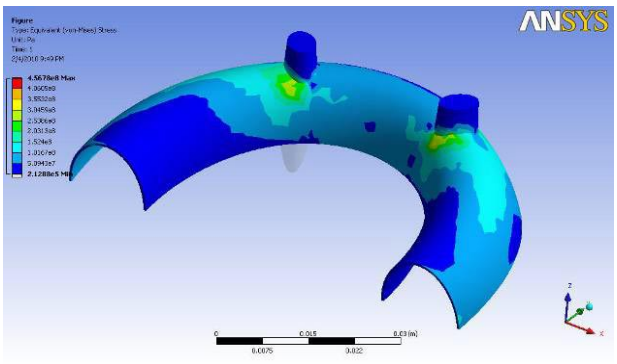

Fig. 2: Stress distribution in the removable framework.

DISCUSSION & CONCLUSIONS: Within the limitation of this study, the effect of the preparation angle is not important for the stress values in the conical double crowns. The stress values increase with the taper only in the removable partial framework (with 21.13%) for the studied cases. In the inner crowns similar variations were observed (21.01%), but they didn't vary with the taper.

REFERENCES: [1] K. Nagata, H. Takahashi, M. Ona, H. Hosomi, N Wakabayashi, Y.Igarashi (2009) *Dent Mater J* 28(5):649-56. [2] M.A. Gungor, C. Artunc, M. Sonugelen, M. Toparli (2002) *J Oral Rehabil* 29(11):1069-75. [3] B. Wostmann, M. Balkenhol, A. Weber, P. Ferger, P. Rehmann (2007) *J Dent* 35(12):939-45. [4] I. Stancic, A. Jelenkovic (2008) *Gerodontology* 25(3):162-7.

ACKNOWLEDGEMENTS: This study was supported by the Grant ID_1264 from the Ministry of Education and Research, Romania.